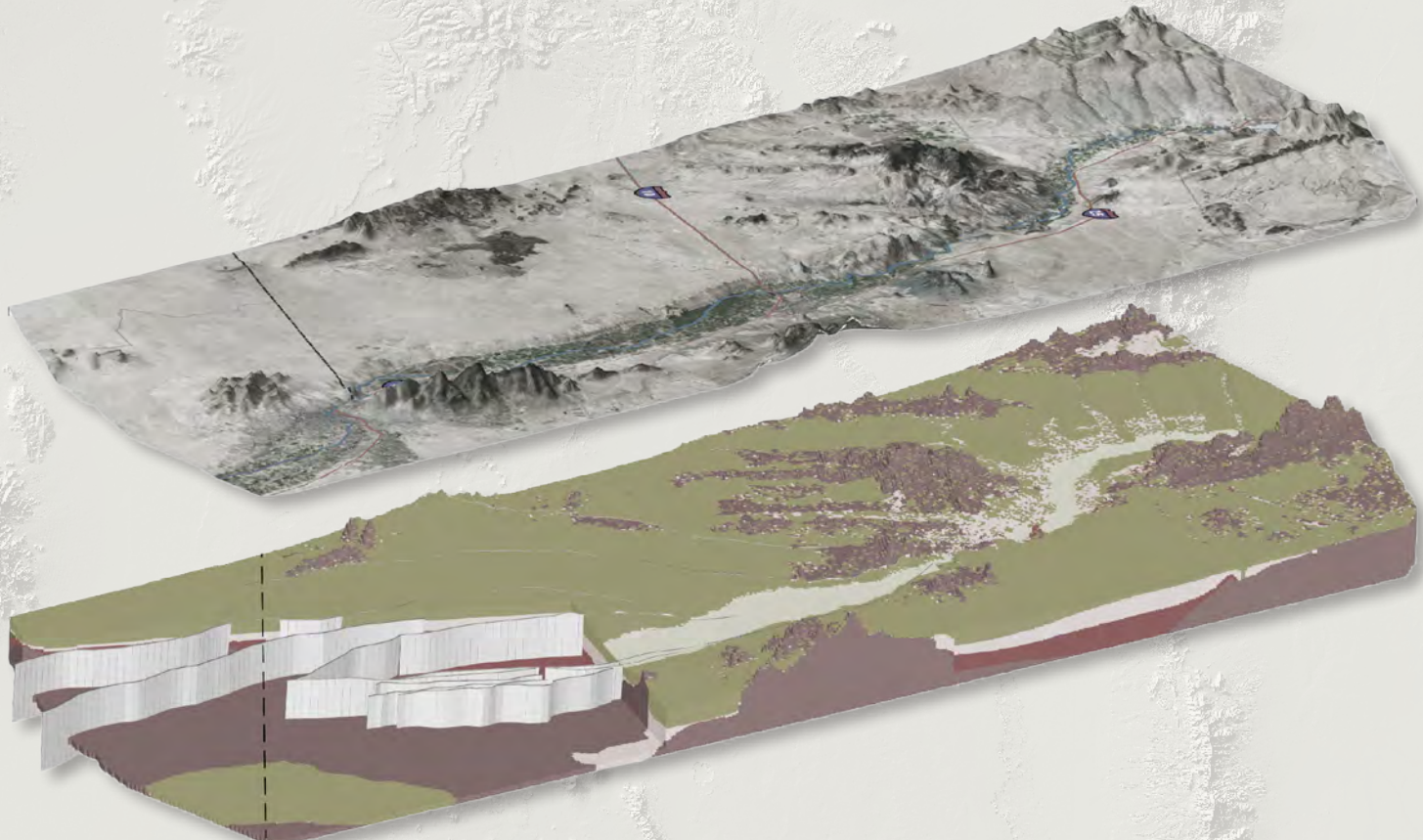


Prepared in cooperation with the Bureau of Reclamation

Three-Dimensional Hydrogeologic Framework Model of the Rio Grande Transboundary Region of New Mexico and Texas, USA, and Northern Chihuahua, Mexico



Scientific Investigations Report 2017–5060

Cover. Example of LANDSAT 7 imagery draped on a digital elevation model and aligned with a corresponding three-dimensional hydrogeologic framework solid model, based on animation shown in appendix 1.

Three-Dimensional Hydrogeologic Framework Model of the Rio Grande Transboundary Region of New Mexico and Texas, USA, and Northern Chihuahua, Mexico

By Donald S. Sweetkind

Prepared in cooperation with the Bureau of Reclamation

Scientific Investigations Report 2017–5060

**U.S. Department of the Interior
U.S. Geological Survey**

U.S. Department of the Interior
RYAN K. ZINKE, Secretary

U.S. Geological Survey
William H. Werkheiser, Acting Director

U.S. Geological Survey, Reston, Virginia: 2017

For more information on the USGS—the Federal source for science about the Earth, its natural and living resources, natural hazards, and the environment—visit <https://www.usgs.gov> or call 1–888–ASK–USGS.

For an overview of USGS information products, including maps, imagery, and publications, visit <https://store.usgs.gov/>.

Any use of trade, firm, or product names is for descriptive purposes only and does not imply endorsement by the U.S. Government.

Although this information product, for the most part, is in the public domain, it also may contain copyrighted materials as noted in the text. Permission to reproduce copyrighted items must be secured from the copyright owner.

Suggested citation:
Sweetkind, D.S., 2017, Three-dimensional hydrogeologic framework model of the Rio Grande transboundary region of New Mexico and Texas, USA, and northern Chihuahua, Mexico: U.S. Geological Survey Scientific Investigations Report 2017-5060, 49 p., <https://doi.org/10.3133/sir20175060>.

ISSN 2328-0328 (online)

Acknowledgments

This work was funded by, and conducted in cooperation with, the Bureau of Reclamation. The author acknowledges the efforts of Sarah McKean and Laura Breitner, former employees of the U.S. Geological Survey (USGS) New Mexico Water Science Center, in developing preliminary versions of digital datasets for the Transboundary Aquifer Assessment Program. Randy Hanson (USGS California Water Science Center) organized these preliminary datasets and provided them to the author. Bryanna Sudman (Geographic Information System [GIS] Department, City of Northfield, Minn.) developed and edited GIS datasets while working as a National Association of Geoscience Teachers (NAGT)/USGS summer intern. The author thanks Jeremy Havens (ADC Management Services, Inc.) for assistance with the preparation of the report figures and animations.

Contents

Acknowledgments.....	iii
Abstract.....	1
Introduction.....	1
Purpose and Scope	3
Description of Study Area	3
Stratigraphic and Structural Setting	3
Stratigraphy	3
Structural Setting.....	6
Tectonic Setting and Basin Evolution.....	8
Hydrostratigraphic Units For 3D Hydrogeologic Framework Model.....	9
Data Sources.....	11
Geologic Maps	11
Cross Sections.....	11
Faults.....	11
Structure Contour Maps.....	13
Well Data.....	13
Geophysical Data.....	13
Modeling Methodology.....	15
Creation of Top Surfaces of the Major Hydrostratigraphic Units	15
Modeling of Facies Variations for HSUs	19
Elevation, Thickness, Unit Extent, and Facies Patterns of Hydrostratigraphic Units.....	19
River Channel (RC).....	19
Upper Santa Fe (USF).....	21
Middle Santa Fe (MSF)	21
Lower Santa Fe (LSF).....	21
Basement (BSMT).....	21
Visualization of the 3D Hydrogeologic Framework Model.....	37
Model Evaluation, Use, and Limitations	40

Evaluation of Fit—Comparison to Input Data.....	40
Applicability and Limitations.....	40
Summary and Conclusions.....	43
References Cited.....	43
Appendix 1. Animation—Solid Model Reveal	48
Appendix 2. Animation—Cross Section Panels.....	49

Figures

1. Map of Rio Grande transboundary region of New Mexico and Texas, USA, and northern Chihuahua, Mexico, showing location of study area 2
2. Stratigraphic and hydrostratigraphic units of study area 4
3. Map of Rio Grande transboundary region of New Mexico and Texas, USA, and northern Chihuahua, Mexico, showing generalized geology of study area 5
4. Map of Rio Grande transboundary region of New Mexico and Texas, USA, and northern Chihuahua, Mexico, showing structural features of study area 7
5. Example cross section within the model domain..... 10
6. Map of Rio Grande transboundary region of New Mexico and Texas, USA, and northern Chihuahua, Mexico, showing study area and locations of published geologic cross sections used as input data for three-dimensional hydrogeologic framework model..... 14
7. Chart showing process of development of digital data for the three-dimensional hydrogeologic framework model 16
8. Diagrammatic cross section showing relative elevation of hydrostratigraphic unit tops and resultant thickness within the three-dimensional hydrogeologic framework model..... 17
9. Map of Rio Grande transboundary region of New Mexico and Texas, USA, and northern Chihuahua, Mexico, showing the location and types of input geologic data sets used for gridding of top of lower Santa Fe hydrostratigraphic unit in the three-dimensional hydrogeologic framework model..... 18
10. Map of Rio Grande transboundary region of New Mexico and Texas, USA, and northern Chihuahua, Mexico, showing elevation of base of river channel hydrostratigraphic unit used in the three-dimensional hydrogeologic framework model 20
11. Map of Rio Grande transboundary region of New Mexico and Texas, USA, and northern Chihuahua, Mexico, showing zone codes for upper part of river channel hydrostratigraphic unit used in the three-dimensional hydrogeologic framework model 22
12. Map of Rio Grande transboundary region of New Mexico and Texas, USA, and northern Chihuahua, Mexico, showing gridded elevation of top of upper Santa Fe hydrostratigraphic unit as used in the three-dimensional hydrogeologic framework model 23
13. Map of Rio Grande transboundary region of New Mexico and Texas, USA, and northern Chihuahua, Mexico, showing gridded thickness of upper Santa Fe hydrostratigraphic unit as used in the three-dimensional hydrogeologic framework model..... 24

14.	Map of Rio Grande transboundary region of New Mexico and Texas, USA, and northern Chihuahua, Mexico, showing zone codes for upper part of upper Santa Fe hydrostratigraphic unit as used in the three-dimensional hydrogeologic framework model.....	25
15.	Map of Rio Grande transboundary region of New Mexico and Texas, USA, and northern Chihuahua, Mexico, showing zone codes for lower part of upper Santa Fe hydrostratigraphic unit as used in the three-dimensional hydrogeologic framework model.....	26
16.	Map of Rio Grande transboundary region of New Mexico and Texas, USA, and northern Chihuahua, Mexico, showing gridded elevation of top of middle Santa Fe hydrostratigraphic unit as used in the three-dimensional hydrogeologic framework model.....	27
17.	Map of Rio Grande transboundary region of New Mexico and Texas, USA, and northern Chihuahua, Mexico, showing gridded thickness of middle Santa Fe hydrostratigraphic unit as used in the three-dimensional hydrogeologic framework model.....	28
18.	Map of Rio Grande transboundary region of New Mexico and Texas, USA, and northern Chihuahua, Mexico, showing zone codes for upper part of middle Santa Fe hydrostratigraphic unit as used in the three-dimensional hydrogeologic framework model.....	29
19.	Map of Rio Grande transboundary region of New Mexico and Texas, USA, and northern Chihuahua, Mexico, showing zone codes for lower part of middle Santa Fe hydrostratigraphic unit as used in the three-dimensional hydrogeologic framework model.....	30
20.	Map of Rio Grande transboundary region of New Mexico and Texas, USA, and northern Chihuahua, Mexico, showing gridded elevation of top of lower Santa Fe hydrostratigraphic unit as used in the three-dimensional hydrogeologic framework model.....	31
21.	Map of Rio Grande transboundary region of New Mexico and Texas, USA, and northern Chihuahua, Mexico, showing gridded thickness of lower Santa Fe hydrostratigraphic unit as used in the three-dimensional hydrogeologic framework model.....	32
22.	Map of Rio Grande transboundary region of New Mexico and Texas, USA, and northern Chihuahua, Mexico, showing zone codes for upper part of lower Santa Fe hydrostratigraphic unit as used in the three-dimensional hydrogeologic framework model.....	33
23.	Map of Rio Grande transboundary region of New Mexico and Texas, USA, and northern Chihuahua, Mexico, showing zone codes for lower part of lower Santa Fe hydrostratigraphic unit as used in the three-dimensional dydrogeologic framework model.....	34
24.	Map of Rio Grande transboundary region of New Mexico and Texas, USA, and northern Chihuahua, Mexico, showing gridded elevation of top of basement hydrostratigraphic unit as used in the three-dimensional hydrogeologic framework model.....	35
25.	Map of Rio Grande transboundary region of New Mexico and Texas, USA, and northern Chihuahua, Mexico, showing zone codes for basement hydrostratigraphic unit as used in the three-dimensional hydrogeologic framework model.....	36
26.	Perspective view of three-dimensional hydrogeologic framework solid model with cutout.....	38

27. Perspective view of vertical cross sections cut through three-dimensional hydrogeologic framework solid model.....	39
28. Perspective view of input hydrogeologic cross sections and three-dimensional hydrogeologic framework modeled top of lower Santa Fe hydrostratigraphic unit.....	41
29. Difference in elevation of the top of middle Santa Fe between input data and three-dimensional hydrogeologic framework model	42

Tables

1. Zone definitions for river channel, lower Santa Fe, middle Santa Fe, and upper Santa Fe Group hydrostratigraphic units used in three-dimensional hydrogeologic framework model.....	12
2. Zone definitions for pre-Santa Fe Group basement hydrostratigraphic unit used in three-dimensional hydrogeologic framework model	13

Conversion Factors

International System of Units to Inch/Pound

Multiply	By	To obtain
Length		
millimeter (mm)	0.03937	inch (in.)
centimeter (cm)	0.3937	inch (in.)
meter (m)	3.281	foot (ft)
kilometer (km)	0.6214	mile (mi)
Area		
square meter (m^2)	10.76	square foot (ft^2)
square kilometer (km^2)	0.3861	square mile (mi^2)

Datum

Model X and Y coordinates are Transverse Mercator Projection, Universal Transverse Mercator (UTM) Zone 13 in meters, North American Datum 1983 (NAD 83). Z values are elevation in feet, North American Vertical Datum 1988 (NAVD 88).

Elevation, as used in this report, refers to distance above the vertical datum.

Abbreviations

2D	two-dimensional
3D	three-dimensional
3D HFM	three-dimensional hydrogeologic framework model
BSMT	basement
DEM	digital elevation model
DOD	U.S. Department of Defense
EPA	U.S. Environmental Protection Agency
ESRI	Environmental Science Research Institute
HSU	hydrostratigraphic unit
GIS	geographic information system
LSF	lower Santa Fe
Ma	mega-annum (10^6 years)
MSF	middle Santa Fe
NAGT	National Association of Geoscience Teachers
ppm	parts per million
RC	river channel
TEM	time-domain electromagnetic
USF	upper Santa Fe
USGS	U.S. Geological Survey

Three-Dimensional Hydrogeologic Framework Model of the Rio Grande Transboundary Region of New Mexico and Texas, USA, and Northern Chihuahua, Mexico

By Donald S. Sweetkind

Abstract

As part of a U.S. Geological Survey study in cooperation with the Bureau of Reclamation, a digital three-dimensional hydrogeologic framework model was constructed for the Rio Grande transboundary region of New Mexico and Texas, USA, and northern Chihuahua, Mexico. This model was constructed to define the aquifer system geometry and subsurface lithologic characteristics and distribution for use in a regional numerical hydrologic model. The model includes five hydrostratigraphic units: river channel alluvium, three informal subdivisions of Santa Fe Group basin fill, and an undivided pre-Santa Fe Group bedrock unit. Model input data were compiled from published cross sections, well data, structure contour maps, selected geophysical data, and contiguous compilations of surficial geology and structural features in the study area. These data were used to construct faulted surfaces that represent the upper and lower subsurface hydrostratigraphic unit boundaries. The digital three-dimensional hydrogeologic framework model is constructed through combining faults, the elevation of the tops of each hydrostratigraphic unit, and boundary lines depicting the subsurface extent of each hydrostratigraphic unit. The framework also compiles a digital representation of the distribution of sedimentary facies within each hydrostratigraphic unit. The digital three-dimensional hydrogeologic model reproduces with reasonable accuracy the previously published subsurface hydrogeologic conceptualization of the aquifer system and represents the large-scale geometry of the subsurface aquifers. The model is at a scale and resolution appropriate for use as the foundation for a numerical hydrologic model of the study area.

Introduction

The region surrounding the Rio Grande between Caballo Reservoir, New Mexico, and El Paso, Texas, (fig. 1) lies within the lower Rio Grande surface-water and groundwater basins (New Mexico Office of the State Engineer/Interstate Stream Commission, 2017). Groundwater and instream flows supply

water for urban, agricultural, and industrial uses and support recreational and environmental interests (Hanson and others, 2013). The conjunctive use of surface water and groundwater occurs under numerous legal and operational constraints including the Rio Grande Compact (an international treaty) and the Rio Grande Project of the Bureau of Reclamation (Hanson and others, 2013). As in many arid regions, the water supply is limited in quantity and there is substantial annual variability in rainfall, yet increasing demands from both agricultural and urban users are being placed on the interconnected surface and groundwater system.

Analysis of the complex relations between the use and movement of water in the groundwater basins requires an integrated hydrologic model capable of tracking the three-dimensional movement of groundwater and the impacts of surface-water and groundwater use on water availability in the context of changing land use, irrigation practices, and climate (Hanson and others, 2013). The U.S. Geological Survey (USGS), in cooperation with the Bureau of Reclamation, is building on previous hydrologic modeling efforts to develop a regional integrated hydrologic model of the transboundary aquifers and interconnected surface waters of Rincon Valley, the informally named Mesilla groundwater basin in New Mexico and Texas, and the informally named Conejos-Medanos basin of northern Mexico (fig. 1). The hydrologic model will be used to evaluate and test the conceptual model of the system and may be used as a management tool for surface-water flows and to evaluate groundwater availability under alternative development and climate scenarios. The hydrogeologic framework model described in this report is the geologic foundation for numerical simulation of the hydrologic system.

Management of surface-water and groundwater resources in the region requires a knowledge of the groundwater system, which in turn requires an understanding of the configuration and properties of aquifers. Previous hydrogeologic framework studies of the shallow alluvial and deep-basin aquifer system have been developed for the region (King and others, 1971; Hawley, 1984; Hawley and Lozinsky, 1992; Nickerson and Myers, 1993; Hawley and Kennedy, 2004). These reports include a series of geologic maps, cross sections, and well data (Hawley and Kennedy, 2004; Hawley and others,

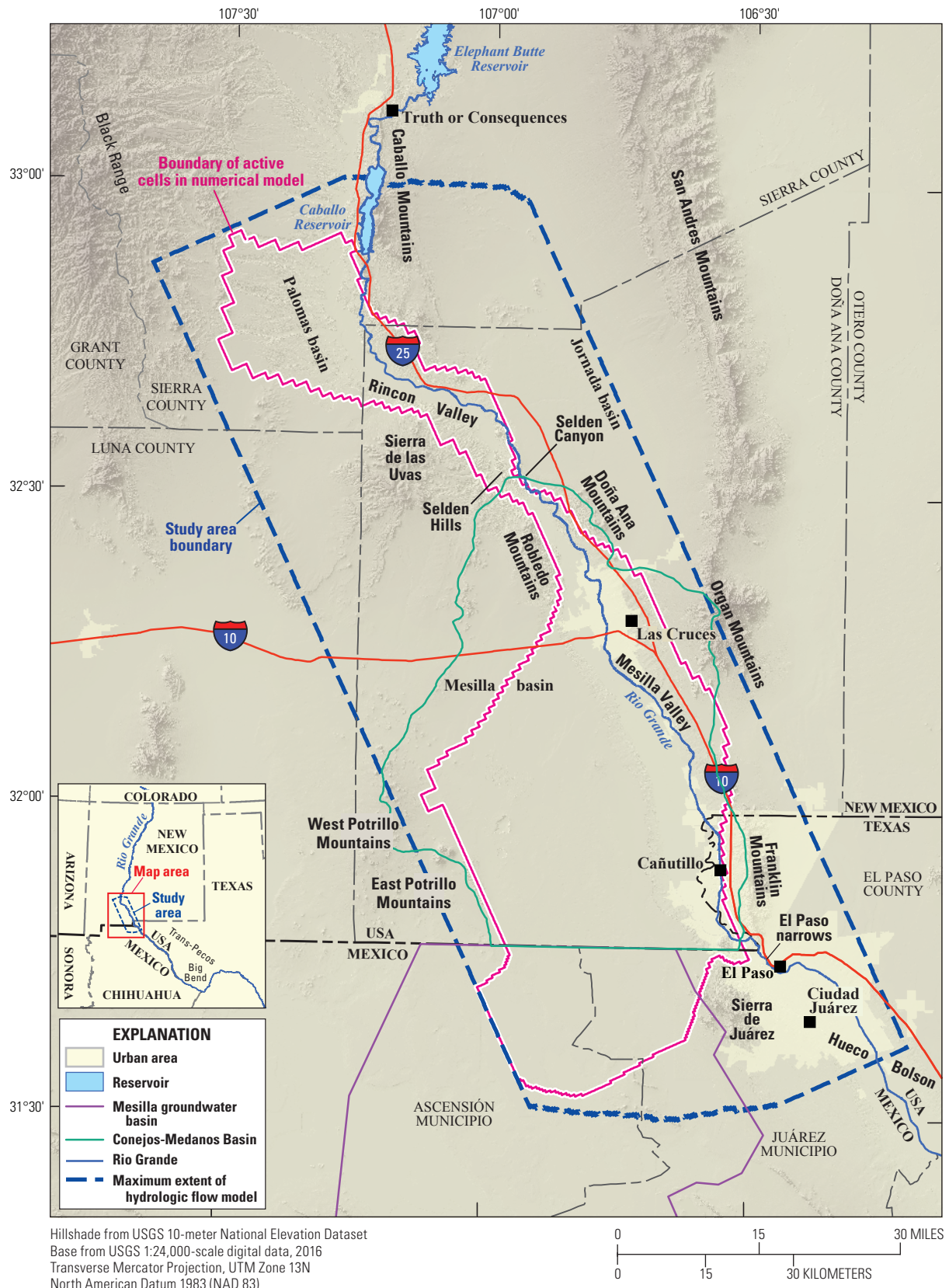


Figure 1. Map of Rio Grande transboundary region of New Mexico and Texas, USA, and northern Chihuahua, Mexico, showing location of study area.

2009), but these data have never been combined digitally in three dimensions. Published numerical groundwater models generalize aquifer geometry and properties within three model layers above a basement rock layer (Frenzel, 1992; Hamilton, 1993; Lang and Maddock, 1995; Weeden and Maddock, 1999; Boyle Engineering and Parsons Engineering Science, 2000). Recent numerical models use additional layering and focus on specific aquifer horizons, such as the base of shallow unconsolidated alluvial deposits and the top of deep, fine-grained clay-rich deposits (S.S. Papadopoulos & Associates, Inc., 2007; Hanson and others, 2013), but do not incorporate a fully three-dimensional hydrogeologic framework model as the basis for numerical simulation.

Purpose and Scope

This report describes the development of a digital three-dimensional hydrogeologic framework model (3D HFM) of the study area (fig. 1), which defines the extent and geometry of the basin-filling deposits and older bedrock units that serve as the geohydrologic layering for the framework model. The 3D HFM also describes the spatial distribution of sedimentary facies, which provides an initial condition for defining hydraulic properties of the aquifer layers, and includes the location of faults and igneous dikes, both of which could potentially be used as horizontal-flow barriers within a numerical hydrologic model.

The study area modeled by the 3D HFM covers approximately 4,660 square miles (mi^2) within New Mexico and Texas, USA, and northern Chihuahua, Mexico (fig. 1). The study area is centered on two adjacent structural basins, the Palomas and Mesilla basins, which are connected by Selden Canyon (fig. 1). Parts of two adjacent structural basins, the Jornada del Muerto basin, hereafter called the Jornada basin, in the northeast part of the study area and the Hueco Bolson to the southeast of El Paso, Texas, are included in the 3D HFM to provide control on grid elevations and fault offsets near the edges of the model, but they are not part of the region that will actively participate in the numerical hydrologic model (fig. 1; Randall Hanson, USGS, written commun., 2015). The digital 3D HFM described in this report captures the hydrogeologic conceptualization of Hawley and Kennedy (2004) and additional data developed in conjunction with the USGS during the Trans-boundary Aquifer Assessment Program (Alley, 2013).

Description of Study Area

The study area includes parts of south-central New Mexico, El Paso County, Texas, and northwestern Chihuahua, Mexico, and surrounds the Rio Grande from Caballo Reservoir, New Mexico, for approximately 80 miles (mi) southeastward, south of El Paso, Texas (fig. 1). The study area includes two generally northwest-southeast-trending topographic valleys that form the floodplain adjacent to the Rio Grande: Rincon Valley between Caballo Reservoir and Selden Canyon,

and to the south Mesilla Valley between Leasburg, New Mexico, and the El Paso narrows to the west of El Paso, Texas. Rincon and Mesilla Valleys are linked by Selden Canyon, a narrow valley incised into the Selden Hills uplift (fig. 1).

The Palomas structural basin in the northwestern part of the study area is bounded on the west and south by the Black Range and the Sierra de las Uvas and on the east by the Caballo Mountains. In this report, the Palomas basin includes the east-west-trending Hatch-Rincon basin as used by Mack and others (2006). The large intermontane Jornada basin lies between the Caballo Mountains on the west and the San Andres Mountains on the east and occupies the northeast part of the study area (fig. 1). The Mesilla structural basin occupies most of the southern half of the study area between Selden Canyon on the north and the El Paso narrows on the southeast. The Mesilla basin is bounded on the northeast by the Doña Ana Mountains; on the east by the Organ Mountains, Franklin Mountains, and Sierra de Juarez; and on the west by the East Potrillo, West Potrillo, and Robledo Mountains (fig. 1). The Rio Grande exits Mesilla Valley and the Mesilla basin through the El Paso narrows between the Franklin Mountains and Sierra de Juarez uplifts and flows southeastward down the Hueco Bolson toward the Big Bend area of Trans-Pecos Texas (fig. 1).

Stratigraphic and Structural Setting

The study area is located in the southern part of the Rio Grande rift, a tectonic feature that is characterized by generally north-south-trending structural basins bounded by volcanic highlands and fault-block ranges that expose tilted pre-Cenozoic rocks (Chapin and Seager, 1975; Hawley, 1978; Chapin and Cather, 1994). The Rio Grande flows through a series of extensional basins filled with up to 12,000 feet (ft) of Paleogene volcanic rocks and Neogene alluvial, fluvial, playa, and lacustrine sediments (Chapin and Cather, 1994).

Stratigraphy

The stratigraphic framework of the study area consists, from oldest to youngest, of a

- thick sequence of pre-Cenozoic rocks,
- Paleogene sedimentary and volcanic rocks,
- locally thick sequence of Neogene basin-fill deposits,
- late Pliocene to Pleistocene alluvial fan and fluvial deposits and local Pleistocene basalt flows, and
- local Pleistocene and Holocene deposits (figs. 2 and 3).

Pre-Cenozoic rocks include Precambrian granitic and metamorphic rocks overlain by about 1,600 meters (m) of Paleozoic rocks including dolomite, limestone, and sandstone, with interbedded shale and local gypsum beds. Paleozoic strata are unconformably overlain by as much as 2,500 ft of

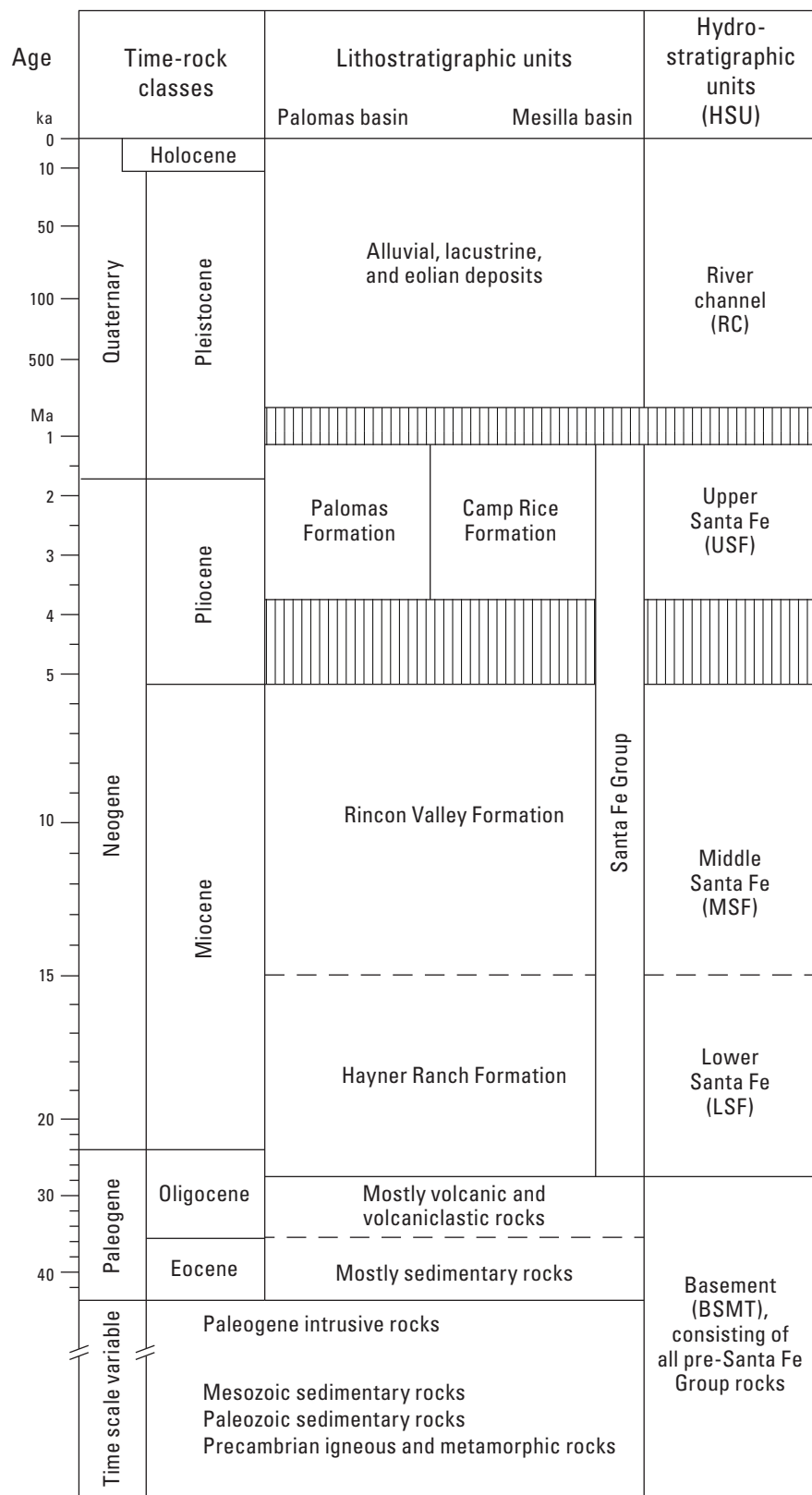


Figure 2. Stratigraphic and hydrostratigraphic units of study area. (ka, kilo annum [10^3 years]; Ma, mega-annum [10^6 years])

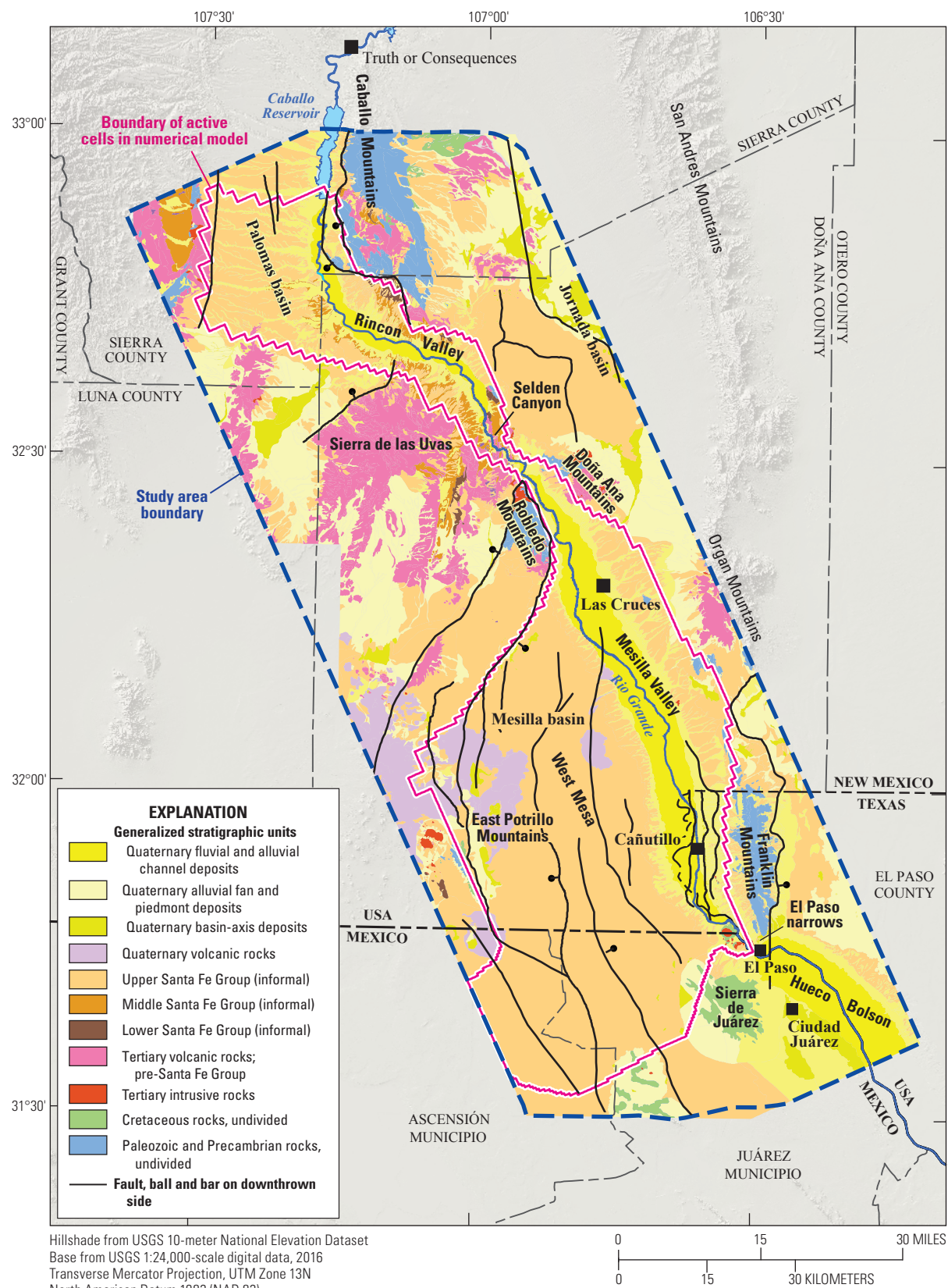


Figure 3. Map of Rio Grande transboundary region of New Mexico and Texas, USA, and northern Chihuahua, Mexico, showing generalized geology of study area.

6 Three-Dimensional Hydrogeologic Framework Model of the Rio Grande Transboundary Region, USA and Mexico

Upper Cretaceous marine and nonmarine sandstone and shale. Rocks of Paleozoic and Lower Cretaceous age are exposed in the Caballo, Franklin, East Portillo, and Robledo Mountains and Sierra de Juarez (fig. 3; Harbour, 1972; Seager and others, 1987, 2008). Intrusive rocks of intermediate composition and probable Paleogene age crop out in the El Paso narrows between the Franklin Mountains and Sierra de Juárez (fig. 3; Hoffer, 1969).

Basal Cenozoic strata are pre-rift siliciclastic strata associated with the erosion of Laramide uplifts (Epis and Chapin, 1975). These strata are overlain by a 3,000-ft sequence of Neogene intermediate-composition lavas and associated volcaniclastic rocks capped with silicic ash-flow tuffs and basaltic andesite erupted from multiple volcanic centers (Seager and others, 1984) (fig. 2). Tertiary igneous intrusive rocks, primarily granite to monzonite in composition, are the dominant rocks exposed in the Doña Ana Mountains and southern part of the Organ Mountains (fig. 3; Seager and others, 1976; Seager, 1981).

Neogene and earliest Pleistocene strata that record synrift basin filling are included in the Santa Fe Group (Spiegel and Baldwin, 1963; Hawley and others, 1969; Mack, 2004). Santa Fe Group strata correspond to at least four formations mapped in the study area:

- Hayner Ranch Formation, early to middle Miocene fanglomerate and sandstone;
- Rincon Valley Formation, middle to late Miocene fanglomerate, alluvial basin and playa deposits; and
- Palomas and Camp Rice Formations, late Pliocene to Pleistocene coarse-grained sand and gravel deposits that represent alluvial fan and fluvial deposits associated with the ancestral Rio Grande

(fig. 2; Lozinsky and Hawley, 1986; Mack and others, 1993; Hawley and others, 2001; Hawley and Kennedy, 2004).

The Santa Fe Group is subdivided into informal upper Santa Fe (USF), middle Santa Fe (MSF), and lower Santa Fe (LSF) hydrostratigraphic units (HSUs) on the basis of genesis, age, and stratigraphic position (fig. 2; Hawley and Lozinsky, 1992; Hawley and others, 2001; Hawley and Kennedy, 2004). The Santa Fe Group sediments record deposition in pre-, syn-, and post-extensional settings and the transition from a closed-basin deposition in early to middle Miocene to an open-basin, fluvial system in the Pleistocene (Seager, 1975; Seager and others, 1984; Mack and Seager, 1990; Mack and others, 2006). Quaternary deposits include fluvial deposits of the entrenched Rio Grande channel, eolian deposits, and alluvial channel fill (figs. 2 and 3; Hawley and Kennedy, 2004).

Structural Setting

Older, pre-rift structures in the study area include Laramide foreland contractile structures (Seager and others, 1997; Seager, 2004) and late Paleozoic to Mesozoic structures potentially related to reactivation of original passive-margin

normal faults (Muehlberger, 1980; Dickinson and Lawton, 2001; Lawton, 2004). Laramide structures are only intermittently exposed as a result of burial by Cenozoic deposits and segmentation by faults of the Rio Grande rift. A Laramide uplift and associated syntectonic basin were identified in the Caballo Mountains (Seager and others, 1997). These older, pre-rift structures appear unrelated to evolution of Neogene basins and fault patterns and are not considered in the 3D HFM.

The Texas lineament (fig. 4) is described as a broad, northwest-trending regional structural zone that serves as a boundary between regional geologic and geomorphic terranes (DeFord, 1969; Hildebrand, 2015). The lineament is believed to have been most active during the Precambrian but may have had repeated periods of offset (Muehlberger, 1980). Northwest-striking, graben-bounding normal faults in the Hueco Bolson of the border region of Texas may be controlled by the Texas lineament (Muehlberger, 1980; Collins and Raney, 1994). Muehlberger (1980) inferred the lineament to be a broad distributed zone of shear tens of kilometers wide. In the study area, the north boundary of the lineament is in the El Paso narrows and projects northwestward to the north of the East Portillo Mountains; areas to the southwest of this line could be affected by lineament-associated structures (fig. 4). Within the study area, the lineament has no surface expression and appears unrelated to the location of Neogene basins and fault patterns; however, the presence of the lineament may explain the abrupt bedrock discontinuity between the west-tilted Paleozoic rock section in the Franklin Mountains and the highly folded Cretaceous rocks exposed to the south in the Sierra de Juarez (fig. 3).

The study area lies at the south end of a series of generally north-south-trending structural basins and flanking mountain uplifts that compose the Rio Grande rift (Chapin and Seager, 1975; Seager and Morgan, 1979). The rift extends from the San Luis basin of south-central Colorado through New Mexico to the Hueco Bolson area of west Texas and northern Chihuahua, Mexico (Hawley, 1978). In the study area, intermontane structural basins, or bolsons, are flanked by fault-bounded mountain-block uplifts of late Cenozoic age (fig. 4). In the northwestern part of the study area, the Palomas basin is an east-tilted half-graben where the thickest basin fill is adjacent to the Caballo Mountains and the basin-bounding west-side-down Red Hills and Derry faults (figs. 3 and 4; Hawley and Kennedy, 2004, plate R4). At the end of the Rincon Valley, the Rio Grande exits the Palomas basin through Selden Canyon, a narrow bedrock-floored canyon incised into uplifted pre-Santa Fe Group volcanic rocks (figs. 3 and 4). In the northeastern part of the study area is the Jornada basin, a complexly faulted basin flanked on the east by the San Andres Mountains, which are bounded on the west side by west-side-down faults (Hawley and Kennedy, 2004, plate R4). The Jornada basin is bounded on the southwest by the Jornada fault (fig. 4; Seager and others, 1976, 1987). The Jornada fault is the northern structural boundary of a partly buried bedrock ridge that forms the boundary between the Mesilla and Jornada structural basins; the Doña Ana Mountains are the largest surface expression of the bedrock ridge (figs. 3 and 4).

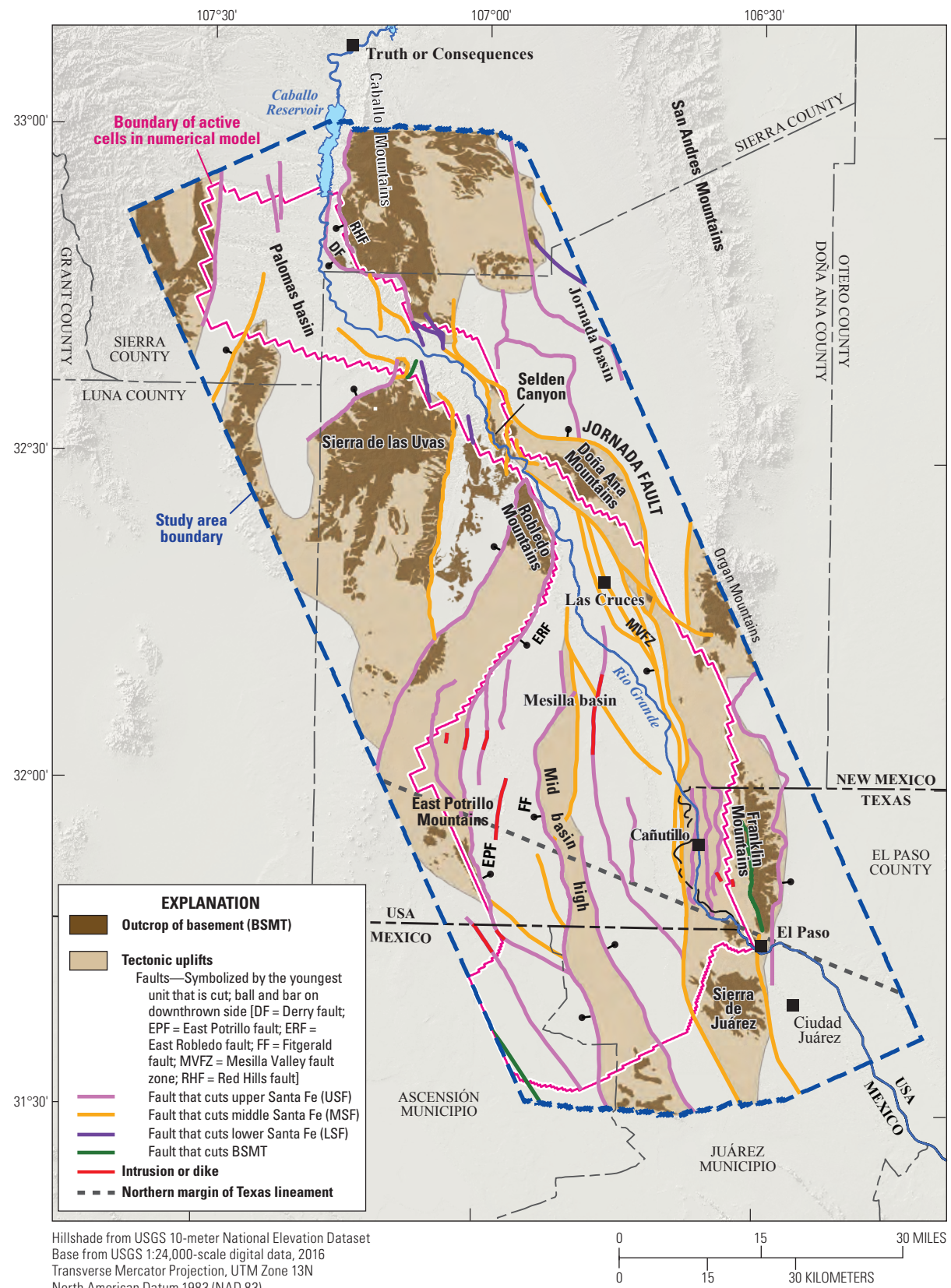


Figure 4. Map of Rio Grande transboundary region of New Mexico, USA, and northern Chihuahua, Mexico, showing structural features of study area.

The southern half of the study area is dominated by the Mesilla structural basin, which covers an area of about 1,100 mi² (2,590 square kilometers [km²]), and extends southward about 60 mi (100 km) from the Robledo and Doña Ana Mountains to west of Ciudad Juarez in northern Chihuahua, Mexico (fig. 1). Basin width varies from about 5 mi (8 km) in the north to about 25 mi (40 km) near its center (figs. 3 and 4). The northeastern structural boundary of the basin is formed by the partly buried bedrock ridge that includes the Doña Ana Mountains; the ridge is bounded on its southwest side by the Mesilla Valley fault zone, which is known in the subsurface along the entire eastern edge of the Mesilla basin (Lovejoy, 1976; Hawley and Kennedy, 2004, plates 3 and 4). The Mesilla basin is bounded on the west by the East Robledo fault to the northwest and the East Potrillo fault to the southwest (fig. 4; Hawley and Kennedy, 2004, plates 3 and 4). The Mesilla basin is internally faulted; a buried mid-basin uplift separates an eastern subbasin, the La Union-Mesquite subbasin of Hawley and others (2001), from a western subbasin that includes the southwestern and northwestern subbasins of Hawley and others (2001) (fig. 4).

Hawley and Kennedy (2004) interpret almost all basin-bounding and intrabasinal faults as nearly vertical normal faults, in part based on interpreted gentle dips of strata in the central basin areas. Other interpretive geologic cross sections of parts of the study area show gently listric fault geometry (Seager and others, 1975, 1982, 1987) or complex geometries within fault transfer zones (Mack and Seager, 1995). The 3D HFM presented in this report depicts faults as vertical, in order to maintain consistency with input geologic data and to meet the needs of the anticipated numerical hydrologic model.

Tectonic Setting and Basin Evolution

Extension, fault-block uplift, and basin subsidence have occurred in the study area in multiple pulses of deformation over a prolonged period from Oligocene to Pleistocene time (Seager, 1975; Mack, 2004). The tectonic evolution of the region is documented in Santa Fe Group rocks, aided by local interbedded volcanic rocks that serve as time-stratigraphic markers. Block faulting, uplift, basin subsidence, and sedimentation were initiated in late Eocene to early Oligocene time, contemporaneous with volcanism in other parts of the southern Rio Grande rift (Seager and others, 1984; Mack and others, 1994). A major phase of rift-related extensional faulting and basin subsidence occurred throughout most of the Miocene, resulting in deposition of about 6,500 ft of basin-fill sediments of the Hayner Ranch and Rincon Valley Formations deposited in a number of separate subbasins (Mack and others, 1994; Mack, 2004). By late Miocene time, basin aggradation occurred and intrabasin uplifts were buried by lower and middle Santa Fe Group deposits, resulting in larger, less segmented depositional basins (Mack and others, 1994). A second major pulse of deformation in the southern Rio Grande rift began near the Miocene-Pliocene boundary, resulting in the maximum

differential displacement between the major basin and range structural blocks (Chapin and Seager, 1975). During this period, the older deposits were deformed and tilted and new faults developed, many of which uplifted parts of earlier Miocene basins. Following this faulting, basin aggradation formed a single broad depositional basin throughout middle Pliocene to early Pleistocene time (Mack and Seager, 1990; Mack and others, 1993, 2006). The Camp Rice and Palomas Formations represent this pulse of basin filling; these deposits have a maximum thickness of about 500 ft (Mack and Seager, 1990; Mack and others, 2006).

Within the study area, evidence for multiple phases of rift-related faulting and basin-filling episodes is observed in uplifted outcrops of lower and middle Santa Fe Group rocks in the Robledo Mountains, Caballo Mountains, and Sierra de las Uvas (fig. 3). In these areas, late Miocene to Pliocene uplifts expose sediments that were deposited in older Miocene basins, showing that patterns of late Cenozoic basins and uplifts differ from the extent of the earlier formed basins (Chapin and Seager, 1975; Mack and others, 2006). Subsurface distribution of the lower, middle, and upper Santa Fe Group rocks help to constrain the timing of motion on basin-bounding faults. The regions of greatest thickness of Santa Fe Group rocks in the Mesilla basin and southern part of the Jornada basin are adjacent to the most active fault segments within the Mesilla Valley, East Potrillo, East Robledo, and Jornada fault zones (Hawley and Kennedy, 2004). However, not all faults cut the Pliocene-Pleistocene Camp Rice and Palomas Formations, and some faults cut only older units and were apparently inactive during Pliocene and younger time (fig. 4; Seager, 1975; Hawley and Kennedy, 2004, plates 3 and 4; Mack and others, 2006).

Widespread basin filling ceased in middle Pleistocene time because of regional entrenchment of the present Rio Grande (Mack and others, 2006). Incision and subsequent aggradation by the ancestral Rio Grande and its tributaries during the past 0.78 million years (m.y.) deposited a few tens of meters of coarse channel fill, and dissection locally exposed all or part of the Camp Rice and Palomas Formations, as well as some older Santa Fe Group strata (Mack and others, 1993, 2006). In the Palomas basin, the Rio Grande flows in the deeply entrenched Rincon Valley, incised into broad mesas capped by upper Santa Fe Group rocks in the west-central part of the Palomas basin (fig. 3). The mesas are remnants of piedmont slopes graded to ancestral Rio Grande base levels as much as 400 to 500 ft above the present Rincon Valley floor (Hawley and Kottlowski, 1969). The Mesilla basin features the broadly incised recent floodplain of the Rio Grande in the Mesilla Valley on the east side of the basin (fig. 3). A broad geomorphic surface known locally as West Mesa or La Mesa lies to the west of and above the level of the Rio Grande channel (fig. 3; Myers and Orr, 1985). This surface is a remnant of an extensive basin floor preserved between Mesilla Valley and the East Potrillo and Robledo uplifts that predates river-valley incision (Gile and others, 1981; Mack and others, 2006).

Hydrostratigraphic Units For 3D Hydrogeologic Framework Model

The main water-bearing units in the study area are Quaternary fluvial deposits of the inner Rio Grande Valley and the Neogene sedimentary basin-fill deposits of the Santa Fe Group (King and others, 1971; Hawley, 1984; Hawley and Lozinsky, 1992; Hawley and Kennedy, 2004). These units and the underlying bedrock are subdivided into five informal hydrostratigraphic units (HSUs; fig. 2), defined as a stratigraphic unit, a part of a stratigraphic unit, or a combination of adjacent stratigraphic units with consistent hydraulic properties (Maxey, 1964; American Nuclear Society, 1980; Seaber, 1988). A basement (BSMT) HSU consists of all pre-Santa Fe Group rocks, including Paleogene sedimentary and volcanic rocks; Paleozoic carbonate, siliciclastic, and igneous rocks; and Precambrian crystalline rocks (fig. 2). The informal HSUs, described below, serve to group rocks in the study area according to age, lithology, and general water-transmitting properties (fig. 2; Hawley, 1984; Hawley and Lozinsky, 1992; Hawley and others, 2001, 2009; Hawley and Kennedy, 2004).

River channel (RC): The RC HSU (fig. 2) is the Quaternary alluvium of the Rio Grande floodplain, including river channel, overbank deposits, and interfingered alluvial-fan deposits along the margin of the floodplain (Hawley and Kennedy, 2004). The approximately 80-ft-thick channel gravel and sand deposits were deposited in the past 0.8 Ma during a period of incision and partial backfilling by the Rio Grande and its tributaries, forming the relatively narrow floodplain of the current river (Mack and others, 2006). In the Palomas and Mesilla basins, the RC HSU unconformably overlies Santa Fe Group basin fill; in the El Paso narrows and Selden Canyon areas, the channel incision was in pre-Santa Fe Group rocks and the coarse deposits of the RC HSU were deposited above these older units (King and others, 1969; Hawley and Kennedy, 2004).

Upper Santa Fe (USF): The USF HSU (fig. 2) roughly corresponds to the Pliocene-Pleistocene Camp Rice Formation in the Mesilla basin and the Palomas Formation in the Palomas basin (Hawley and others, 2001; Hawley and Kennedy, 2004). This HSU is dominated by fluvial sediments of the ancestral Rio Grande and coeval alluvial-fan detritus (Hawley and Kennedy, 2004; Mack and others, 2006). These deposits are 50 to 450 ft thick and consist of pebbly, medium to coarse sands of braided-stream channel deposits and various finer-grained floodplain deposits. Piedmont-slope deposits are composed of fan alluvium and associated debris-flow deposits (Lozinsky and Hawley, 1986).

Middle Santa Fe (MSF): The MSF HSU generally corresponds to the Rincon Valley Formation (fig. 2). Rocks of this HSU were deposited about 10 to 4 Ma when rift tectonism was most active and basin aggradation adjacent to the major basin-boundary fault zones was accelerated (Mack and others, 1994; Mack, 2004). Rift tectonism resulted in depositional environments that ranged from broad, rapidly aggrading basin

floors to alluvial flats that terminated in extensive playa-lake plains (Hawley and Kennedy, 2004; Mack and others, 2006). Sediment lithofacies include alternating beds of clean sand, silty sand, and silt-clay mixtures in much of the central basin areas (Hawley and Lozinsky, 1992; Hawley and Kennedy, 2004). In the southern parts of the Jornada and Mesilla basins, basin-floor facies include extensive and thick playa-lacustrine deposits that are clay rich and can be confining units (Hawley and Kennedy, 2004; Mack and others, 2006).

Lower Santa Fe (LSF): The LSF HSU generally corresponds to the Hayner Ranch Formation of the Santa Fe Group (fig. 2). Rocks of this HSU were mostly deposited in closed basins and are dominated by fine-grained, clay-rich basin-floor sediments that interfinger with distal-facies alluvial fan deposits from bordering piedmont slopes. In the southern parts of the Jornada del Muerto and Mesilla basins, basin-floor facies include thick, extensive playa-lacustrine deposits (Hawley and Kennedy, 2004; Mack and others, 2006). Locally, thick sheets and lenticular bodies of sandy eolian sediments are interbedded with both basin-floor and piedmont-slope deposits in the southern part of the Mesilla basin (Leggat and others, 1962; Nickerson, 1989; Hawley and others, 2001).

Basement (BSMT): The basement HSU includes all rocks that predate Santa Fe Group rocks. This HSU contains a wide variety of rock types, including Precambrian crystalline rocks; Paleozoic and Mesozoic dolomite, limestone, and sandstone; intrusive rocks; and Paleogene sedimentary and volcanic rocks. These units form the hydrologic basement beneath the basin-fill aquifer system (Hawley and Kennedy, 2004).

Published hydrogeologic cross sections in the study area (Hawley and Kennedy, 2004, plates 3, 4, R4, and R5; Hawley and others, 2009, plate 2) show the HSUs for the Santa Fe Group rocks subdivided into upper and lower parts (red dashed lines in fig. 5A). The subdivisions designate lithofacies changes during deposition of a specific HSU. In this report, HSUs for the Santa Fe Group rocks were split into two subunits within the 3D HFM in order to maintain consistency with the published sections and to provide flexibility in the assignment of hydraulic properties to HSUs within the numerical hydrologic model. For the 3D HFM, subdivisions shown on published hydrogeologic cross sections were captured by splitting the USF, MSF, and LSF HSUs in half; each subunit represents half the total thickness of the unit. In each case, the upper subunit is designated with the number 1 appended to the HSU name, for example USF1, and the lower subunit is designated with the number 2 appended to the HSU name, for example USF2 (Sweetkind and others, 2017). The RC HSU was also split: the upper unit (RC1) was assigned as five-eighths of the total HSU thickness and the lower unit (RC2) is three-eighths of the total HSU thickness.

Each of the HSUs is lithologically heterogeneous, resulting in highly variable hydraulic properties (Nickerson, 1989; Haase and Lozinsky, 1992; Hawley and Kennedy, 2004). The published cross sections show the HSUs for the Santa Fe Group rocks divided into a series of lithofacies assemblages defined to represent geologic materials that likely have fairly

- A.** After Hawley and Kennedy, 2004; Santa Fe Group hydrostratigraphic unit (HSU) names followed by numeral 1 or 2, denoting piedmont or basinal depositional setting, respectively; two HSU names are shown divided by horizontal line where stratigraphic order is inferred but subsurface elevations are unknown; lithofacies codes shown in parentheses below HSU name; 1, basin-flow fluvial; 2, basin-floor fluvial and eolian; 3, basin-flow fluvial overbank; 5, distal to medial piedmont slope; 7, distal to medial piedmont slope, partly indurated; 8, proximal to medial piedmont slope, partly indurated; 9, basin-floor playa.

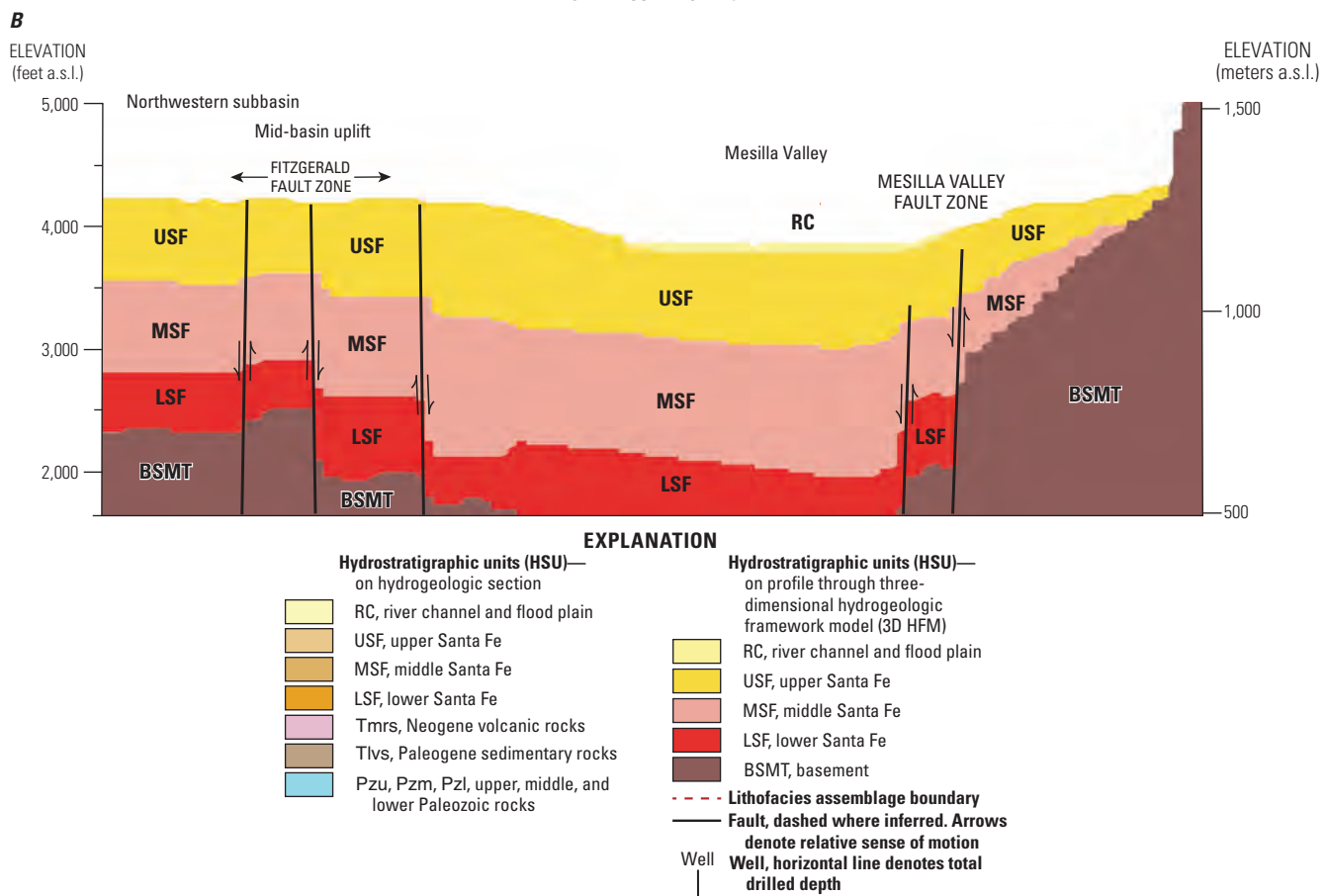
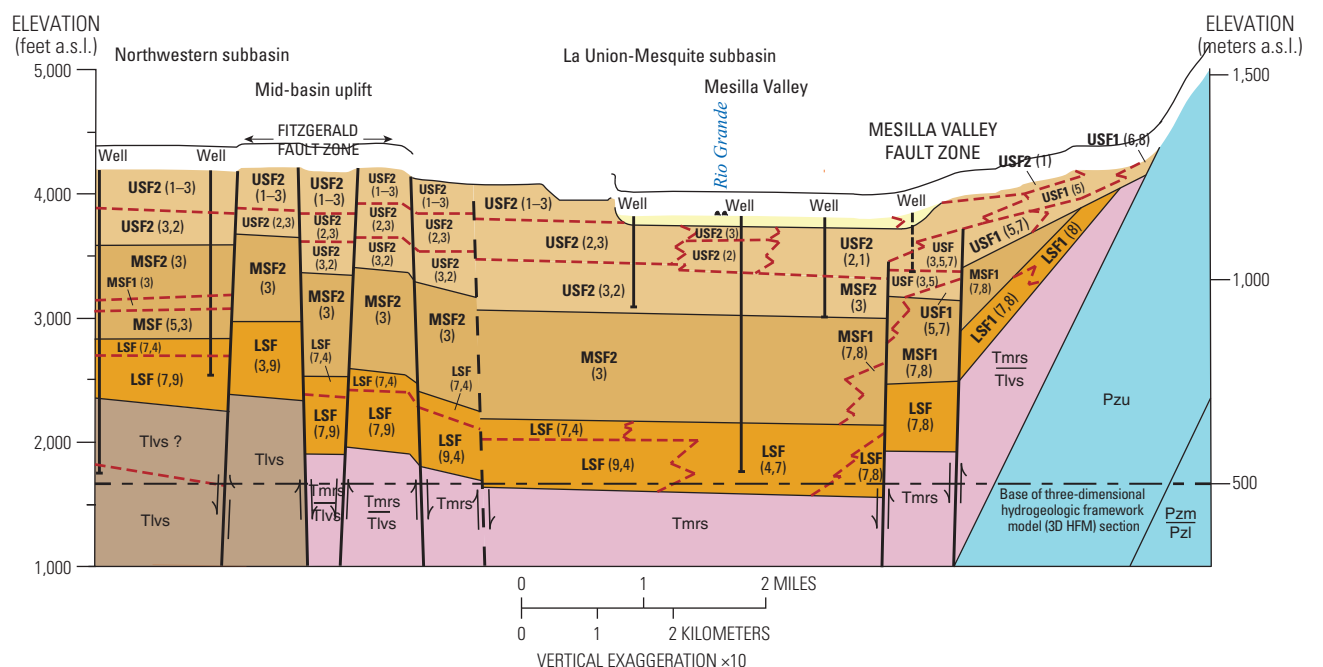


Figure 5. Example cross section within the model domain. **A**, Example of published geologic cross section showing hydrostratigraphic units and lithofacies designations. **B**, Profile cut through three-dimensional hydrogeologic framework model along same line of section. (a.s.l., above sea level)

uniform hydraulic properties (fig. 5A; Hawley and Lozinsky, 1992; Hawley and others, 2001, 2009; Hawley and Kennedy, 2004). The lithofacies assemblages were defined on the basis of grain size and sorting, degree of compaction, rock lithology and competency, degree of post-depositional alteration, and inferred environments of deposition (Hawley and others, 2001). Lithofacies-based zones within the 3D HFM are defined for the basin-fill deposits RC, USF, MSF, and LSF (table 1) and for BSMT, the pre-Santa Fe Group rocks (table 2). Zone definitions in the 3D HFM are based on the lithofacies assemblages of Hawley and others (2001), with slight changes in nomenclature to facilitate use within the numerical hydrologic model (tables 1 and 2).

Data Sources

Multiple sources of data were used to construct the 3D HFM in this report. Surface and subsurface data were used to define the top surface, thickness, and spatial distribution of each HSU. Data used as input to the 3D HFM included

- topographic data,
- geologic maps,
- cross sections,
- stratigraphic tops interpreted from borehole data,
- structure contour maps, and
- geophysical data.

Textural properties of the basin-fill deposits were derived from previously published cross-section interpretations (Hawley and Kennedy, 2004; Hawley and others, 2009).

Geologic Maps

Published geologic maps of the Mesilla basin (Hawley and Kennedy, 2004, plate 1), the Palomas and Jornada basins (Hawley and Kennedy, 2004, plate R1), and Hueco Bolson (Hawley and others, 2009, plate 1) were digitized within a geographic information system (GIS) and edge matched by the USGS during the Transboundary Aquifer Assessment Program (Alley, 2013). Larger-scale, nondigital geologic maps of parts of the study area (Seager, 1981, 1995; Seager and others, 1976, 1987, 2008; Servicio Geológico Mexicano, 2011) were consulted but were not included in the digital compilation. A generalized geologic map of the study area (fig. 3) shows the results of this digital compilation, although in this figure numerous geologic units are grouped into broad age ranges.

A hydrogeologic map was created from the digital geologic map by using a GIS to merge the mapped stratigraphic units into the five HSUs described above. Digital datasets of HSU extent and top elevation were created by merging map polygons from the hydrogeologic map with topographic

information. Outcrop areas for each HSU were sampled at regularly spaced points within a GIS. These points were assigned coordinate locations from the map base and elevations from a 1 arc-second (approximately 30-m resolution) digital elevation model (DEM) and exported as a series of files, one for each stratigraphic unit, containing x, y, and z coordinates, which were subsequently used in gridding the stratigraphic unit tops.

Cross Sections

Published hydrogeologic cross sections (fig. 6) depicting interpreted subsurface relations in the Mesilla basin (Hawley and Kennedy, 2004, plates 3 and 4), Palomas and Jornada basins (Hawley and Kennedy, 2004, plates R4 and R5), and Hueco Bolson (Hawley and others, 2009, plate 2) were fundamental as data input to the 3D HFM. Figure 5A is an example of a published cross section (Hawley and Kennedy, 2004, section G-G') showing the typical level of geologic detail present on these sections. Each published section shows the elevation and thickness of each HSU; the interpreted lithologic facies patterns (shown on the sections as lithofacies codes); and the location, sense, and magnitude of fault offset (fig. 5A). A cross section cut through the digital 3D HFM at the same location (fig. 5B) is discussed later in this report.

The elevation of the tops of HSUs shown on all published cross sections were extracted as horizontal (x, y) and elevation (z) coordinates at selected points along each section trace. A scanned image of each published cross section was scaled and georeferenced in a GIS along the cross-section trace (fig. 6). Points were digitized along each section trace, and the elevation of the top surface of each HSU represented in cross section was interpolated from the cross-section vertical scale. A series of files containing x, y, and z coordinates for each HSU horizon was exported.

Faults

Faults in the 3D HFM (fig. 4) were compiled from the following published sources: Figuers (1987), Imana (2002), Khatun (2003), Hawley and Kennedy (2004), Khatun and others (2007), Hawley and others (2009), and Servicio Geológico Mexicano (2011).

Cross sections in the Mesilla basin (Hawley and Kennedy, 2004, plates 3 and 4), Palomas and Jornada basins (Hawley and Kennedy, 2004, plate R4 and R5), and Hueco Bolson (Hawley and others, 2009, plate 2) provide fault location, sense, magnitude, and units offset (fig. 5A). Structure contour maps showing the elevation of the base of the Santa Fe Group (the top of pre-Santa Fe Group basement rocks) portray the traces of faults within the basin, including faults that do not cut surficial units (Hawley and Kennedy, 2004, plates 7 and R3; Alley, 2013). Fault locations were compared to the Quaternary fault and fold database of the United States (U.S. Geological Survey and New Mexico Bureau of Mines and Mineral Resources, 2006) and adjusted where necessary.

12 Three-Dimensional Hydrogeologic Framework Model of the Rio Grande Transboundary Region, USA and Mexico

Table 1. Zone definitions for river channel (RC), lower Santa Fe (LSF), middle Santa Fe (MSF), and upper Santa Fe (USF) Group hydrostratigraphic units used in three-dimensional hydrogeologic framework model.

Zone code	Lithofacies; dominant depositional setting	Lithology, sediment texture	Occurrence	Equivalent Hawley facies designation
10	River-valley, fluvial—basal channel deposits	Pebble to cobble gravel and sand	Axial parts of RC unit	a1
15	Basin-floor fluvial plain	Sand and pebble gravel, lenses of silty clay	Common in USF	1
20	River-valley, fluvial—Braided plain, channel deposits	Sand and pebbly sand	Adjacent to axis of RC unit	a2
25	Basin-floor fluvial, locally eolian	Sand; lenses of pebble sand, and silty clay	Common in USF	2
30	River-valley, fluvial—Overbank, meander-belt, oxbow deposits	Silty clay, clay, and sand	Adjacent to axis of RC unit	a3
35	Basin-floor, fluvial-overbank fluvial-deltaic and playa-lake; eolian	Interbedded sand and silty clay; lenses of pebbly sand	Major component of middle Santa Fe hydrostratigraphic unit, and minor constituent of unit upper Santa Fe: sand, pebbly sand and silty sand beds form a major part of the medial aquifer system	3
40	Eolian, basin-floor alluvial	Sand and sandstone; lenses of silty sand to clay	Major component of lower Santa Fe hydrostratigraphic unit; sand and silty sand beds form a large part of deep aquifer system in LSF	4
50	Distal to medial piedmont-slope, alluvial fan	Gravel, sand, silt, and clay; common loamy (sand-silt-clay)	Component of both the USF and MSF hydrostratigraphic units; clean to loamy sand and gravel lenses form parts of the medial and upper aquifer system	5
51	River-valley, fluvial—terrace deposits, arroyo channels, reworked distal alluvial fan	Sand, gravel, silt, and clay	Margins of RC deposit and in small upland drainages	b
55	Distal to medial piedmont-slope, alluvial fan	Partly indurated gravel, sand, silt, and clay; common loamy (sand-silt-clay)	Major component of LSF hydrostratigraphic unit; weakly-cemented sand and gravel beds form part of the deep aquifer system	7
60	Proximal to medial piedmont-slope, alluvial-fan	Coarse gravelly, loamy sand and sandy loam; lenses of sand and cobble to boulder gravel	Component of both the USF and MSF hydrostratigraphic units; clean to loamy sand and gravel lenses form parts of the medial and upper aquifer system	6
65	Proximal to medial piedmont-slope, alluvial-fan	Partly indurated coarse gravelly, loamy sand and sandy loam; lenses of sand and cobble to boulder gravel	Minor component of all the SF Group hydrostratigraphic units; weakly-cemented sand and gravel beds form part of the upper, medial, and deep aquifer systems	8
90	Basin-floor—alluvial flat, playa, lake, and fluvial-lacustrine; distal-piedmont alluvial	Silty clay interbedded with sand, silty sand and clay	Makes up fine-grained part of MSF hydrostratigraphic unit; sand and silty beds form very minor to negligible component of the medial aquifer system.	9
100	Basin-floor—alluvial flat, playa, lake, with evaporite processes	Silty clay interbedded with sand, silty sand and clay with gypsumiferous and alkali-impregnated zones	Major component of LSF hydrostratigraphic unit; weakly-cemented sand and gravel beds form a very minor to negligible component of the deep aquifer system	10
0	This code is used for units that have been eroded at the upper surface of the model and are absent, with a normal stratigraphic sequence of older units present			
999	This code is used where a unit is absent within the stratigraphic stack and was given an arbitrary thickness of 5 feet. Zone code is intended to be a pass-through; no lithologic significance is implied.			

Table 2. Zone definitions for pre-Santa Fe Group basement (BSMT) hydrostratigraphic unit used in three-dimensional hydrogeologic framework model.

Zone code	Rock unit
Bedrock units	
10	Precambrian rocks, undivided
20	Lower and middle Paleozoic, primarily carbonate rocks
30	Pennsylvanian and Permian rocks
40	Cretaceous rocks
Tertiary sediments	
50	Lower Eocene-Paleocene sedimentary rocks
55	Lower Tertiary volcaniclastic sedimentary rocks and andesite flows
Intrusive rocks	
60	Oligocene intermediate to silicic plutonic rocks
65	Lower Tertiary intermediate-composition volcanic rocks
Volcanic rocks	
70	Middle Tertiary silicic to intermediate composition lavas
73	Middle Tertiary silicic pyroclastic and volcaniclastic rocks
76	Middle to upper Tertiary basaltic-andesite lava flows

For use within a numerical hydrologic model, faults were classified according to their recency and the stratigraphic units that each fault offsets (fig. 4; Sweetkind and others, 2017). Fault recency describes the youngest HSU that the fault cuts completely. Fault recency was determined through comparison with the Quaternary fault and fold database of the United States (U.S. Geological Survey and New Mexico Bureau of Mines and Mineral Resources, 2006) and through inspection of the structural offset of each fault as shown on geologic cross sections (Hawley and Kennedy, 2004).

Fault lines were converted to a series of regularly spaced points which were assigned x and y coordinates and exported as a series of files. These files were used within horizon-gridding software to incorporate offsets in HSUs during the gridding process. For computational convenience and to maintain consistency with published interpretations (Hawley and Kennedy, 2004; Hawley and others, 2009), all faults in the study area were generalized as vertical boundaries.

Structure Contour Maps

Hawley and Kennedy (2004) published structure contour maps showing the elevation of the base of the Santa Fe Group (top of pre-Santa Fe Group basement rocks) for the Mesilla, Palomas, and Jornada structural basins. Structure contour maps showing the elevation of the base of the USF and MSF HSUs were created for the Mesilla basin in conjunction with the USGS during the Transboundary Aquifer Assessment Program (J. W. Hawley, HAWLEY GEOMATERS, written commun., 2011; Alley, 2013) and southern Palomas basin (this study) based on available surface and subsurface data.

Structure contour lines were digitized in a GIS and converted to a series of regularly spaced points, which were assigned horizontal coordinate locations from the map base and elevations from the contour elevation. A series of files that contained x, y, and z coordinates for each HSU horizon was exported.

Well Data

Hawley and Kennedy (2004) compiled well data from numerous sources that include subsurface intercepts of HSU tops for the Mesilla, Palomas, and Jornada basins. Well data from the Chihuahuan part of the Mesilla basin are from Servicio Geológico Mexicano (2011) and from well data compiled during the Transboundary Aquifer Assessment Program (Alley, 2013). Well data were incorporated during the drafting of the structure-contour maps for each HSU rather than used explicitly during horizon gridding. Well data were used as a check of the resultant gridded horizons.

Geophysical Data

Servicio Geológico Mexicano (2011) published the results of a high-resolution aeromagnetic survey and profiles based upon time-domain electromagnetic (TEM) soundings for the Chihuahuan part of the Mesilla basin. The aeromagnetic data were used in refining and interpreting the locations of faults in the southern part of the Mesilla basin; profiles from the TEM soundings were used to define the elevation of HSU tops along the line of profile. The locations of three faults near the west flank of the Franklin Mountains were based on modeling results of detailed gravity data (Imana, 2002; Khatun, 2003; Khatun and others, 2007) and an east-west seismic profile (Figuers, 1987).

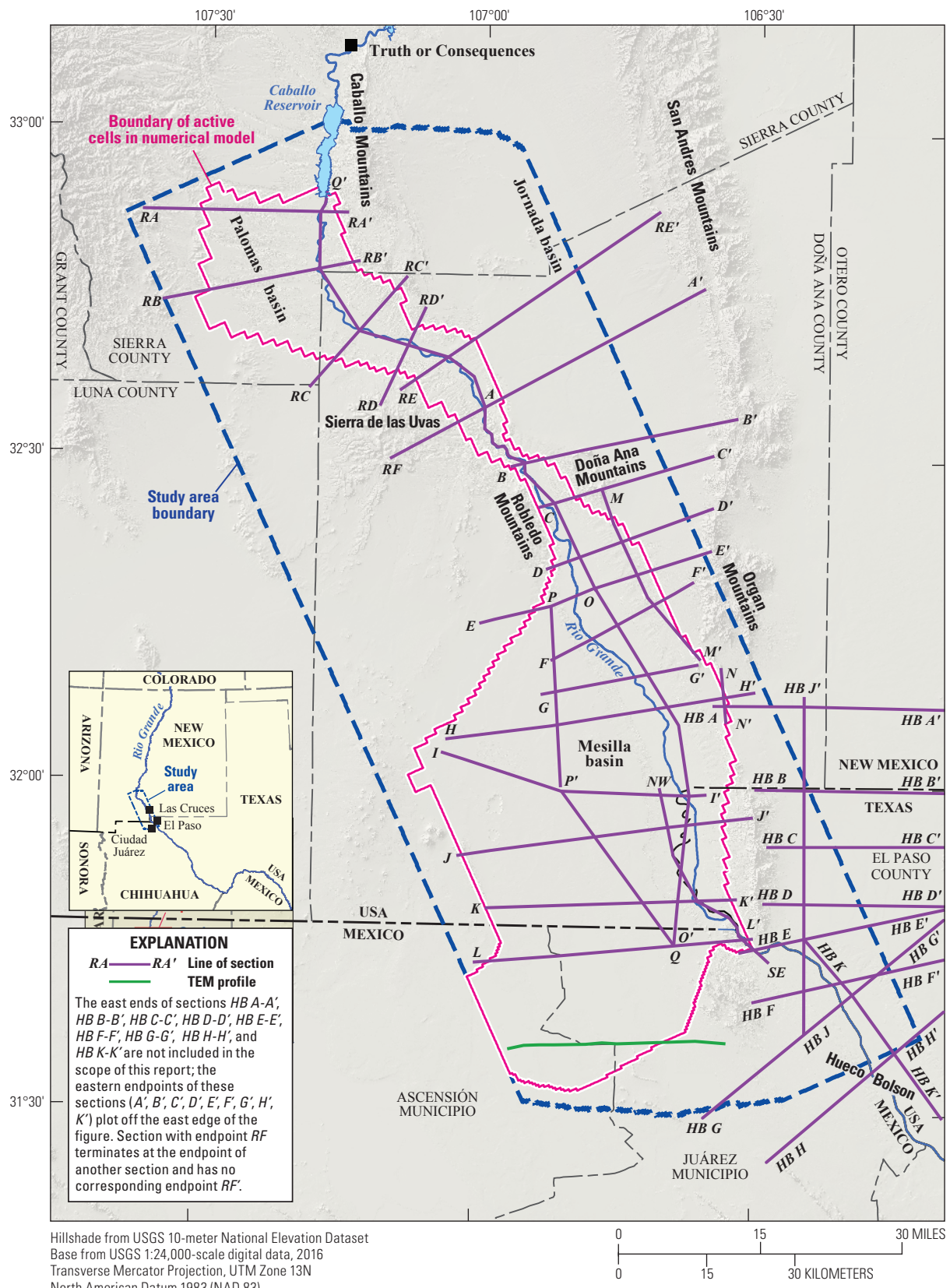


Figure 6. Map of Rio Grande transboundary region of New Mexico and Texas, USA, and northern Chihuahua, Mexico, showing study area and locations of published geologic cross sections used as input data for three-dimensional hydrogeologic framework model.

Modeling Methodology

A 3D HFM was constructed to represent the subsurface geometry, thickness, and structure of the hydrostratigraphic units RC, USF, MSF, LSF, and BSMT. This digital model provides the fundamental geologic framework for the subsequent development of a transient numerical hydrologic model of the study area (Randall Hanson, USGS, written commun., 2015). The 3D HFM is constructed through combining four digital framework elements:

- faults,
- elevation of the tops of each hydrostratigraphic unit,
- boundary lines depicting the subsurface extent of each HSU, and
- a digital representation of the distribution of sedimentary facies within each HSU.

The comprehensive hydrogeologic conceptualization of Hawley and Kennedy (2004) is the primary dataset used in the subsurface interpretations for the digital 3D HFM presented in this report.

The initial step in constructing the 3D HFM was extracting digital information from a variety of datasets, such as elevation models, geologic maps, borehole data, cross sections, and structure contour maps and combining them in a centralized geospatial database (fig. 7). Geologic data described in the previous sections and used as input to the 3D HFM were compiled using Environmental Science Research Institute (ESRI) ArcGIS™ software (fig. 7). Surfaces, or horizons, representing the elevation of the top of each HSU were created through interpolation of input data points into grids using Golden Software Surfer™ two-dimensional (2D) horizon gridding software (fig. 7). For efficient translation to the numerical hydrologic model, resultant gridded horizons representing the HSU tops were mapped to an x, y array of nodes representing the centroids of cells in the anticipated numerical hydrologic model (Sweetkind and others, 2017). The array of nodes is skewed to the northwest to support the anticipated focus of the numerical hydrologic model on the Mesilla and Palomas basins. The array of nodes for the entire study area represents almost 330,000 square grid cells that are 656 ft (200 m) in both x and y dimensions. Resultant dimensions of the array for the entire study area are 40.8 mi (328 grid cells) in the northeast-southwest direction and 113.3 mi (912 cells) in the northwest-southeast direction; the region of cells that will actively participate in the numerical hydrologic model occupy a much smaller region within the study area (fig. 1; Randall Hanson, USGS, written commun., 2015). Each node within the array is assigned multiple attributes representing the elevation of the top, thickness, and facies zone assignment for each HSU (Sweetkind and others, 2017).

The final 3D HFM was compiled from the gridded surfaces of HSU tops by stacking the individual gridded surfaces in stratigraphic order using Rockware Rockworks17™ three-dimensional (3D) modeling software (fig. 7). Unit thickness is represented by the difference between elevations of successive

stratigraphic tops, such that the elevation of the base of a unit is always equal to the elevation of the top of the unit directly below it in the stacking order. The 3D HFM is calculated as a cell-based solid model where the 3D volume is populated by volume elements, called voxels, that completely define each model-generated HSU at all points in space, filling the volume defined by the HSUs extent, top, and base. Each voxel has a defined x, y, z location at its center and is assigned an attribute that corresponds to a HSU name based upon the location of each voxel with respect to the gridded HSU surfaces.

Creation of Top Surfaces of the Major Hydrostratigraphic Units

Construction of the 3D HFM began with the stacking of gridded surfaces representing the elevation of the top of each HSU. Because of the requirement for grids to be continuous, in some x, y locations stratigraphically lower units are exposed at land surface, and corresponding grid cells in all overlying units are forced to have the same land-surface elevation and zero thickness at those x, y locations. Elevation and thickness for each HSU with respect to the elevations of other HSUs in the geologic framework model may be described by four general geometric cases (fig. 8):

1. The HSU of interest is present in the subsurface beneath other HSUs, such that the elevation of the HSU top is defined by geologic data or by the thickness of the overlying HSU and the thickness of the unit is defined by geologic data.
2. The HSU of interest crops out at land surface, such that the eroded top of the unit is defined by the digital elevation model and the thickness of the unit is defined by geologic data or, in the case of BSMT, as an arbitrary thickness.
3. The HSU of interest has been removed by erosion where an older HSU crops out at land surface. In this case, the grid representing the elevation of the top of the HSU of interest is assigned the land-surface elevation from the digital elevation model and assigned zero thickness.
4. The HSU of interest is absent in the subsurface because of the presence of an unconformity; for example, where HSU USF might directly overlie HSU BSMT with no intervening MSF or LSF HSUs. Within the subsurface modeling domain, computational requirements of the anticipated numerical hydrologic model require a non-zero thickness for every HSU. Therefore, in this special case, the HSU of interest is assigned an arbitrary thickness of 5 ft and the top of the underlying HSU is forced downward by 5 ft at those x, y locations (fig. 8).

Using the geometric rules described above, the elevations of the tops of the RC and USF HSUs were constructed using the digital elevation model and the digital geologic map, without gridding of geologic input data. Where RC exists within the incised floodplain of the Rio Grande, the top

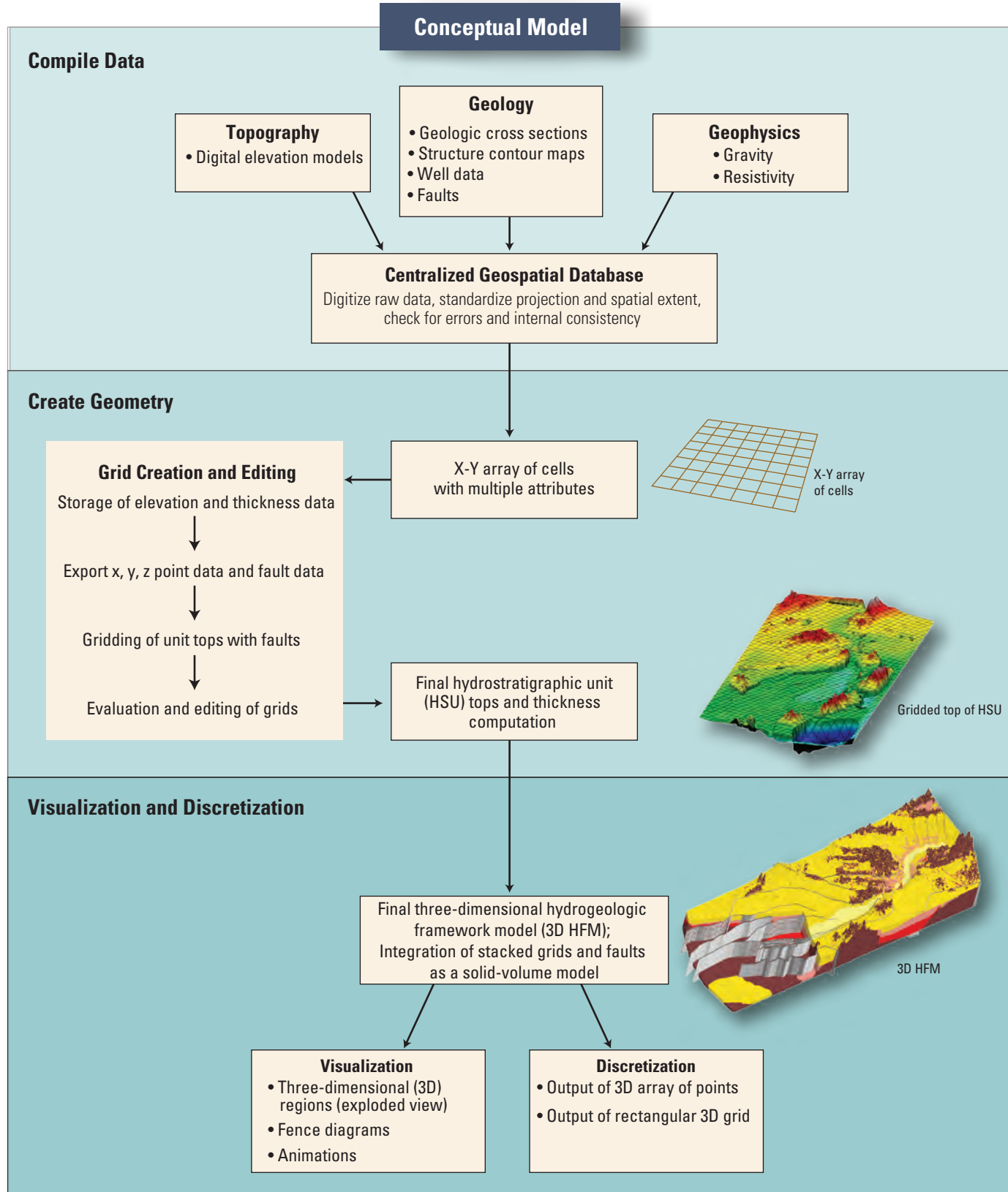


Figure 7. Chart showing process of development of digital data for the three-dimensional hydrogeologic framework model.

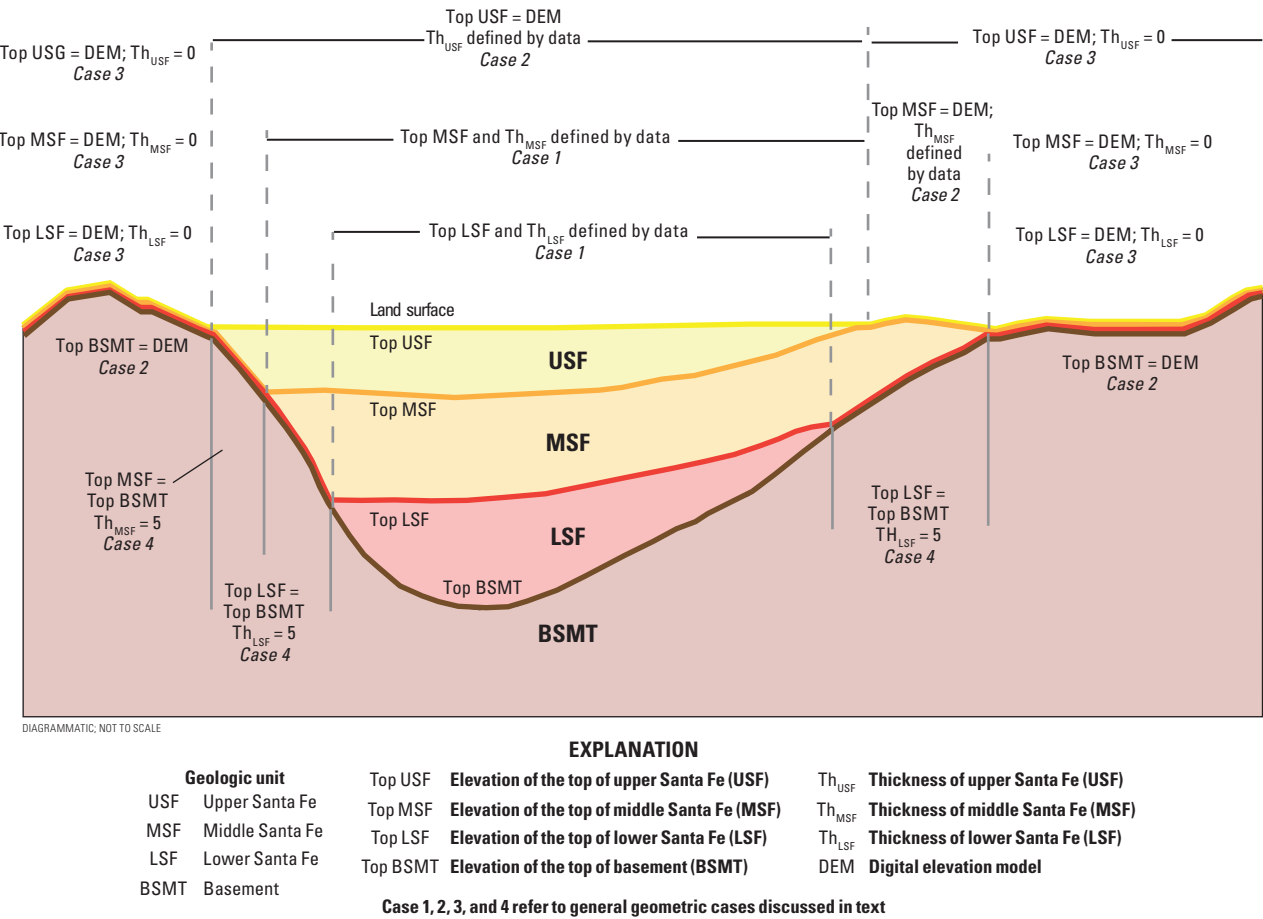


Figure 8. Diagrammatic cross section showing relative elevation of hydrostratigraphic unit tops and resultant thickness within the three-dimensional hydrogeologic framework model.

of RC is defined by land surface. Grid nodes within the unit extent of RC were assigned z values by sampling the digital elevation model at each cell centroid location. Outside the RC unit extent boundary, cells were assigned an arbitrary null value of -99999. The base of the fluvial deposits of RC is interpreted to be about 80 ft below the inner-valley floor, based on analyses of well driller's logs and borehole geophysical logs (Nickerson, 1986, 1989). In the 3D HFM, RC was assigned a thickness of 80 ft and the base of RC was defined as 80 ft below land surface.

For the upper surface of USF, the elevation of the HSU top is everywhere defined by the digital elevation model except where the unit is overlain by RC, such that the top of USF is dependent on the thickness of RC. For those areas where USF crops out at land surface—identified by querying the digital geologic map—grid nodes were assigned z values by sampling the digital elevation model at each cell centroid location. For areas where HSUs that underlie USF crop out at land surface and USF is absent because of erosion, grid nodes were assigned z values by sampling the digital elevation model at each cell centroid location but the thickness of USF was set to zero (fig. 8). Where inferred to be present beneath RC, the top of USF was assigned as 80 ft below land surface elevation.

The upper surfaces of HSUs MSF, LSF, and BSMT were defined by gridding geologic data (fig. 9). Structure contour maps that were constructed from cross section and well data and depict the elevation of each HSU top (Hawley and Kennedy, 2004; Alley, 2013) were digitized in a GIS. Structure contour lines were digitized and then converted to a series of regularly spaced points which were assigned coordinate locations from the map base and elevations from the contour elevation (fig. 9). Outcrop areas of each HSU were sampled from the digital geologic map with points at a 500-ft x, y spacing, and points were assigned an elevation from a digital elevation model (fig. 9). For each HSU, data from structure contour lines and outcrops were combined and gridded using a minimum curvature contouring algorithm with square grid cells of 250-ft dimension in both the x- and y-direction, with no preprocessing to filter or decluster the data. Data were contoured using faults as two-dimensional boundaries that acted as a barrier to information flow during horizon gridding. Only those faults inferred to completely cut the HSU of interest were included during gridding. For example, in gridding HSU MSF, only those faults interpreted to cut USF or MSF were used; faults interpreted to cut only LSF or BSMT were not used. The resulting grids were clipped to a unit extent boundary interpreted from the geologic data. Where an

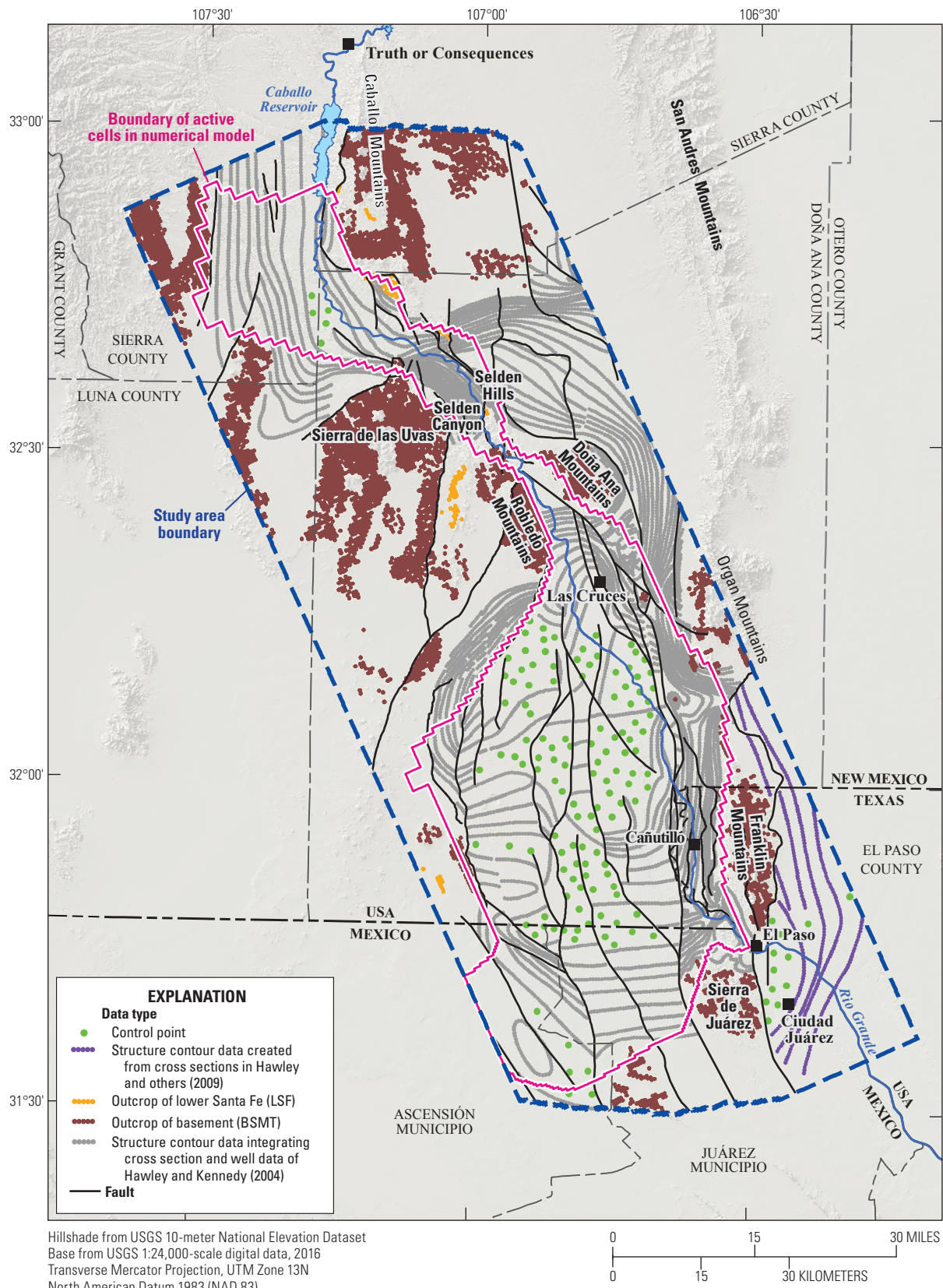


Figure 9. Map of Rio Grande transboundary region of New Mexico and Texas, USA, and northern Chihuahua, Mexico, showing the location and types of input geologic datasets used for gridding of top of lower Santa Fe (LSF) hydrostratigraphic unit in the three-dimensional hydrogeologic framework model.

HSU is present (model cell lies within the unit extent), the HSU has a defined elevation and thickness; where an HSU is absent in the 3D HFM (model cell lies outside of the unit extent polygon), thickness is zero and a null value of -99999 is used for the elevation of the unit and subunit tops for that cell.

Final gridded surfaces representing the tops of HSUs MSF, LSF, and BSMT were derived through an iterative process involving multiple cycles of grid creation, evaluation, and editing (fig. 7). Data control points were locally added to control gridding behavior in data-poor areas, at the margins of the grid domain, and adjacent to large-displacement faults where the absolute elevation change of the surface across a fault presented difficulties for the minimum curvature contouring routine (fig. 9). Locally, specific grid nodes were hand edited to remove gridding artifacts, grid overextrapolation, and to explicitly honor fault locations. Grids were edited or clipped to force HSU tops to be at or below land surface elevation and to ensure that the elevation of the top of each HSU was not higher than the bottom of an overlying HSU grid nor lower than the tops of underlying HSUs.

Modeling of Facies Variations for HSUs

The spatial variability of material properties for each HSU is represented using a number of hydrogeologic zones (tables 1 and 2). Zones were defined to represent geologic materials that likely have fairly uniform hydraulic properties and were derived from previously published interpretations of lithofacies assemblages (Hawley and Lozinsky, 1992; Hawley and others, 2001, 2009; Hawley and Kennedy, 2004). The hydrogeologic zonation presented for each HSU is intended as a starting point for assignment of horizontal hydraulic conductivity values to an HSU within the numerical hydrologic model (Randall Hanson, USGS, oral commun., 2015).

For the HSUs that represent Santa Fe Group rocks, lithofacies-based zones (table 1) were derived from lithofacies assemblages shown on previously published cross sections of the study area (Hawley and Kennedy, 2004, plates 3, 4, R4, and R5; Hawley and others, 2009, plate 2). A scanned image of each cross section was scaled and georeferenced in a GIS along the cross-section trace of the digital source map. In a GIS, polygons were drawn in map view that corresponded to lithofacies assemblages shown on each cross section, surface-mapped outcrops and faults were used as guides in the construction of polygons. The network of published sections (fig. 6) allowed for internal consistency checks between adjacent and crossing sections. The configuration of hydrogeologic zones for each HSU was also checked against published facies interpretations of Santa Fe Group rocks (Mack and others, 1994, 2006; Mack, 2004). The resultant hydrogeologic zones within the 3D HFM (table 1) are based on the previously defined lithofacies assemblages (Hawley and others, 2001), with slight changes in nomenclature to facilitate use within the numerical hydrologic model.

For RC, zonation (table 1) was based on interpretation of soil survey data from the Natural Resources Conservation Service for Doña Ana, Grant, and Luna Counties, New Mexico,

and El Paso County, Texas (U.S. Department of Agriculture, 2017). Reported soil textural classes were ranked by grain size and presence of clay into four general hydrogeologic categories (table 1) that are similar to previously published lithofacies zones (Hawley and others, 2001; Hawley and Kennedy, 2004):

- active river channel (gravels and sands of the river channel),
- braided plain (sands, gravels, and silts),
- overbank (clay dominated deposits), and
- reworked alluvial fan.

In a GIS, numerous small polygons from the original soil surveys were generalized into hydrogeologic zones based on dominant textural type and location (Sweetkind and others, 2017). Zonation was applied to only the upper subdivision RC1; RC2 was left unzoned because surficial soils data were not appropriate to use for the lower part of the unit and published cross sections do not include textural data for RC.

BSMT was subdivided into hydrogeologic zones based on lithology (table 2). In a GIS, polygons representing outcrops of all pre-Santa Fe Group rocks were displayed and classified. A scanned image of each published cross section was scaled and georeferenced in a GIS along the cross-section trace of the digital source map. In a GIS, basement lithology polygons were drawn in map view to be consistent with interpreted lithology shown on the cross sections and surface-mapped outcrops (table 2).

Elevation, Thickness, Unit Extent, and Facies Patterns of Hydrostratigraphic Units

This section presents the results of the construction of the subsurface geometry, including unit extent, elevation, and thickness, for each hydrostratigraphic unit. The spatial variability of interpreted depositional facies for each HSU is represented using hydrogeologic zones. The results presented here are available as a digital GIS dataset accessible at <https://doi.org/10.5066/F7JM27T6>.

River Channel (RC)

RC underlies the river-valley floor across the entire study area and fills the incised inner valley floodplain, which in places is as much as 5 mi wide (fig. 10). The floodplain alluvial deposits of RC range in thickness from 60 to 100 ft (Wilson and others, 1981; Nickerson, 1986, 1989); in the 3D HFM, the base of RC was defined as 80 ft below land surface (fig. 8). Throughout most of the study area, deposits of RC are incised into USF or, in the Palomas basin, into MSF. In Selden Canyon and El Paso narrows, the RC deposits are incised into pre-Santa Fe Group bedrock units with no intervening alluvial basin fill (fig. 3).

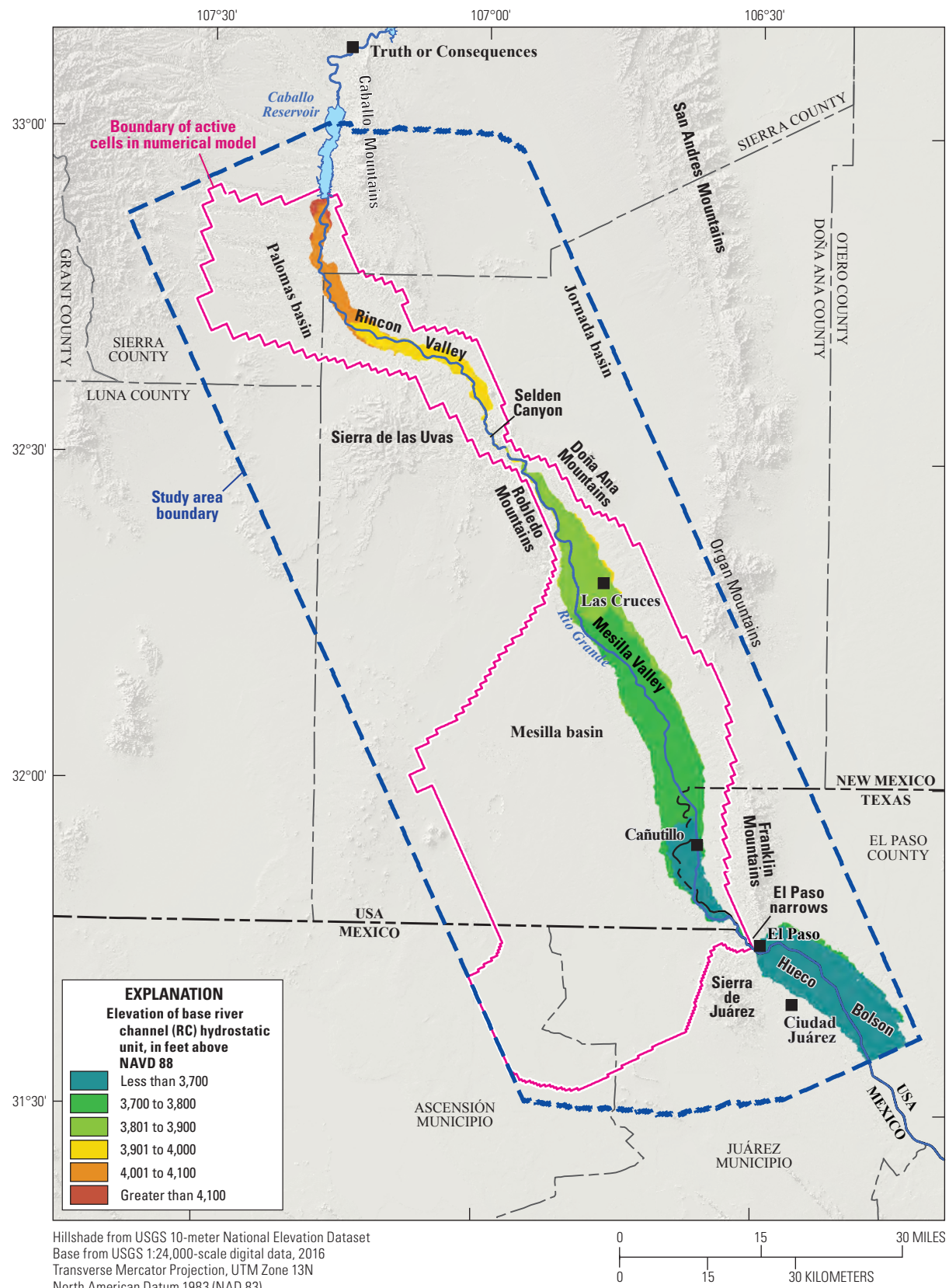


Figure 10. Map of Rio Grande transboundary region of New Mexico and Texas, USA, and northern Chihuahua, Mexico, showing elevation of base of river channel (RC) hydrostratigraphic unit used in the three-dimensional hydrogeologic framework model. (NAVD 88, North American Vertical Datum of 1988)

RC includes river-channel and overbank deposits consisting of poorly sorted gravel and coarse- to medium-grained sand with lenses of silt and clay (Wilson and others, 1981; Hawley and Kennedy, 2004). RC1 is divided into hydrogeologic zones on the basis of surficial soils data (fig. 11); the lower zone RC2 is undivided. Wilson and others (1981) report that the basal part of the floodplain alluvium is generally a layer of well-rounded siliceous gravel ranging from 20 to 40 ft in thickness.

Upper Santa Fe (USF)

The top of USF is at land surface except where overlain by RC (fig. 12). In the Palomas basin, USF is generally less than 250 ft thick and is absent where the Rio Grande has incised into MSF units (fig. 13). USF ranges in thickness in the Mesilla basin from less than 250 ft to as much as 1,250 ft east of the mid-basin high (fig. 13). USF thickness in the Mesilla basin and much of the Jornada basin is relatively thin when compared to USF in the adjacent Hueco Bolson, where it is greater than 1,500 ft thick (fig. 13; Hawley and others, 2009).

The pattern of facies zones in the upper part of USF (USF1, fig. 14) corresponds to the modern depositional setting of coarse-grained deposits along the Rio Grande, flanked by sandy basin floor fluvial plain deposits, both of which are inset into broad, distal to medial facies piedmont-slope and alluvial fan deposits. During the time period equivalent to the lower part of USF (fig. 15, USF2), the ancestral Rio Grande occupied a broad fluvial plain wider than the present topographic Mesilla Valley (Mack and others, 2006), resulting in thick sequences of medium-grained fluvial deposits that grade southward into finer-grained basin floor and lacustrine facies, flanked by narrow bands of piedmont-slope alluvium (fig. 15).

Middle Santa Fe (MSF)

MSF lies at very shallow depths beneath much of the Palomas and Jornada basins (fig. 16). MSF is deeper in the Mesilla basin, particularly to the east and west of the mid-basin high and along the Mesilla Valley fault zone (fig. 16). In the Mesilla basin, MSF ranges in thickness from less than 250 ft to about 1,000 ft, being thickest to the east and west of the mid-basin high, and thinning south of the international border (fig. 17). In contrast, both the Jornada and Palomas basins feature regions where MSF is 1,500 ft thick or more, providing evidence for a northwest-trending depositional trough present during MSF time (Mack and others, 1994; Mack, 2004). In the Jornada and Palomas basins, MSF is thickest against basin-bounding normal faults including the Jornada, Red Hills, and Derry faults (fig. 17) as a result of syntectonic deposition of MSF sediment (Mack and others, 1994; Mack, 2004).

In the Mesilla basin, MSF1 and MSF2 are dominated by basin-floor, fluvial-overbank, fluvial-deltaic, and playa-lake lithofacies (figs. 18 and 19, zones 35 and 90) consisting of fine-grained, interbedded sand and silt-clay beds up to 1,000 ft thick (Leggat and others, 1962). This sequence interfingers with

piedmont-slope alluvium within narrow bands on the east, west, and southern margins of the basin (figs. 18 and 19, zones 50 and 55). In Palomas basin, MSF1 is dominated by a thick sequence of fine-grained basin-floor sediments, including silty clay beds interbedded with evaporites (figs. 18 and 19, zones 90 and 100). These sediments represent deposition in restricted, closed-basin environments as a result of active uplift of surrounding mountain blocks (Mack and others, 1994; Mack, 2004).

Lower Santa Fe (LSF)

The elevation of the top of LSF (fig. 20) shows the Palomas basin as a half graben that dips eastward into the basin-bounding Derry and Red Hills faults, the Jornada basin dipping southwestward into the Jornada fault, and two subbasins within the Mesilla basin separated by the mid-basin high (fig. 20). LSF is thickest in the southern part of the Jornada basin and is as much as 1,000 ft thick on the eastern side of the Palomas basin and within the two subbasins of the Mesilla basin that flank the mid-basin high (fig. 21).

Lithofacies zones for LSF differ markedly between the Palomas and Mesilla basins (figs. 22 and 23). Active uplift of the Caballo Mountains resulted in the deposition of relatively coarse-grained piedmont-slope and alluvial fan deposits in the Palomas basin (figs. 22 and 23, zone 55; Mack and others, 1994; Mack, 2004). In contrast, uplifts bounding the Mesilla basin were distant, resulting in deposition of fine- to medium-grained fluvial-deltaic and playa-lake deposits (figs. 22 and 23, zones 90 and 100; Hawley and others, 2001; Hawley and Kennedy, 2004). On the east side of Mesilla basin, LSF includes a distinctive eolian sand facies (figs. 22 and 23, zone 40) that consists of as much as 600 ft of clean, fine to medium sand interpreted as paleo-dune deposits (Hawley and others, 2001; Hawley and Kennedy, 2004). These deposits form a productive aquifer zone at 1,000 to 1,500 ft depth in the Anthony-Cañutillo area (Leggat and others, 1962; Nickerson, 1989; Hawley and Kennedy, 2004). Similar deposits are present on the west flank of the Mesilla basin where eolian sands may be as thick as 1,000 ft (Hawley and Kennedy, 2004).

Basement (BSMT)

The elevation of the top of BSMT shows the three main structural basins (Palomas, Jornada, and Mesilla) between uplifts of pre-Santa Fe Group rocks (fig. 24). The zonation of BSMT (fig. 25) is based on published cross sections (Hawley and Kennedy, 2004; Hawley and others, 2009) and include data from deep drill holes (Gross and Ierman, 1983; Seager and others, 1987; Woodward and Myers, 1997). Drill hole data from the center part of the Mesilla basin support the interpretation that Neogene volcanic and volcaniclastic rocks underlie Santa Fe Group rocks beneath most of the basin (Seager and others, 1987; Hawley and Kennedy, 2004). Santa Fe Group HSUs are interpreted to overlie Precambrian, Paleozoic, and Cretaceous rocks adjacent to the Caballo, Robledo, East Potrillo, and Franklin Mountains and Sierra de Juarez (fig. 25; Hawley and Kennedy, 2004).

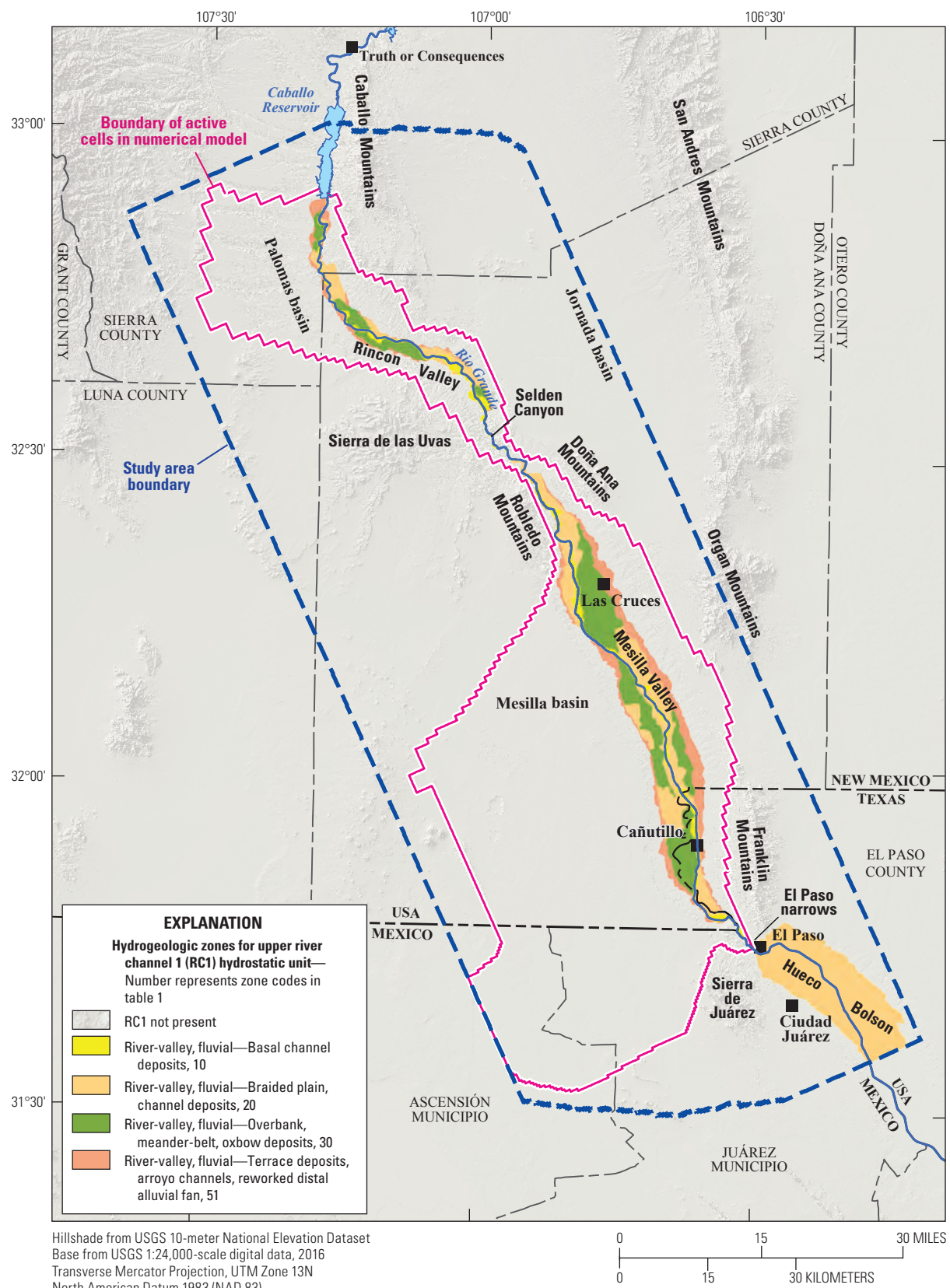


Figure 11. Map of Rio Grande transboundary region of New Mexico and Texas, USA, and northern Chihuahua, Mexico, showing zone codes for upper part of river channel (RC1) hydrostratigraphic unit used in the three-dimensional hydrogeologic framework model.

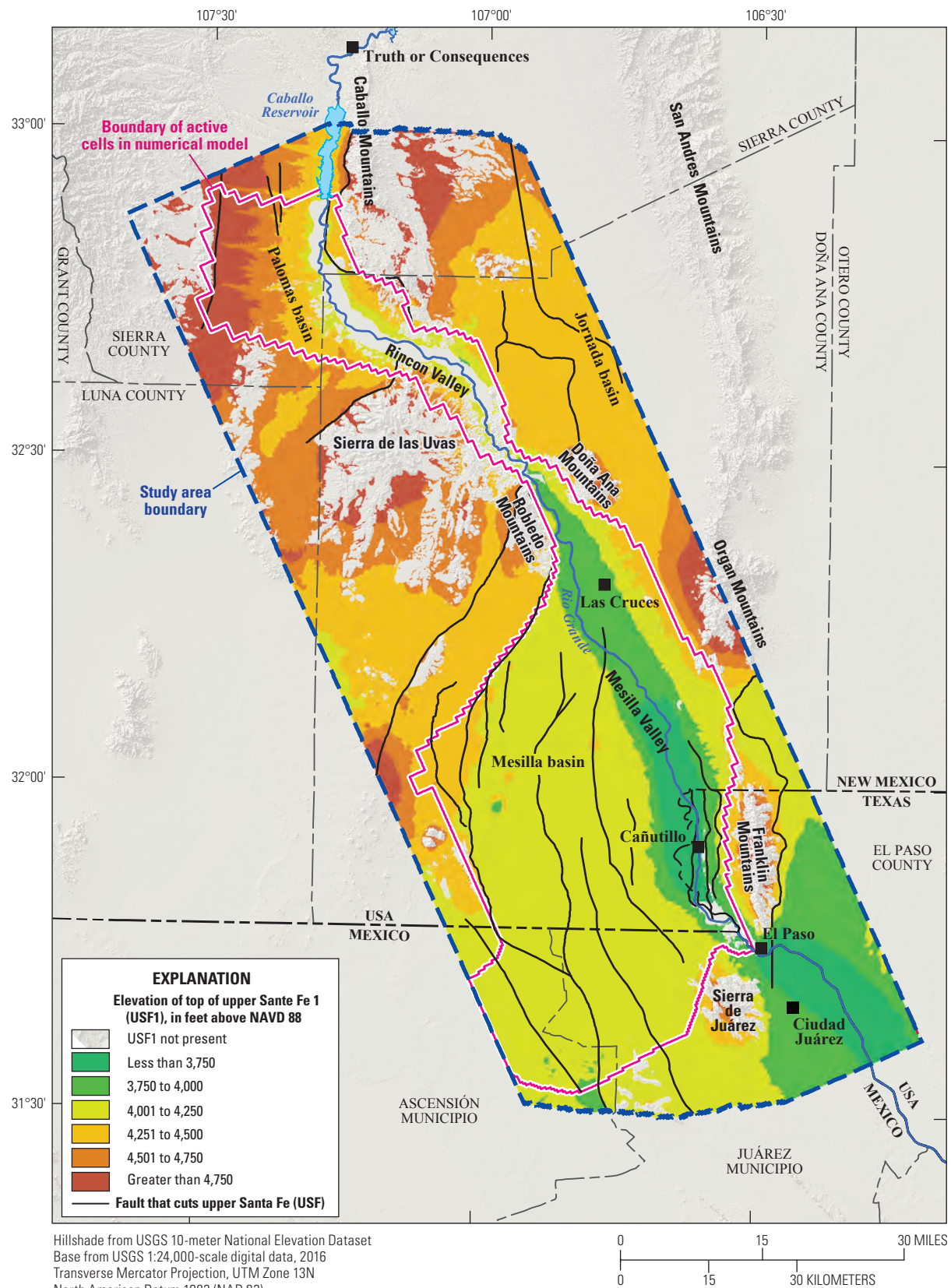


Figure 12. Map of Rio Grande transboundary region of New Mexico and Texas, USA, and northern Chihuahua, Mexico, showing gridded elevation of top of upper Santa Fe (USF) hydrostratigraphic unit as used in the three-dimensional hydrogeologic framework model. (NAVD 88, North American Vertical Datum of 1988)

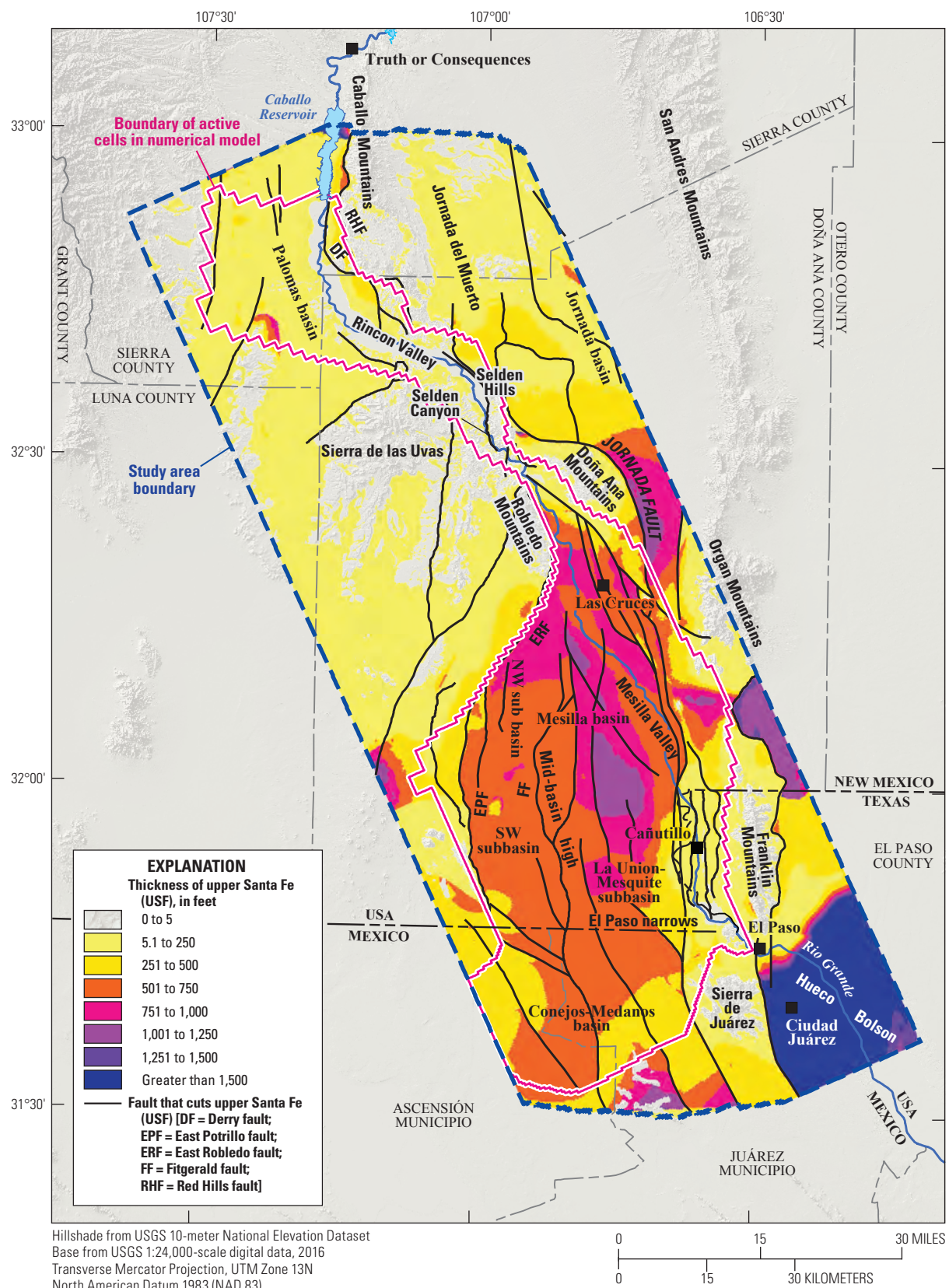


Figure 13. Map of Rio Grande transboundary region of New Mexico and Texas, USA, and northern Chihuahua, Mexico, showing gridded thickness of upper Santa Fe (USF) hydrostratigraphic unit as used in the three-dimensional hydrogeologic framework model. (NW, northwest; SW, southwest)

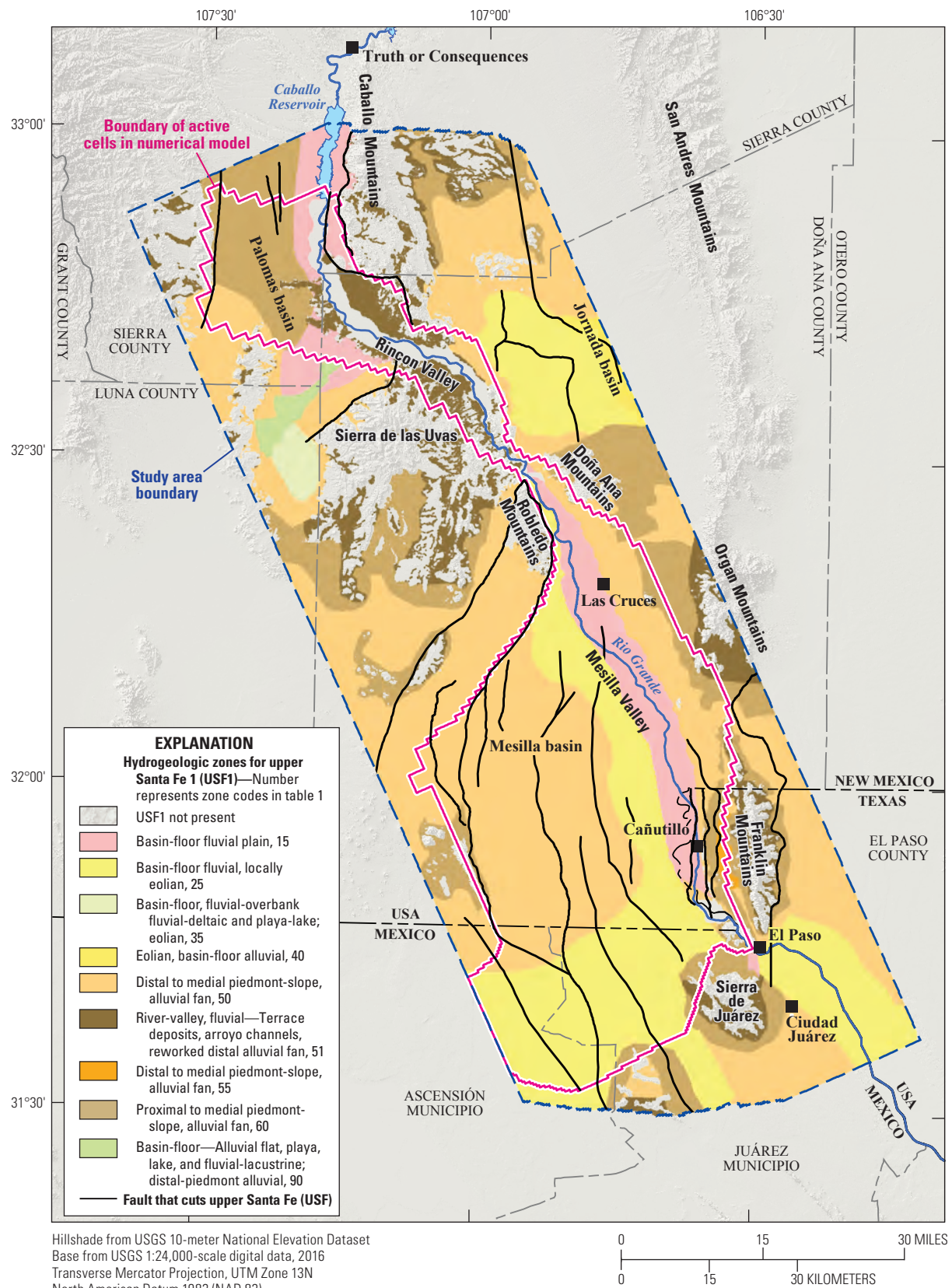


Figure 14. Map of Rio Grande transboundary region of New Mexico and Texas, USA, and northern Chihuahua, Mexico, showing zone codes for upper part of upper Santa Fe hydrostratigraphic unit (USF1) as used in the three-dimensional hydrogeologic framework model.

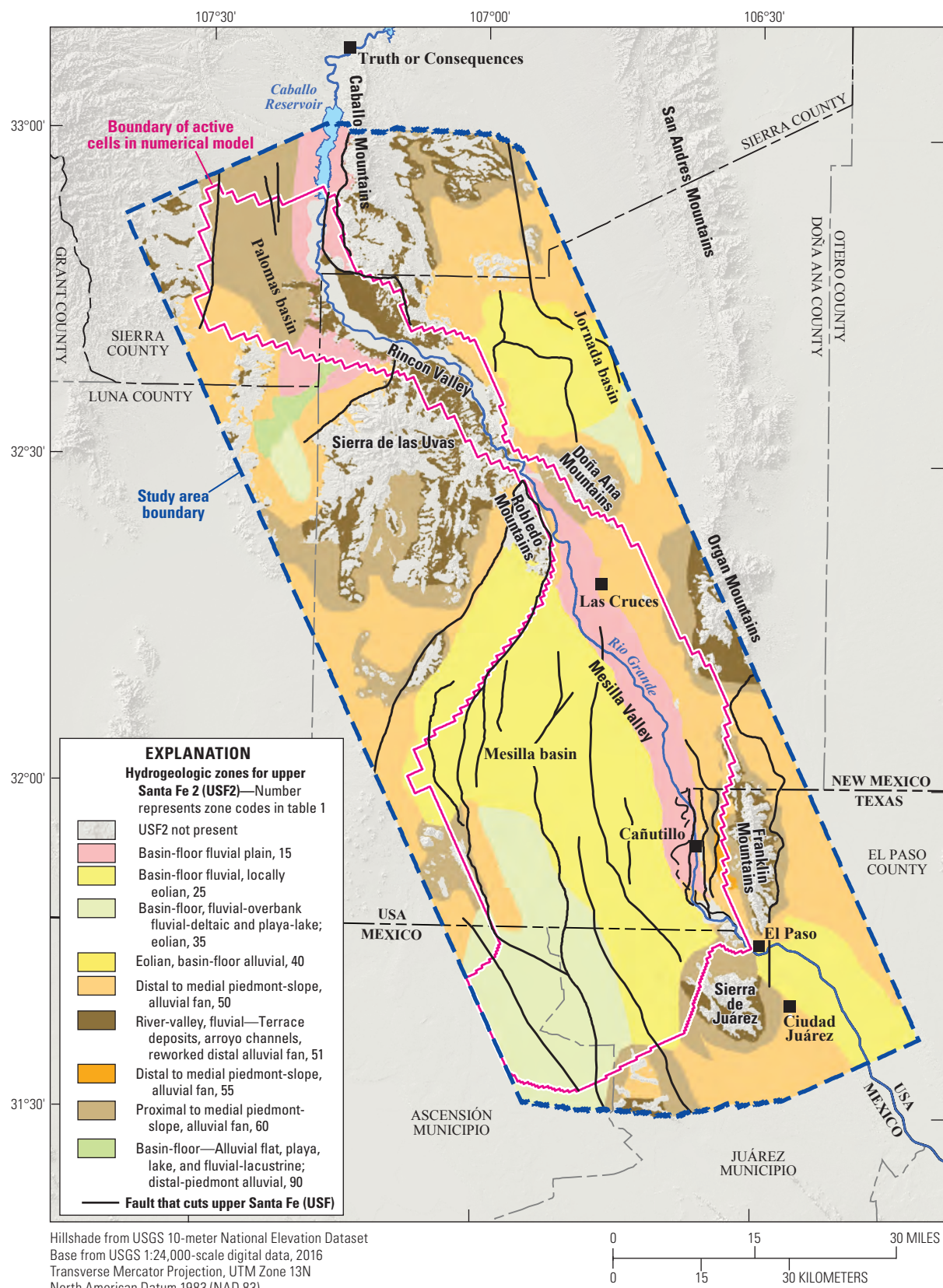


Figure 15. Map of Rio Grande transboundary region of New Mexico and Texas, USA, and northern Chihuahua, Mexico, showing zone codes for lower part of upper Santa Fe hydrostratigraphic unit (USF2) as used in the three-dimensional hydrogeologic framework model.

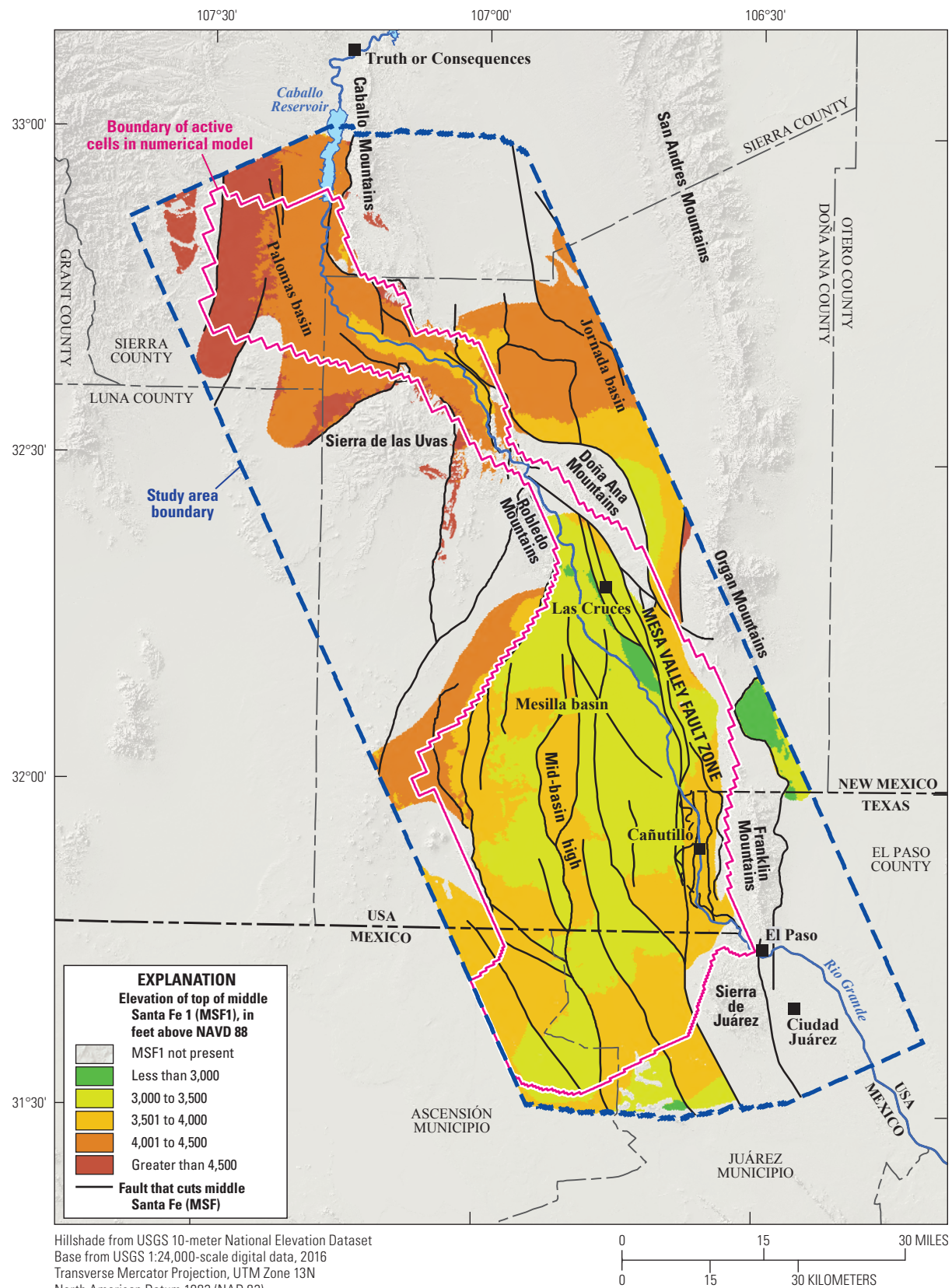


Figure 16. Map of Rio Grande transboundary region of New Mexico and Texas, USA, and northern Chihuahua, Mexico, showing gridded elevation of top of middle Santa Fe (MSF) hydrostratigraphic unit as used in the three-dimensional hydrogeologic framework model. (NAVD 88, North American Vertical Datum of 1988)

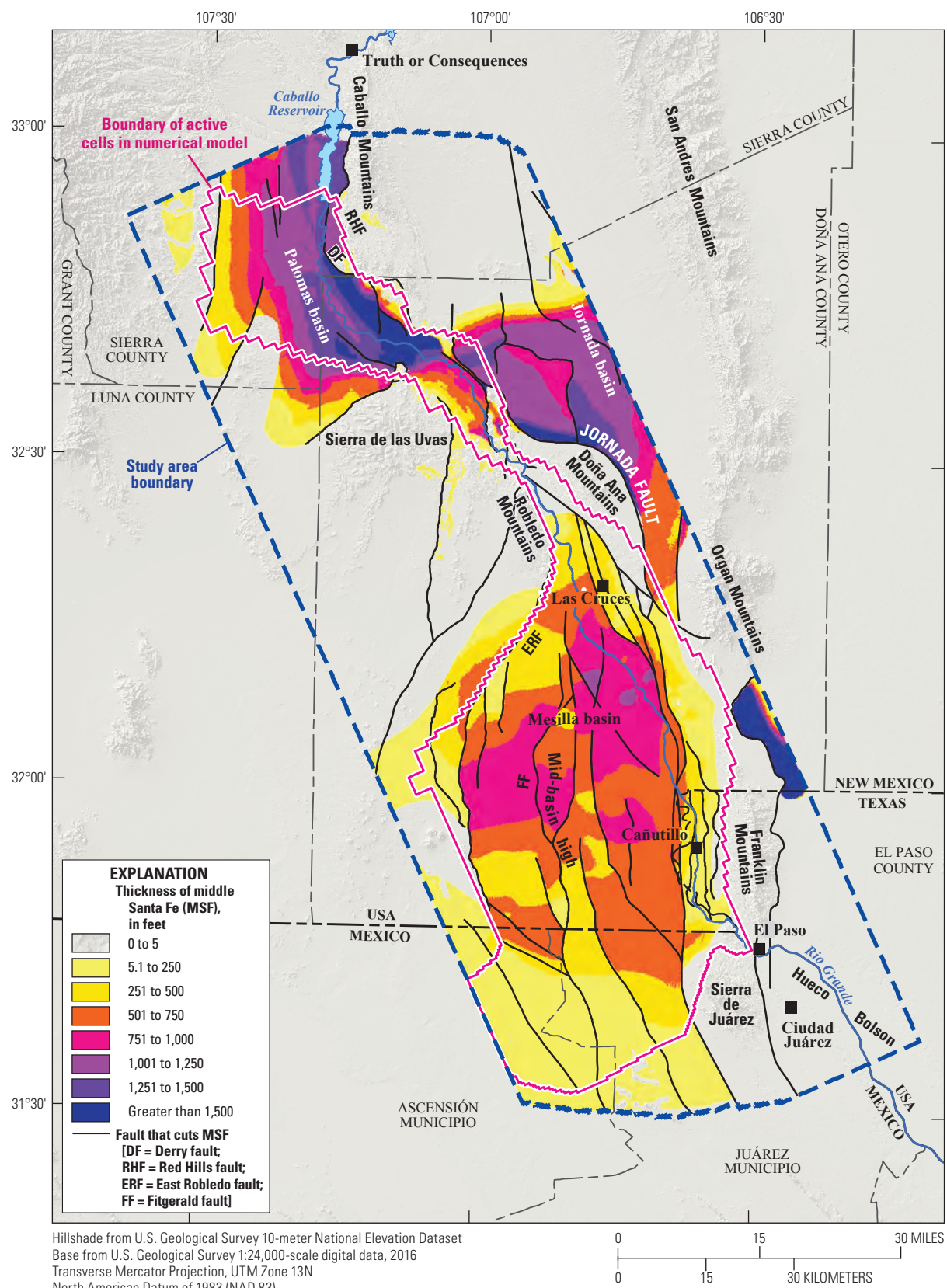


Figure 17. Map of Rio Grande transboundary region of New Mexico and Texas, USA, and northern Chihuahua, Mexico, showing gridded thickness of middle Santa Fe (MSF) hydrostratigraphic unit as used in the three-dimensional hydrogeologic framework model.

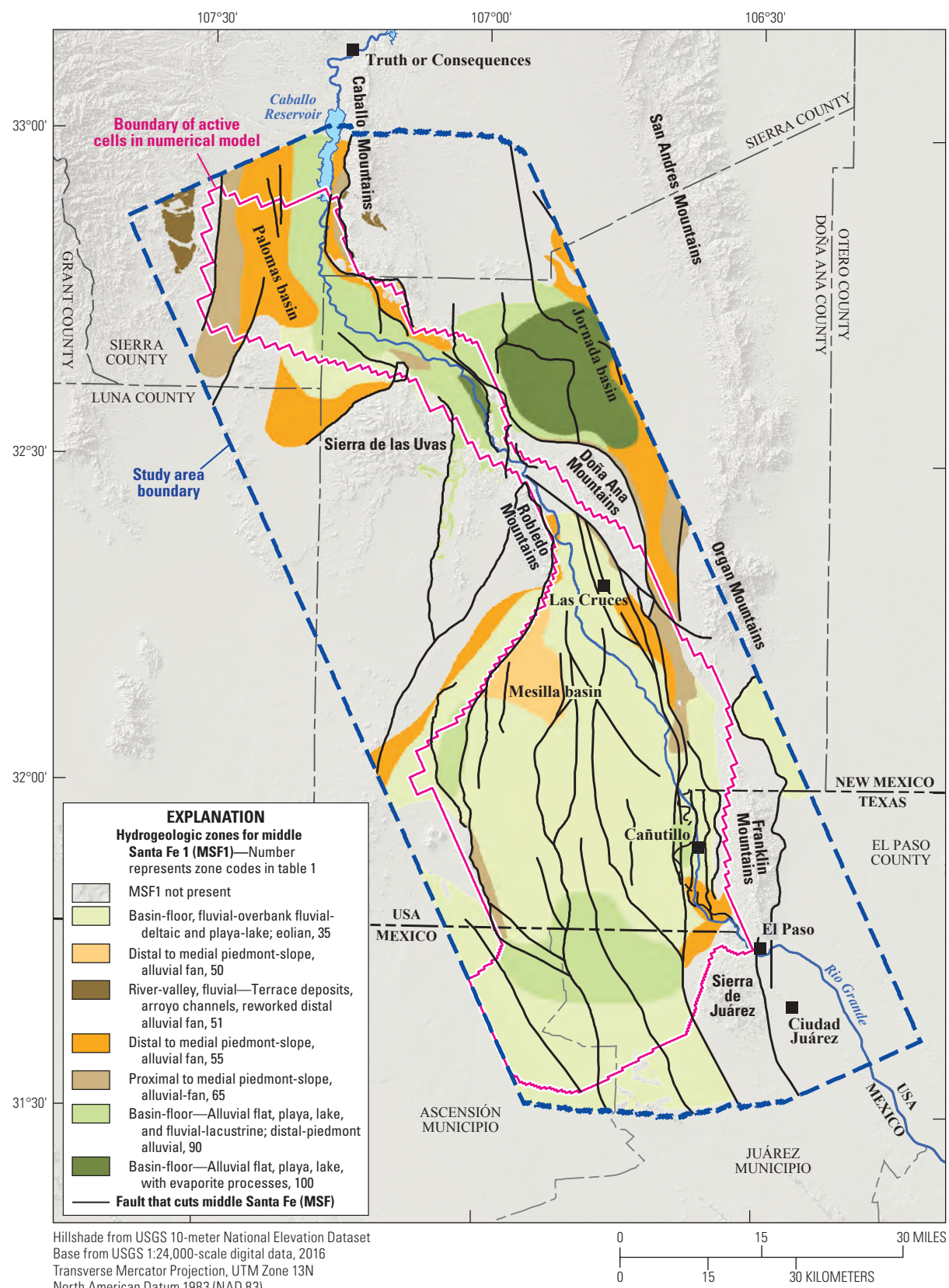


Figure 18. Map of Rio Grande transboundary region of New Mexico and Texas, USA, and northern Chihuahua, Mexico, showing zone codes for upper part of middle Santa Fe hydrostratigraphic unit (MSF1) as used in the three-dimensional hydrogeologic framework model.

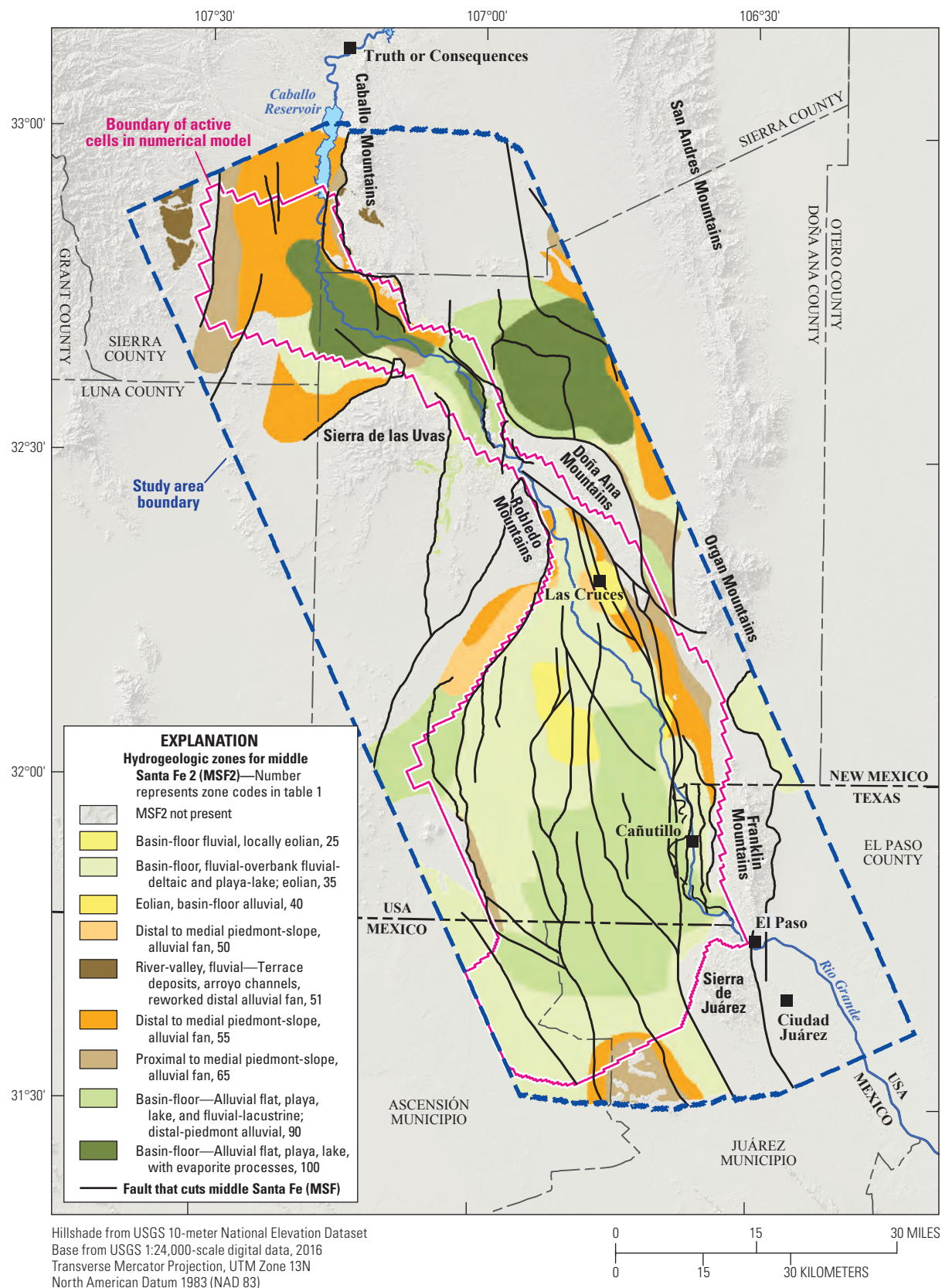


Figure 19. Map of Rio Grande transboundary region of New Mexico and Texas, USA, and northern Chihuahua, Mexico, showing zone codes for lower part of middle Santa Fe hydrostratigraphic unit (MSF2) as used in the three-dimensional hydrogeologic framework model.

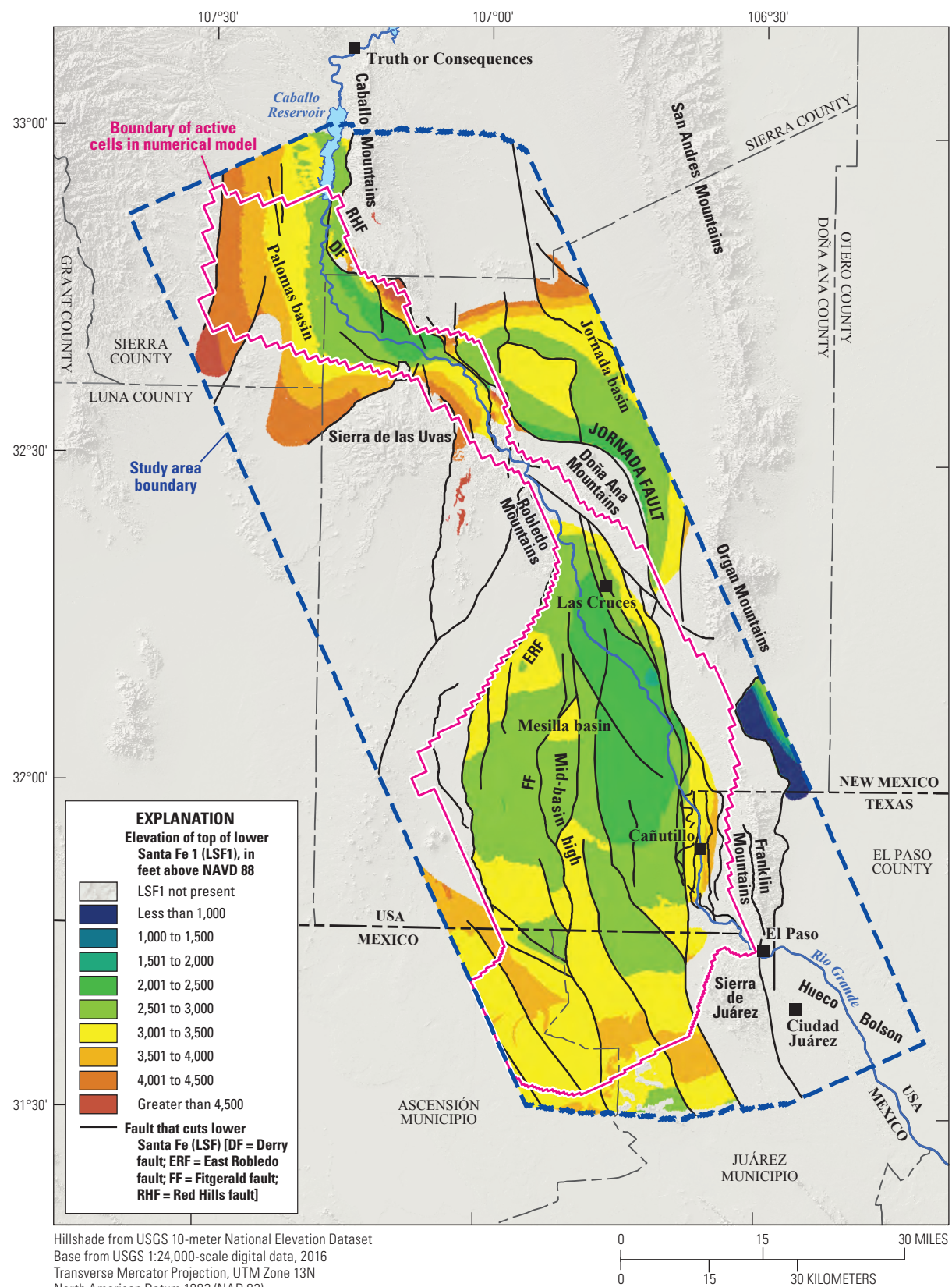


Figure 20. Map of Rio Grande transboundary region of New Mexico and Texas, USA, and northern Chihuahua, Mexico, showing gridded elevation of top of lower Santa Fe (LSF) hydrostratigraphic unit as used in the three-dimensional hydrogeologic framework model. (NAVD 88, North American Vertical Datum of 1988)

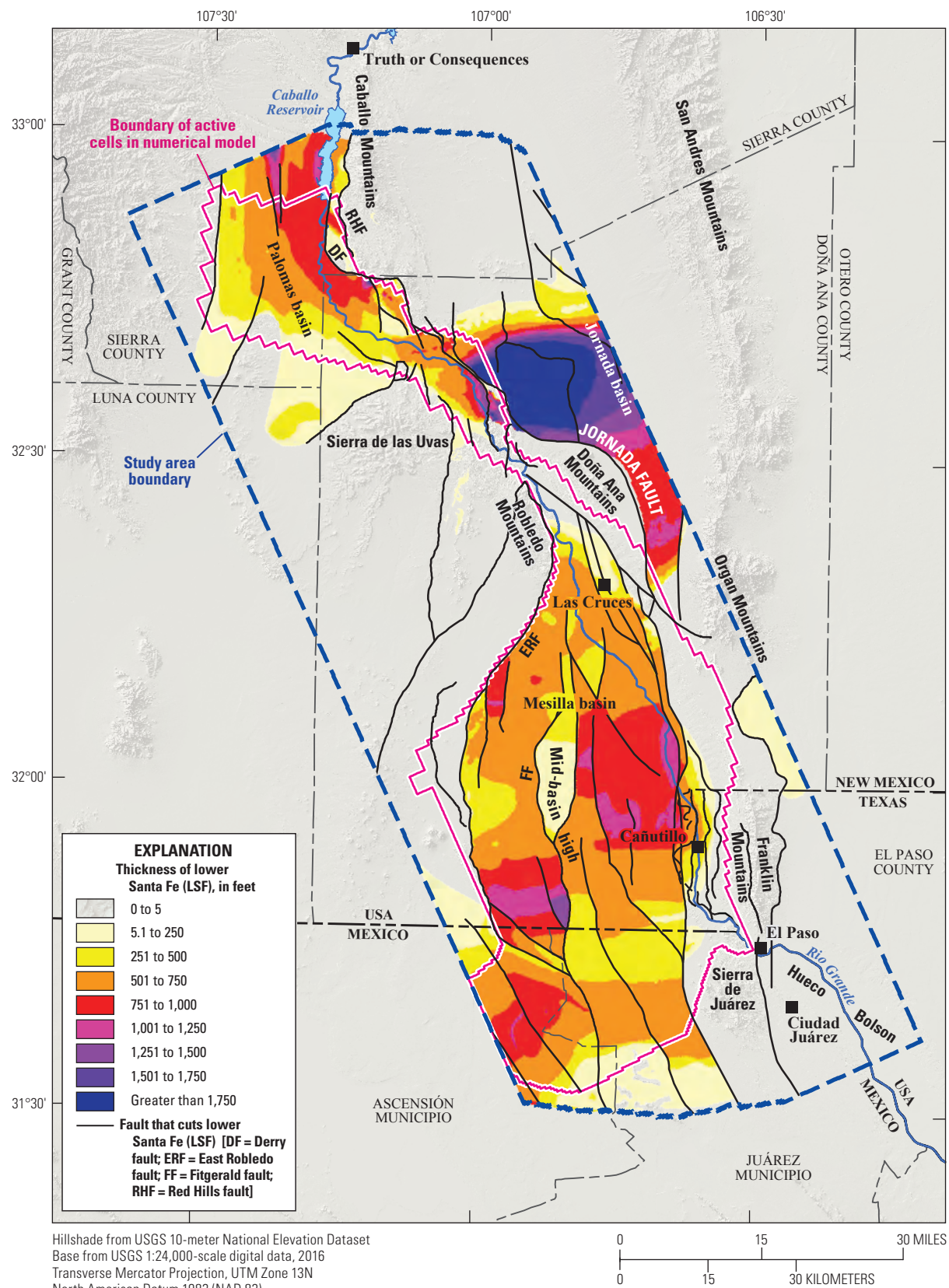


Figure 21. Map of Rio Grande transboundary region of New Mexico and Texas, USA, and northern Chihuahua, Mexico, showing gridded thickness of lower Santa Fe (LSF) hydrostratigraphic unit as used in the three-dimensional hydrogeologic framework model.

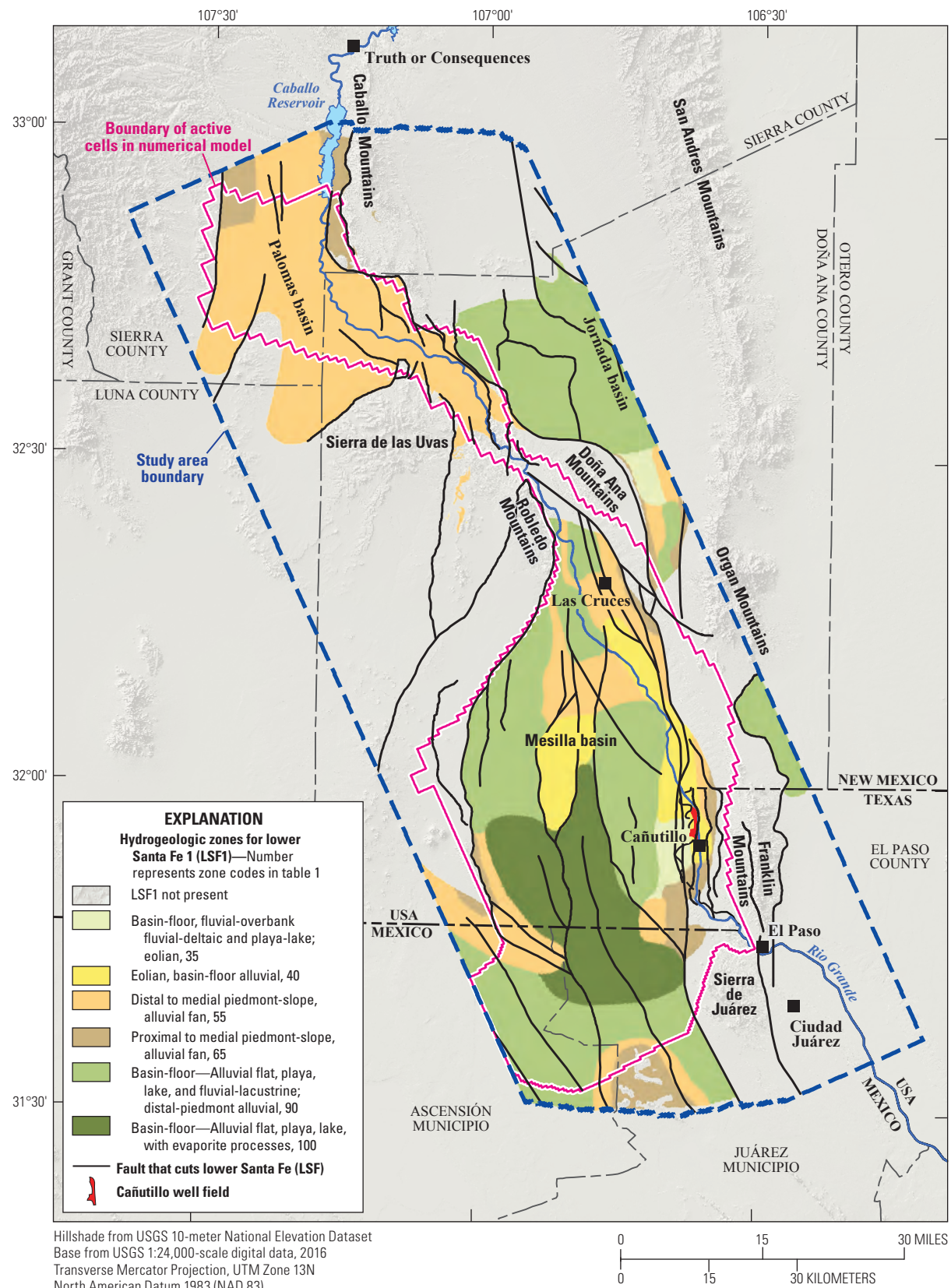


Figure 22. Map of Rio Grande transboundary region of New Mexico and Texas, USA, and northern Chihuahua, Mexico, showing zone codes for upper part of lower Santa Fe hydrostratigraphic unit (LSF1) as used in the three-dimensional hydrogeologic framework model.

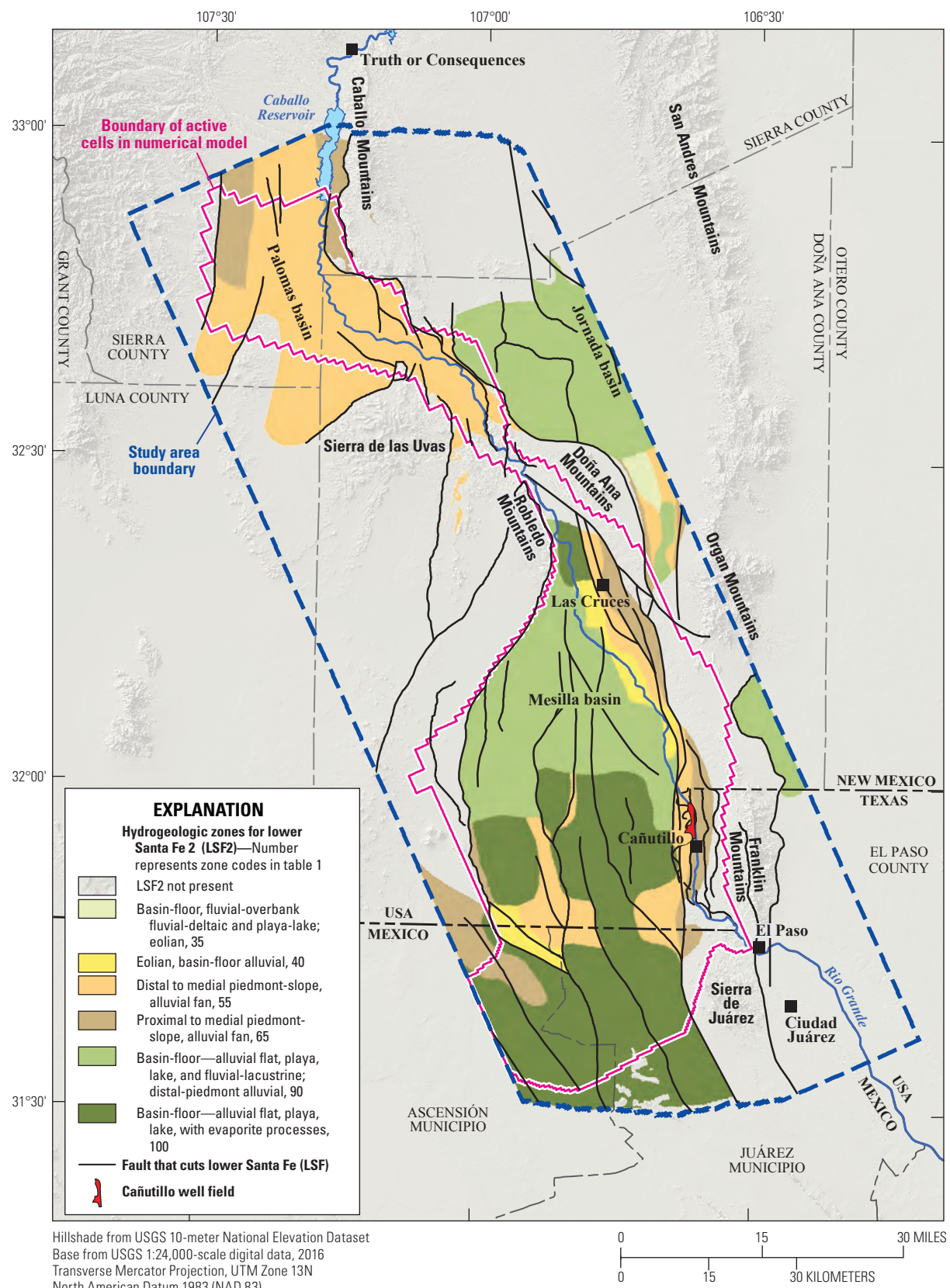


Figure 23. Map of Rio Grande transboundary region of New Mexico and Texas, USA, and northern Chihuahua, Mexico, showing zone codes for lower part of lower Santa Fe hydrostratigraphic unit (LSF2) as used in the three-dimensional hydrogeologic framework model.

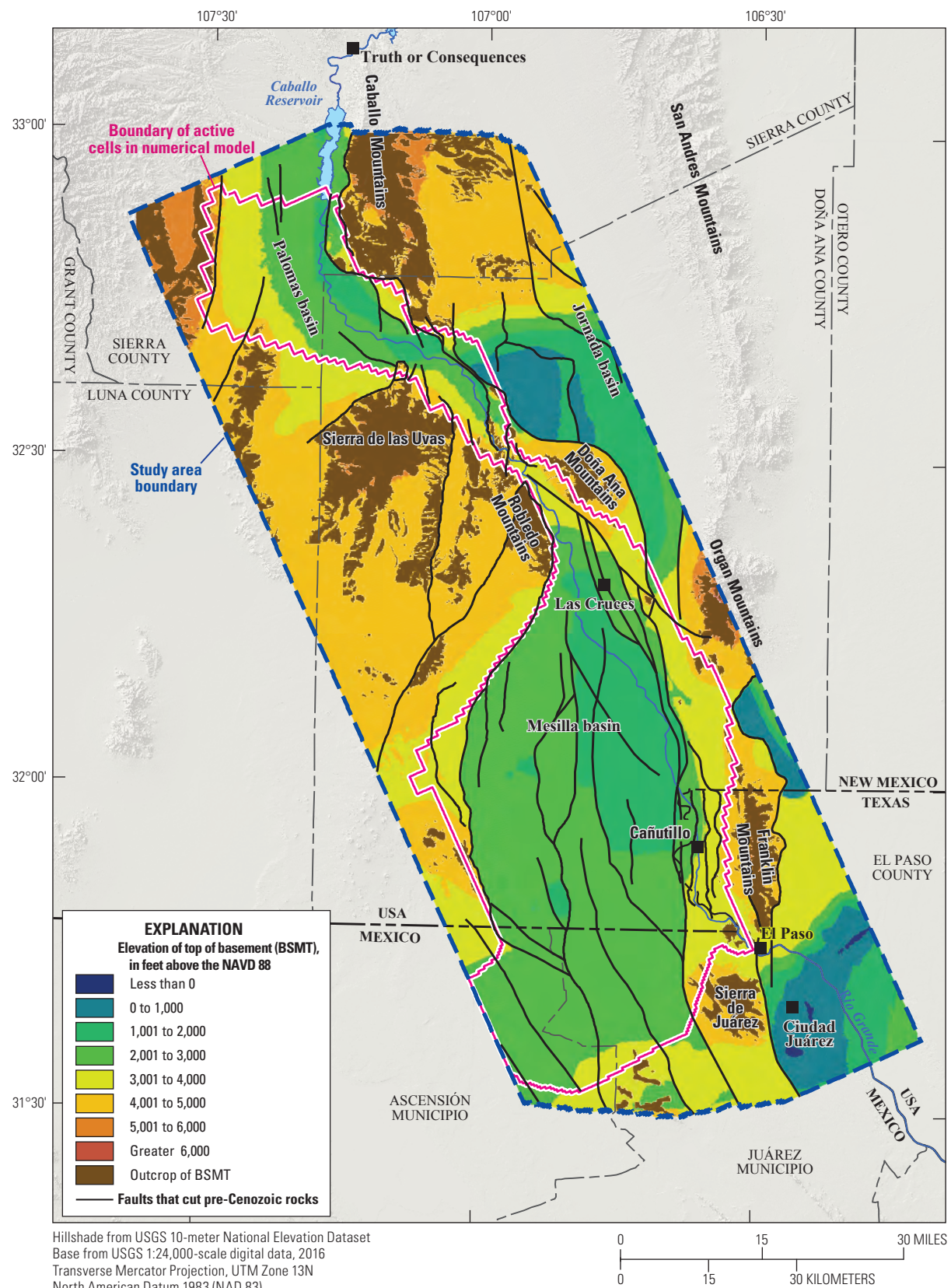


Figure 24. Map of Rio Grande transboundary region of New Mexico and Texas, USA, and northern Chihuahua, Mexico, showing gridded elevation of top of basement hydrostratigraphic unit (BSMT) as used in the three-dimensional hydrogeologic framework model. (NAVD 88, North American Vertical Datum of 1988)

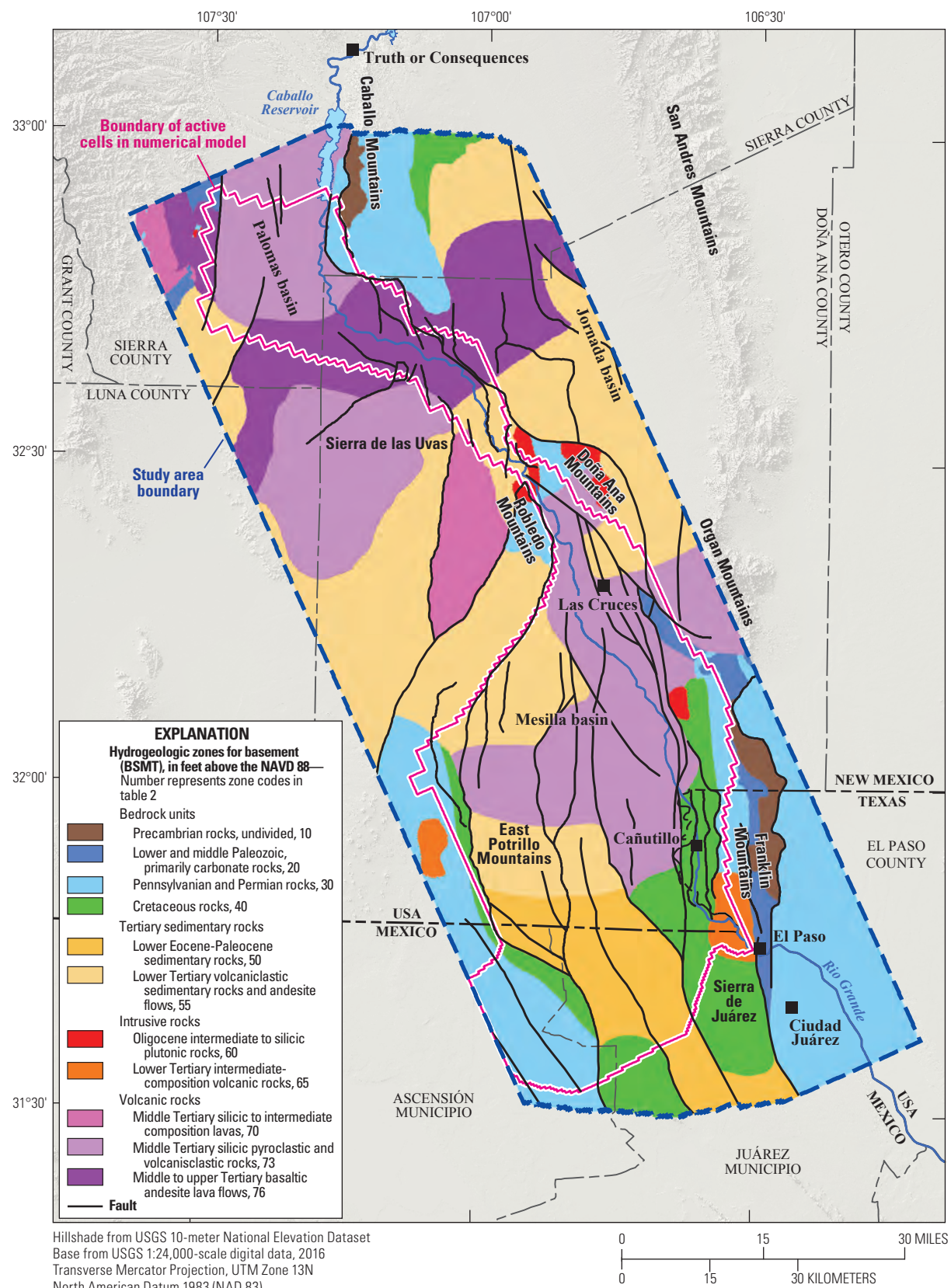


Figure 25. Map of Rio Grande transboundary region of New Mexico and Texas, USA, and northern Chihuahua, Mexico, showing zone codes for basement hydrostratigraphic unit (BSMT) as used in the three-dimensional hydrogeologic framework model. (NAVD 88, North American Vertical Datum of 1988)

Visualization of the 3D Hydrogeologic Framework Model

A perspective view of the 3D HFM shows the upper surface of the model and subsurface geology in the southeastern part of the model (fig. 26). In this view, the solid volume of the 3D HFM fills the skewed northwest-trending rectangular polygon of the study area boundary; the solid model has been cut away at its southeast corner so that some of the interior of the model volume can be viewed. Faults in the subsurface are modeled as curved vertical panels and are visible in the cutaway view. In this perspective view, model cells or voxels representing the five HSUs are symbolized and labeled RC, USF, MSF, LSF, and BSMT (fig. 26). The upper surface of the 3D HFM is limited by a digital elevation model and represents a map of the hydrostratigraphic units predicted by the model to be present at land surface. The patterns of the hydrostratigraphic units at the upper surface of the 3D HFM generally correspond to outcrops shown in the geologic map of the basin (fig. 3), providing a first-order check on the model's validity.

In the perspective view of the 3D HFM, modeled bedrock highs of HSU BSMT are evident in the Sierra de las Uvas and the Caballo, Robledo, Doña Ana, and Organ Mountains (fig. 26). BSMT units are dotted with isolated voxels of USF as a result of differences in x, y resolution and orientation of the input grids for USF and BSMT and the x, y voxel resolution chosen for solid model. Outcrops of MSF are simulated along the incised inner valley of the Rio Grande in the Palomas basin where RC has incised through USF (fig. 26, location 1). The 3D HFM correctly simulates the geologic relations in Selden Canyon where the Rio Grande, underlain by RC, is confined to a narrow canyon through uplifted MSF and BSMT HSUs (fig. 26, location 2). Surface exposures of LSF are limited to localized outcrops in the study area (fig. 3), which are visible on the upper surface of the 3D HFM as bright red voxels in the southern part of the Caballo Mountains and to the north of the Robledo Mountains (fig. 26, location 3).

HSUs in the subsurface are shown on the east edge of the solid block and in the cutaway in the southeast corner of the model (fig. 26). In the cutaway view, BSMT at the north end of the Franklin Mountains are shown along the vertical profile (fig. 26, location 4), but most of the Franklin Mountains block is higher in elevation than the base of the cutout and is not visible within the cutaway view. The cutaway displays the subsurface geology of the Mesilla basin and the stratigraphic stack of USF, MSF, and LSF. RC is not apparent in section view because it is only 80 ft (24 m) thick. Offset across faults is visible in the cutout as changes of elevation of the HSU top; the actual offset at the fault is obscured by the 3D fault panel (fig. 26, location 5). The horizontal floor of the cutout shows the subsurface geology in plan view at an elevation of 400 m above sea level. On this plane in the southeast corner of the model, USF is preserved in the deep basin of the Hueco

Bolson to the east of the Franklin Mountains uplift (fig. 26, location 6). Near the west edge of the cutout, the mid-basin high appears as an area of BSMT flanked to the east and west by down-dropped sections of LSF (fig. 26, location 7).

An auxiliary animation (appendix 1) shows this same perspective view, but instead of a single cutout, the interior of the solid model is revealed from south to north by a succession of cross sections that display the interior volume of the model.

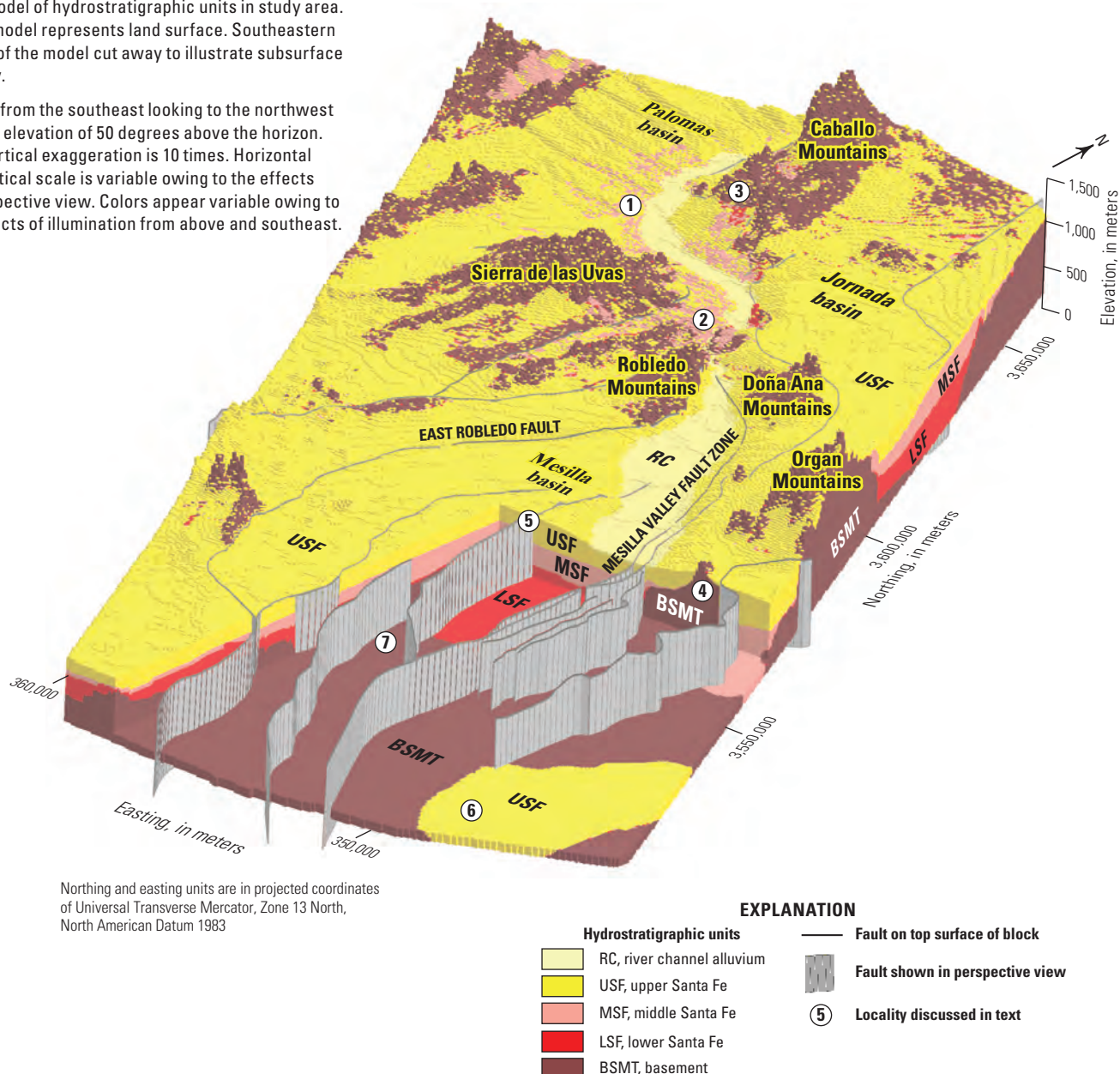
Multiple vertical cross sections cut through the 3D HFM are another way to analyze and better understand the geometry and structure of the basin-fill aquifers as portrayed by the 3D HFM (fig. 27). Vertical cross sections cut through the 3D HFM are symbolized with colors representing the HSUs RC, USF, MSF, LSF, and BSMT. Cross sections extend to a depth of 1,640 ft (500 m) above sea level; the top edge of each section represents the topographic profile at land surface. Cross sections can be cut through the 3D HFM in any orientation. In figure 27, model cross sections are shown in similar orientations to some of the input sections (fig. 6; Hawley and Kennedy, 2004), but the length and location of the model sections differ from input sections for illustration clarity. A select number of the faults from the 3D HFM are shown in figure 27 for reference; faults are shown as curving 3D panels. The offset created by faults that are not depicted is readily seen in the vertical profiles as abrupt changes in elevation of the hydrostratigraphic unit tops. For reference, an index map similar to figure 1 is included as a base. The index map is hung at an arbitrary elevation of 820 ft (250 m) above sea level, so that the sections appear to be extruded above the surface of the map.

Cross sections through the Mesilla basin dominate the lower half of figure 27; sections cut through the Palomas basin are in the upper part of the figure. BSMT uplifts bounding the east side of Mesilla basin include the Sierra de Juarez and the Franklin and Organ Mountains, and on the west side, the Robledo and East Potrillo Mountains (fig. 27). Palomas basin is bounded on the east by the BSMT uplift of the Caballo Mountains and on the south by the Sierra de las Uvas. The simulated uplifted block of the mid-basin high is apparent near the center of Mesilla basin (fig. 27, location 1). On the east flank of the Mesilla basin, fault offsets of LSF and MSF along the Mesilla Valley fault zone are buried by generally post-faulting USF (fig. 27, location 2). In the northeast part of the 3D HFM, the Jornada fault separates the BSMT uplift of the Doña Ana Mountains on the south from the thick package of basin fill in the southern part of the Jornada basin to the north (fig. 27, location 3). The most striking difference within the 3D HFM between the Mesilla and Palomas basins is the relative absence of USF in Palomas basin. The cross section in the Palomas basin that generally follows the course of the Rio Grande shows relatively thick sections of MSF that directly underlie the inner valley of the Rio Grande and RC in this area (fig. 27, location 4).

In the associated animation (appendix 2), these same cross sections are rotated in 3D space so that the model results may be explored from different viewpoints.

Solid model of hydrostratigraphic units in study area. Top of model represents land surface. Southeastern corner of the model cut away to illustrate subsurface geology.

View is from the southeast looking to the northwest from an elevation of 50 degrees above the horizon. Map vertical exaggeration is 10 times. Horizontal and vertical scale is variable owing to the effects of perspective view. Colors appear variable owing to the effects of illumination from above and southeast.



Northing and easting units are in projected coordinates of Universal Transverse Mercator, Zone 13 North, North American Datum 1983

Figure 26. Perspective view of three-dimensional hydrogeologic framework solid model with cutout.

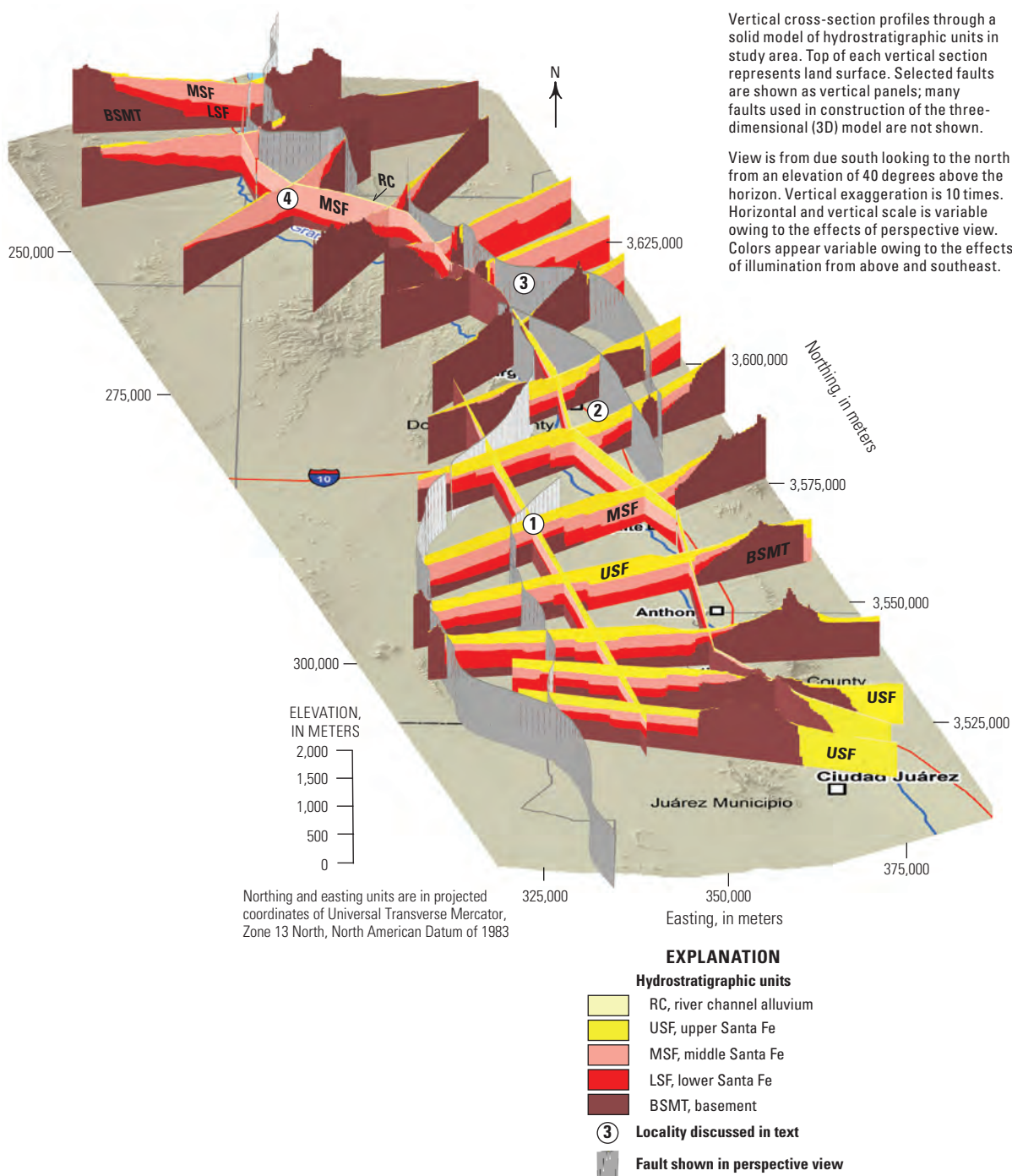


Figure 27. Perspective view of vertical cross sections cut through three-dimensional hydrogeologic framework solid model.

Model Evaluation, Use, and Limitations

The 3D HFM was evaluated for accuracy by visual inspection and by mathematical manipulations of the gridded surfaces to evaluate the elevation and thickness of the HSUs. The 3D HFM was compared to the known extent of HSUs, input cross sections, and geologic maps.

Evaluation of Fit—Comparison to Input Data

Gridded surfaces of the HSU horizons were compared to the input data used to construct the surfaces to assess the accuracy of the gridding processes. A qualitative comparison of the modeled HSU tops generated by the 3D HFM (fig. 5B) and the published hydrogeologic cross section along the same line of section are shown in figure 5A (Hawley and Kennedy, 2004, section G-G'). Model HSU tops closely match the fault locations and changes of HSU surface elevations from the published cross section, showing that model representation of the HSUs is a good match to the input data.

Visually comparing in three dimensions the modeled tops of the HSUs with several hydrogeologic cross sections used as input to the 3D HFM provided another method of evaluating the model accuracy and representation (fig. 28). In this example, the modeled top of LSF is shown in perspective view with faults from the 3D HFM and some of the input hydrogeologic sections referenced in 3D space. On the basis of gross morphology, the modeled top of LSF retains the geometric characteristics from the input cross sections, in all but a few places closely matching the interpreted top of LSF on the sections (fig. 28). No discrepancies of geologic or hydrologic significance were recognized between the input data and the modeled surfaces from the 3D HFM.

The modeled top of MSF from the 3D HFM was evaluated in a quantitative manner by calculating the elevation value of the top MSF in the 3D HFM at every x, y location of input data used to create the top MSF surface. The z value in the 3D HFM was subtracted from the z value of the input data at each location, creating a z-residual value, which was posted on a base map (fig. 29A). Z-residual values are generally less than 50 ft throughout most of the active model domain (fig. 29A); the mean difference in elevation of top MSF between input data and the 3D HFM is 19.3 ft (fig. 29B). This difference was calculated as a percentage of the z-value range of the input data; mean z-residuals are 1 percent of the total range in elevation of the input data. Z-residuals are high in one fault block at the southwest edge of the model, adjacent to some faults, such as the Mesilla Valley fault zone on the east edge of the active model, and near Selden Canyon where close spacing between surface outcrops and subsurface locations of MSF produce gridding instabilities. The elevation value of the

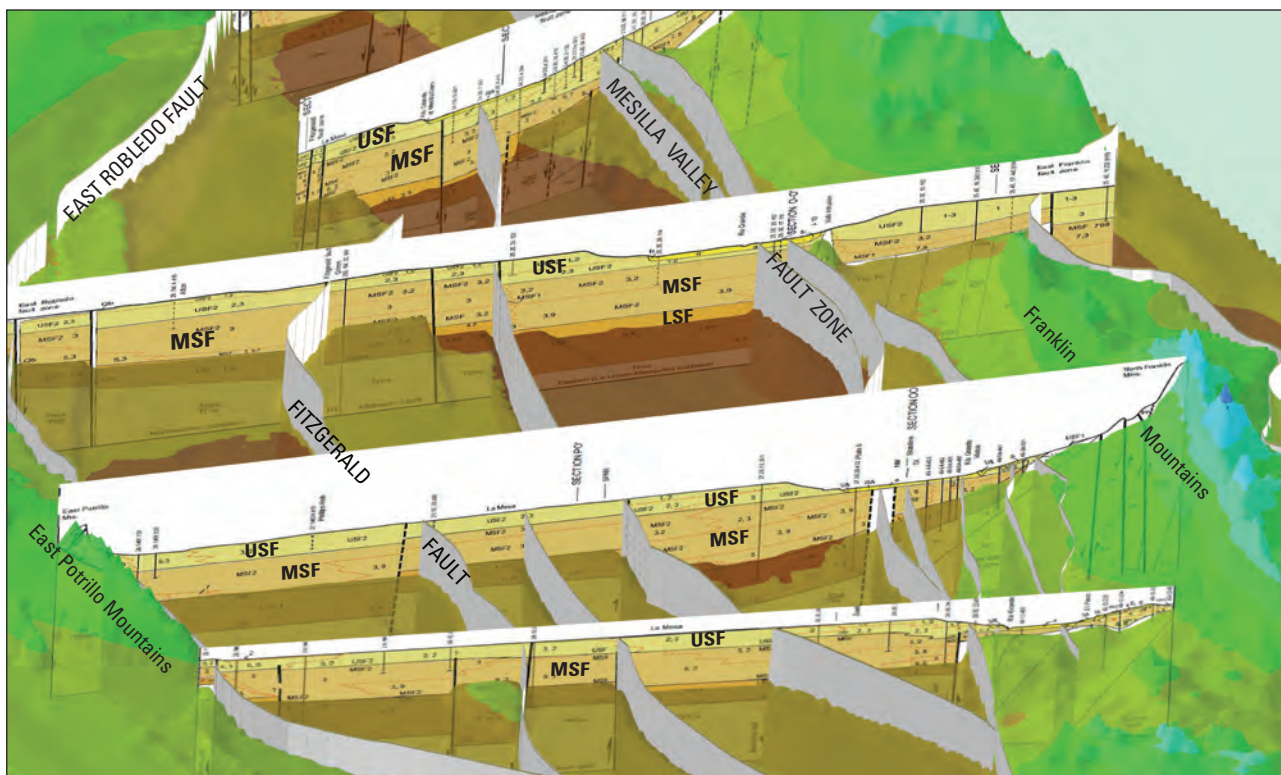
top MSF in the 3D HFM was similarly compared to selected wells from the Palomas basin (figs. 29A and C). Z-residuals are higher for these wells than for the input dataset, averaging -34.6 ft, meaning that on average, 3D HFM elevations are lower than the input data. Most of the largest values of z-residual are for wells that are south of the active model cells, where 3D HFM grids were less rigorously edited (fig. 29A). For the well data, mean z-residuals are 5.7 percent of the total range in elevation of the input well data.

Applicability and Limitations

The intended use of the digital 3D HFM is to provide the hydrogeologic framework input to numerical hydrologic models used for evaluation of the availability and sustainability of surface and groundwater resources. The 3D HFM reproduces with reasonable accuracy the previously published subsurface hydrogeologic conceptualization of the aquifer system and represents the large-scale geometry and structure of the aquifer systems.

Limitations of the 3D HFM include the following:

- The digital 3D HFM described in this report captures the hydrogeologic conceptualization of Hawley and Kennedy (2004), data developed in conjunction with the U.S. Geological Survey during the Transboundary Aquifer Assessment Program (Alley, 2013), and selected other published data. Any more recent data and subsurface interpretations were beyond the scope of this model construction.
- The goal in construction of this 3D HFM was to represent, in digital form, the hydrogeologic conceptualization embodied in the input datasets. Thus, any errors inherent in these input datasets may be propagated into the digital framework.
- Framework model error increases with distance from data. Although uncertainty is unquantified within the framework, it is reasonable to assume that the model is less certain where fewer input data were available to constrain fault locations and the elevation of hydrostratigraphic units. This is the case in the southwestern part of the study area and to the south of the International border, which is beyond the limits of geologic sections; few well data are available, and there is little outcrop control to guide subsurface interpretation. The Palomas basin has a lower density of input geologic sections than the Mesilla basin, but geologic outcrops on both sides of the basin and outcrops of Santa Fe Group rocks within the basin help to constrain the subsurface interpretation.



Vertical input hydrogeologic cross section profiles showing hydrostratigraphic units in study area. Modeled top of LSF shown as transparent colored surface. Faults used in construction of the 3D model are shown as vertical panels.

View is from due south looking to the north from an elevation of 40 degrees above the horizon. Vertical exaggeration is 7 times. Horizontal and vertical scale is variable owing to the effects of perspective view. Colors appear variable owing to the effects of illumination from above and southeast.

EXPLANATION

Hydrostratigraphic units (HSUs)—
on hydrogeologic sections

- USF, upper Santa Fe
- MSF, middle Santa Fe
- LSF, lower Santa Fe

 Fault shown in perspective view

Figure 28. Perspective view of input hydrogeologic cross sections and three-dimensional hydrogeologic framework modeled top of lower Santa Fe (LSF) hydrostratigraphic unit.

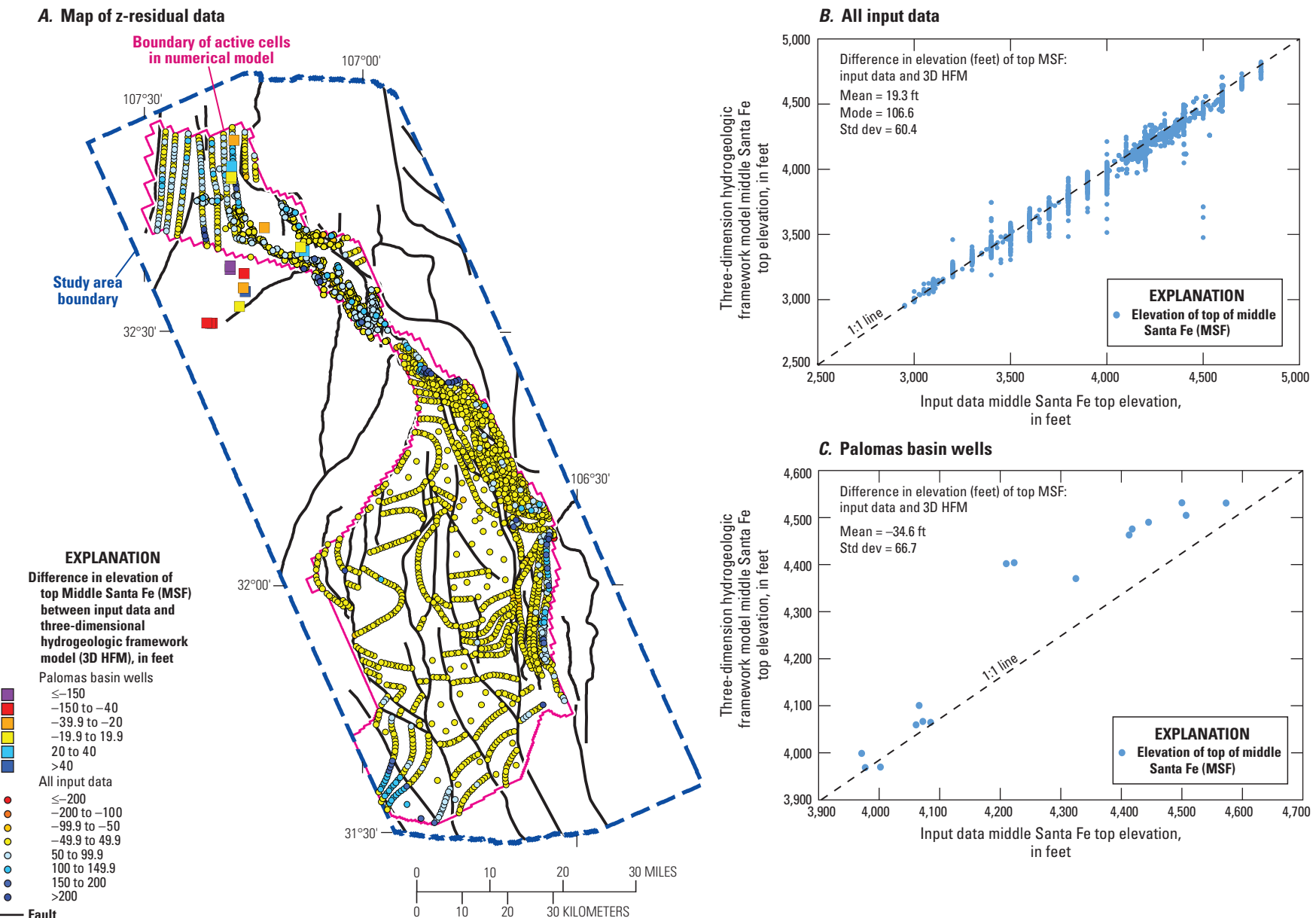


Figure 29. Difference in elevation of the top of middle Santa Fe (MSF) between input data and three-dimensional hydrogeologic framework model (3D HFM) (z-residual). **A.** Map of z-residual data for all input data and select Palomas basin wells. **B.** Graph comparing elevation of the top of MSF between input data and 3D HFM for all input data. **C.** Graph comparing elevation of the top of MSF between input data and 3D HFM for select Palomas basin wells.

Summary and Conclusions

A digital three-dimensional framework model of the major hydrostratigraphic units (HSUs) of the lower Rio Grande basin in New Mexico and Texas and the Conejos-Medanos basin of northern Mexico was developed from existing geologic data. Top surfaces were created for five hydrostratigraphic units and then stacked in three dimensions to create a solid-volume digital model. The solid-volume model is internally consistent in that the calculated base of each HSU is coincident with the top of the underlying HSU, and the thickness of each unit is the difference between the unit top and unit bottom. Major structures and hydrogeologic unit outcrop patterns of this model are generally consistent with published geologic maps and subsurface interpretations (Hawley and Kennedy, 2004; Mack, 2004; Hawley and others, 2009).

The model shows the overall geometry of the Palomas basin, an east-tilted half graben, and the Mesilla basin, a broad graben with complex internal faulting. The model illustrates the spatial extent, elevation, and thickness of alluvium along the Rio Grande and three informal hydrostratigraphic subdivisions of the Santa Fe Group rocks which form the important groundwater aquifer units in these basins. Included in the model are numerous faults which control the overall configuration of the basins and offset the HSUs at basin boundaries and in intrabasin locations. The model is at a scale and resolution appropriate for use as the foundation for a numerical hydrologic model of the study area.

References Cited

- Alley, W.M., ed., 2013, Five-year interim report of the United States–Mexico Transboundary Aquifer Assessment Program—2007–2012: U.S. Geological Survey Open-File Report 2013–1059, 31 p.
- American Nuclear Society, 1980, American National Standard—For evaluation of radionuclide transport in ground water for nuclear power sites: La Grange Park, Ill., American Nuclear Society, 10 p.
- Boyle Engineering Corp. and Parsons Engineering Science, 2000, El Paso–Las Cruces regional sustainable water project, hydrological modeling final report: Boyle Engineering Corp. and Parsons Engineering Science, 202 p.
- Chapin, C.E., and Cather, S.M., 1994, Tectonic setting of the axial basins of the northern and central Rio Grande rift, *in* Keller, G.R., and Cather, S.M., eds., Basins of the Rio Grande rift—Structure, stratigraphy, and tectonic setting: Geological Society of America, Special Paper 291, p. 5–25. [Also available at <https://doi.org/10.1130/SPE291-p5>.]
- Chapin, C.E., and Seager, W.R., 1975, Evolution of the Rio Grande rift in the Socorro and Las Cruces areas, *in* Seager,
- W.R., Clemons, R.E., and Callender, J.F., eds., 26th Annual Fall Field Conference Guidebook: New Mexico Geological Society, p. 297–321.
- Collins, E.W., and Raney, J.A., 1994, Tertiary and Quaternary tectonics of the Hueco Bolson, Trans-Pecos Texas and Chihuahua, Mexico, *in* Keller, G.R., and Cather, S.M., eds., Basins of the Rio Grande rift—Structure, stratigraphy, and tectonic setting: Geological Society of America, Special Paper 291, p. 265–282. [Also available at <https://doi.org/10.1130/SPE291-p265>.]
- DeFord, R.K., 1969, Some keys to the geology of northern Chihuahua, *in* Córdoba, D.A., Wengerd, S.A., and Shomaker, John, eds., 20th Field Conference, Guidebook of the Border Region: New Mexico Geological Society, p. 61–65.
- Dickinson, W.R., and Lawton, T.F., 2001, Carboniferous to Cretaceous assembly and fragmentation of Mexico: Geological Society of America Bulletin, v. 113, no. 9, p. 1142–1160. [Also available at [https://doi.org/10.1130/0016-7606\(2001\)113<1142:CTCAAF>2.0.CO;2](https://doi.org/10.1130/0016-7606(2001)113<1142:CTCAAF>2.0.CO;2).]
- Epis, R.C., and Chapin, C.E., 1975, Geomorphic and tectonic implications of the post-Laramide, late Eocene erosion surface in the southern Rocky Mountains: Geological Society of America Memoir 144, p. 45–74. [Also available at <https://doi.org/10.1130/MEM144-p45>.]
- Figuers, S.H., 1987, Structural geology and geophysics of the pipeline complex, northern Franklin Mountains, El Paso, Texas: El Paso, Tex., University of Texas, Ph.D. dissertation, 279 p. [Also available at <http://digitalcommons.utep.edu/dissertations/AI8729914/>.]
- Frenzel, P.F., 1992, Simulation of ground-water flow in the Mesilla basin, Doña Ana County, New Mexico, and El Paso County, Texas: U.S. Geological Survey Water Resource Investigations Report 91–4155, 152 p. [Also available at <http://pubs.er.usgs.gov/publication/wri914155>.]
- Gile, L.H., Hawley, J.W., and Grossman, R.B., 1981, Soils and geomorphology in the Basin Range area of southern New Mexico—Guidebook to the Desert Project: New Mexico Bureau of Mines and Mineral Resources Memoir 39, 222 p.
- Gross, James, and Iceman, Larry, 1983, Subsurface investigations for the area surrounding Tortugas Mountain, Doña Ana County, New Mexico: New Mexico Energy Research and Development Institute Report NMERDI 2-67-2238(2), 70 p.
- Haase, C.S., and Lozinsky, R.P., 1992, Estimation of hydrologic parameters, *in* Hawley, J.W., and Haase, C.S., comps., Hydrogeologic framework of the northern Albuquerque basin: New Mexico Bureau of Mines and Mineral Resources Open-File Report 387, 176 p.

- Hamilton, S.L., 1993, Application of a ground-water flow model to the Mesilla basin, New Mexico and Texas: Tucson, Ariz., University of Arizona, M.S. thesis, 340 p., accessed December 19, 2016, at <http://arizona.openrepository.com/arizona/handle/10150/278362>.
- Hanson, R.T., Schmid, Wolfgang, Knight, Jake, and Maddock, T., III, 2013, Integrated hydrologic modeling of a transboundary aquifer system—Lower Rio Grande, *in* MODFLOW and more 2013—Translating science into practice: Golden, Colo., Colorado School of Mines, International Ground Water Modeling Center, 5 p.
- Harbour, R.L., 1972, Geology of the northern Franklin Mountains, Texas and New Mexico: U.S. Geological Survey Bulletin 1298, 129 p. [Also available at <https://pubs.er.usgs.gov/publication/b1298>.]
- Hawley, J.W., 1978, Guidebook to the Rio Grande rift in New Mexico and Colorado: New Mexico Bureau of Mines and Mineral Resources Circular 163, 241 p.
- Hawley, J.W., 1984, Hydrogeologic cross sections of the Mesilla bolson, New Mexico and Texas: New Mexico Bureau of Mines and Minerals Resources Open-File Report 190, 10 p.
- Hawley, J.W., and Kennedy, J.F., 2004, Creation of a digital hydrogeologic framework model of the Mesilla basin and southern Jornada del Muerto basin: New Mexico State University, New Mexico Water Resources Research Institute Technical Completion Report 332, 105 p., with 2005 Addendum, accessed April 17, 2017, at <https://nmwrri.nmsu.edu/tr332/>.
- Hawley, J.W., Kennedy, J.F., and Creel, B.J., 2001, The Mesilla basin aquifer system of New Mexico, west Texas and Chihuahua—An overview of its hydrogeologic framework and related aspects of groundwater flow and chemistry, *in* Mace, R.E., and Angle, E.S., eds., Aquifers of west Texas: Texas Water Development Board Report 356, chap. 7, p. 76–99, accessed December 20, 2016, at http://www.twdb.texas.gov/publications/reports/numbered_reports/doc/R356/Report356.asp.
- Hawley, J.W., Kennedy, J.F., Granados-Olivas, Alfredo, and Ortiz, M.A., 2009, Hydrogeologic framework of the binational western Hueco Bolson–Paso del Norte area, Texas, New Mexico, and Chihuahua—Overview and progress report on digital-model development: New Mexico Water Resources Research Institute Technical Completion Report 349, 45 p., 2 plates, accessed December 20, 2016, at <https://nmwrri.nmsu.edu/tr349/>.
- Hawley, J.W., and Kottlowski, F.E., 1969, Quaternary geology of the south-central New Mexico border region, *in* Kottlowski, F.E., and LeMone, D.V., eds., Border stratigraphy symposium: New Mexico Bureau of Mines and Mineral Resources Circular 104, p. 89–115.
- Hawley, J.W., Kottlowski, F.E., Strain, W.S., Seager, W.R., King, W.E., and LeMone, D.V., 1969, The Santa Fe Group in the south-central New Mexico border region, *in* Kottlowski, F.E., and LeMone, D.V., eds., Border stratigraphy symposium: New Mexico Bureau of Mines and Mineral Resources Circular 104, p. 52–76.
- Hawley, J.W., and Lozinsky, R.P., 1992, Hydrogeologic framework of the Mesilla basin in New Mexico and western Texas: New Mexico Bureau of Mines and Mineral Resources Open-File Report 323, 55 p.
- Hildebrand, R.S., 2015, Dismemberment and northward migration of the Cordilleran orogen—Baja-BC resolved: GSA Today, v. 25, no. 11, p. 4–11. [Also available at <https://doi.org/10.1130/GSATG255A.1>.]
- Hoffer, J.M., 1969, Geology and petrography of the Campus Andesite pluton, El Paso County, Texas: New Mexico Geological Society Guidebook 20, p. 102–107.
- Imana, E.C., 2002, The Mesilla bolson—An integrated geo-physical, hydrological, and structural analysis using free-air anomalies: El Paso, Texas, University of Texas, Ph.D. dissertation, 170 p.
- Khatun, Salma, 2003, A precision gravity study of the southern Mesilla bolson, west Texas: El Paso, Texas, University of Texas, M.S. thesis, 75 p. [Also available at <http://digitalcommons.utep.edu/dissertations/AAIEP10570>.]
- Khatun, Salma, Doser, D.I., Imana, E.C., and Keller, G.R., 2007, Locating faults in the southern Mesilla bolson, west Texas and southern New Mexico, using 3-D modeling of precision gravity data: Journal of Environmental & Engineering Geophysics, v. 12, no. 2, p. 149–161. [Also available at <https://doi.org/10.2113/JEEG12.2.149>.]
- King, W.E., Hawley, J.W., Taylor, A.M., and Wilson, R.P., 1969, Hydrogeology of the Rio Grande Valley and adjacent intermontane areas of southern New Mexico: New Mexico Water Resources Research Institute Miscellaneous Report 6, 146 p., accessed December 20, 2016, at <https://nmwrri.nmsu.edu/m6/>.
- King, W.E., Hawley, J.W., Taylor, A.M. and Wilson, R.P., 1971, Geology and ground-water resources of central and western Doña Ana County, New Mexico: New Mexico Bureau of Mines and Mineral Resources Hydrologic Report 1, 64 p.
- Lang, P.T., and Maddock, Thomas, III, 1995, Simulation of groundwater flow to assess the effects of pumping and canal lining on the hydrologic regime of the Mesilla basin, Doña Ana County, New Mexico and El Paso County, Texas: University of Arizona Department of Hydrology and Water Resources HWR no. 95–020. [Also available at <http://arizona.openrepository.com/arizona/bitstream/10150/617628/1/HWR-1995-020.pdf>.]

- Lawton, T.F., 2004, Upper Jurassic and Lower Cretaceous strata of southwestern New Mexico and northern Chihuahua, Mexico, in Mack, G.H., and Giles, K.J., eds., The geology of New Mexico—A geologic history: New Mexico Geological Society Special Publication 11, p. 153–168.
- Leggat, E.R., Lowry, M.E., and Hood, J.W., 1962, Ground-water resources of the lower Mesilla Valley, Texas and New Mexico: U.S. Geological Survey Water-Supply Paper 1669-AA, 191 p. [Also available at <https://pubs.usgs.gov/wsp/1669aa/report.pdf>.]
- Lovejoy, E.M.P., 1976, Neotectonics of the southeast end of the Rio Grande rift along the Mesilla Valley fault zone and the course of the Rio Grande, El Paso, Texas: El Paso Geological Society Symposium on the stratigraphy of the Franklin Mountains, Quinn Memorial volume, p. 123–138.
- Lozinsky, R.P., and Hawley, J.W., 1986, The Palomas Formation of south-central New Mexico—A formal definition: New Mexico Geology, v. 8, no. 4, p. 73–82. [Also available at http://geoinfo.nmt.edu/publications/periodicals/nmg/8/n4/nmg_v8_n4_p73.pdf.]
- Mack, G.H., 2004, Middle and late Cenozoic crustal extension, sedimentation, and volcanism in the southern Rio Grande rift, Basin and Range, and southern transition zone of southwestern New Mexico, in Mack, G.H., and Giles, K.J., eds., The geology of New Mexico—A geologic history: New Mexico Geological Society Special Publication 11, p. 389–406.
- Mack, G.H., Salyards, S.L., and James, W.C., 1993, Magnetostratigraphy of the Plio-Pleistocene Camp Rice and Palomas Formations in the Rio Grande rift of southern New Mexico: American Journal of Science, v. 293, p. 49–77. [Also available at <http://earth.geology.yale.edu/~ajs/1993/01.1993.03Mack.pdf>.]
- Mack, G.H., and Seager, W.R., 1990, Tectonic controls on facies distribution of the Camp Rice and Palomas Formations (Pliocene-Pleistocene) in the southern Rio Grande rift: Geological Society of America Bulletin, v. 102, no. 1, p. 45–53. [Also available at [https://doi.org/10.1130/0016-7606\(1990\)102<0045:TCOFDO>2.3.CO;2](https://doi.org/10.1130/0016-7606(1990)102<0045:TCOFDO>2.3.CO;2).]
- Mack, G.H., and Seager, W.R., 1995, Transfer zones in the southern Rio Grande rift: Journal of the Geological Society, v. 152, no. 3, p. 551–560. [Also available at <https://doi.org/10.1144/gsjgs.152.3.0551>.]
- Mack, G.H., Seager, W.R., and Kieling, John, 1994, Late Oligocene and Miocene faulting and sedimentation, and evolution of the southern Rio Grande rift, New Mexico, USA: Sedimentary Geology, v. 92, v. 1–2, p. 79–96. [Also available at [https://doi.org/10.1016/0037-0738\(94\)90055-8](https://doi.org/10.1016/0037-0738(94)90055-8).]
- Mack, G.H., Seager, W.R., Leeder, M.R., Perez-Arlucea, Marta, and Salyards, S.L., 2006, Pliocene and Quaternary history of the Rio Grande, the axial river of the southern Rio Grande rift, New Mexico, USA: Earth-Science Reviews, v. 79, no. 1–2, p. 141–162. [Also available at <https://doi.org/10.1016/j.earscirev.2006.07.002>.]
- Maxey, G.B., 1964, Hydrostratigraphic units: Journal of Hydrology, v. 2, no. 2, p. 124–129. [Also available at [https://doi.org/10.1016/0022-1694\(64\)90023-X](https://doi.org/10.1016/0022-1694(64)90023-X).]
- Muehlberger, W.R., 1980, Texas lineament revisited, in Dickerson, P.W., Hoffer, J.M., and Callender, J.F., eds., The Trans-Pecos Region: New Mexico Geological Society 31st Field Conference Guidebook, p. 113–121.
- Myers, R.G., and Orr, B.R., 1985, Geohydrology of the aquifer in the Santa Fe Group, northern West Mesa of the Mesilla basin near Las Cruces, New Mexico: U.S. Geological Survey Water-Resources Investigations Report 84-4190, 37 p. [Also available at <https://pubs.er.usgs.gov/publication/wri844190>.]
- New Mexico Office of the State Engineer/Interstate Stream Commission, 2017, Lower Rio Grande: New Mexico Office of the State Engineer/Interstate Stream Commission web page, accessed January 23, 2017, at <http://www.ose.state.nm.us/Basins/RioGrande/lowerRioGrande.php>.
- Nickerson, E.L., 1986, Selected geohydrologic data for the Mesilla basin, Doña Ana County, New Mexico and El Paso County, Texas: U.S. Geological Survey Open-File Report 86-75, 59 p. [Also available at <https://pubs.er.usgs.gov/publication/ofr8675>.]
- Nickerson, E.L., 1989, Aquifer tests in the flood-plain alluvium and Santa Fe Group at the Rio Grande near Canutillo, El Paso County, Texas: U.S. Geological Survey Water-Resources Investigations Report 89-4011, 29 p. [Also available at <https://pubs.usgs.gov/wri/1989/4011/report.pdf>.]
- Nickerson, E.L., and Myers, R.G., 1993, Geohydrology of the Mesilla ground-water basin, Doña Ana county, New Mexico, and El Paso County, Texas: U.S. Geological Survey Water-Resources Investigations Report 92-4156, 89 p. [Also available at <https://pubs.er.usgs.gov/publication/wri924156>.]
- Seaber, P.R., 1988, Hydrostratigraphic units, in Back, William, Rosenschein, J.S., and Seaber, P.R., eds., Hydrogeology: Boulder, Colo., Geological Society of America, v. O-2, p. 9–14.
- Seager, W.R., 1975, Cenozoic tectonic evolution of the Las Cruces area, New Mexico, in Seager, W.R., Clemons, R.E., and Callender, J.F., eds., Las Cruces country: New Mexico Geological Society 26th Annual Fall Field Conference Guidebook, p. 241–250.
- Seager, W.R., 1981, Geology of the Organ Mountains and southern San Andres Mountains, New Mexico: New Mexico Bureau of Mines and Mineral Resources Memoir 36, 97 p.

- Seager, W.R., 1995, Geologic map of the southwest quarter of the Las Cruces and northwest part of the El Paso $1^{\circ} \times 2^{\circ}$ sheets: New Mexico Bureau of Mines and Mineral Resources Geologic Map 60, scale 1:125,000.
- Seager, W.R., 2004, Laramide (Late Cretaceous–Eocene) tectonics of southwestern New Mexico *in* Mack, G.H., and Giles, K.J., eds., The geology of New Mexico—A geologic history: New Mexico Geological Society Special Publication 11, p. 183–202.
- Seager, W.R., Clemons, R.E., and Hawley, J.W., 1975, Geology of Sierra Alta quadrangle Doña Ana County, New Mexico: New Mexico Bureau of Mines and Mineral Resources Bulletin 102.
- Seager, W.R., Clemons, R.E., Hawley, J.W., and Kelley, R.E., 1982, Geology of northwest part of Las Cruces $1^{\circ} \times 2^{\circ}$ sheet, New Mexico: New Mexico Bureau of Mines and Mineral Resources Geologic Map 53, 3 sheets, scale 1:125,000.
- Seager, W.R., Hawley, J.W., Kottlowski, F.E., and Kelley, S.A., 1987, Geologic map of east half of Las Cruces and northeast El Paso $1^{\circ} \times 2^{\circ}$ sheets, New Mexico: New Mexico Bureau of Mines and Mineral Resources Geologic Map 57, 3 sheets, scale 1:125,000.
- Seager, W.R., Kottlowski, F.E., and Hawley, J.W., 1976, Geology of Doña Ana Mountains, New Mexico: New Mexico Bureau of Mines and Mineral Resources Circular 147, 3 sheets.
- Seager, W.R., Kottlowski, F.E., and Hawley, J.W., 2008, Geology of Robledo Mountains and vicinity, Doña Ana County, New Mexico: New Mexico Bureau of Mines and Mineral Resources, Open-File Report 509, scale 1:24,000.
- Seager, W.R., Mack, G.H., and Lawton, T.F., 1997, Structural kinematics and depositional history of a Laramide uplift-basin pair in southern New Mexico—Implications for development of intraforeland basins: Geological Society of America Bulletin, v. 109, no. 11, p. 1389–1401. [Also available at [https://doi.org/10.1130/0016-7606\(1997\)109<1389:SKADHO>2.3.CO;2](https://doi.org/10.1130/0016-7606(1997)109<1389:SKADHO>2.3.CO;2).]
- Seager, W.R., and Morgan, Paul, 1979, Rio Grande rift in southern New Mexico, west Texas and northern Chihuahua, *in* Riecker, R.E., ed., Rio Grande rift—Tectonics and magmatism: Washington D.C., American Geophysical Union, p. 87–106. [Also available at <https://doi.org/10.1029/SP014p0087>.]
- Seager, W.R., Shafiqullah, M., Hawley, J.W., and Marvin, R.F., 1984. New K-Ar dates from basalts and the evolution of the southern Rio Grande Rift: Geological Society of America Bulletin, v. 95, no. 1, p. 87–99. [Also available at [https://doi.org/10.1130/0016-7606\(1984\)95<87:NKDFBA>2.0.CO;2](https://doi.org/10.1130/0016-7606(1984)95<87:NKDFBA>2.0.CO;2).]
- Servicio Geologico Mexicano, 2011, Hydrogeological activities in the Conejos-Medanos/Mesilla Basin Aquifer, Chihuahua: Servicio Geologico Mexicano Report, Phase I, 111 p.
- Spiegel, Zane, and Baldwin, Brewster, 1963, Geology and water resources of the Santa Fe area, New Mexico: U.S. Geological Survey Water-Supply Paper 1525, 258 p. [Also available at <https://pubs.usgs.gov/wsp/1525/report.pdf>.]
- S.S. Papadopoulos & Associates, 2007, Groundwater flow model for administration and management in the lower Rio Grande Basin: Santa Fe, New Mexico, Report prepared for the New Mexico State Engineer, 63 p.
- Sweetkind, D.S., Hanson, R.T., Ritchie, A.B., and Hawley, J.W., 2017, Data release of three-dimensional hydrogeologic framework model of the Rio Grande transboundary region of New Mexico and Texas, USA, and northern Chihuahua, Mexico: U.S. Geological Survey data release, accessed August 3, 2017, at <https://doi.org/10.5066/F7JM27T6>.
- U.S. Department of Agriculture, 2017, Soil data access: U.S. Department of Agriculture web page, accessed April 17, 2017, at <https://sdmdataaccess.nrcs.usda.gov/>.
- U.S. Geological Survey and New Mexico Bureau of Mines and Mineral Resources, 2006, Quaternary fault and fold database for the United States: U.S. Geological Survey web page, accessed June 12, 2015, at <http://earthquake.usgs.gov/hazards/qfaults/>.
- Weeden, A.C., Jr., and Maddock, Thomas, III, 1999, Simulation of groundwater flow in the Rincon Valley area and Mesilla basin, New Mexico and Texas: University of Arizona Research Laboratory for Riparian Studies and Department of Hydrology and Water Resources HWR No. 99-020, 182 p., accessed December 19, 2016, at <http://arizona.aws.openrepository.com/arizona/bitstream/10150/617629/1/HWR-1999-020.pdf>.
- Wilson, C.A., White, R.R., Orr, B.R., and Roybal, R.G., 1981, Water resources of the Rincon and Mesilla Valleys and adjacent areas, New Mexico: New Mexico State Engineer Technical Report 43, 514 p. [Also available at <https://pubs.er.usgs.gov/publication/70042517>.]
- Woodward, D.G., and Myers., R.G., 1997, Seismic investigation of the buried horst between the Jornada del Muerto and Mesilla ground-water basins near Las Cruces, Doña Ana County, New Mexico: U.S. Geological Survey Water-Resources Investigations Report 97-4147, 45 p. [Also available at <https://pubs.er.usgs.gov/publication/wri974147>.]

Appendices

Appendix 1. Animation—Solid Model Reveal

To view the MP4 file for appendix 1, return to <https://doi.org/10.3133/sir20175060>.

The associated file is an animation of a perspective view of the three-dimensional hydrogeologic framework model (3D HFM); it is an animated version of static figure 26 of the report. In this animation, the solid model volume is successively cut from front (south) to back (north) by removing voxel layers in a sequential fashion so that successive panels within the solid model are revealed in each step. Cells within the solid volume are symbolized with colors representing the river channel (RC), upper Santa Fe Group (USF), middle Santa Fe Group (MSF), lower Santa Fe Group (LSF), and basement (BSMT) hydrostratigraphic units. Faults used to build the solid model are shown as curving 3D panels; selected faults are not shown in order to make the simulated subsurface

geology more visible. In this animation, the faults within the 3D model volume are not removed along with the model voxel layers and they remain as vertical 3D panels as the geologic model is successively sliced away. The upper surface of the solid model approximates land surface.

In the animation, the viewpoint is from the southeast at 50° above the horizon, and vertical exaggeration is 10x. Horizontal and vertical scale is variable due to the effects of perspective view. Colors appear variable owing to the effects of illumination from above and the southeast. 3D modeling software requires the vertical dimensions be reported in meters to be consistent with the x, y dimensions of the dimensions of the Universal Transverse Mercator (UTM) coordinates.

Appendix 2. Animation—Cross Section Panels

To view the MP4 file for appendix 2, return to <https://doi.org/10.3133/sir20175060>.

The associated file is an animation of a perspective view of vertical cross section panels cut through the three-dimensional hydrogeologic framework model (3D HFM); it is an animated version of static figure 27 of the report. In this animation, multiple vertical cross section panels cut through the 3D HFM are symbolized with colors representing the river channel (RC), upper Santa Fe Group (USF), middle Santa Fe Group (MSF), lower Santa Fe Group (LSF), and basement (BSMT) hydrostratigraphic units. Hydrostratigraphic unit RC is only 80 feet (24 meters) thick and is nearly invisible in this view. A select number of the faults that were used to build the 3D HFM are shown here for reference; faults are shown as curving 3D panels. The offset created by faults that are not depicted is readily seen in the vertical profiles as abrupt changes in elevation of the hydrostratigraphic unit tops. For

reference, an index map similar to report figure 1 is included. The index map is hung at an arbitrary elevation of 820 feet (250 meters) above sea level, such that the sections appear to be extruded above the surface of the map.

In the animation, vertical exaggeration is 8x. The viewpoint is a constant 40° above the horizon. The animation begins with the viewpoint from due south looking to the north, the same view as report figure 27. The view direction changes sequentially in 1-degree increments in a clockwise manner. Lighting direction remains constant during the animation; the sections are lit from above by a light from due south at 60° above the horizon and from below by a light from the northeast and 15° below the horizon. The effect of lighting results in shadowing and variable colors of the hydrostratigraphic units shown on the sections as the scene rotates.

Publishing support provided by:
Denver Publishing Service Center

For more information concerning this publication, contact:
Center Director, USGS Geosciences and Environmental Change
Science Center
Box 25046, Mail Stop 980
Denver, CO 80225
(303) 236-5344

Or visit the Geosciences and Environmental Change Science Center
website at: <https://gec.cr.usgs.gov/>

